

Adversarially Robust Topological Inference

Siddharth Vishwanath^{*1}, Bharath K. Sriperumbudur¹, Kenji Fukumizu³, and Satoshi Kuriki³

¹*Department of Mathematics, University of California San Diego*

¹*Department of Statistics, The Pennsylvania State University*

³*The Institute of Statistical Mathematics*

The distance function to a compact set plays a crucial role in the paradigm of topological data analysis. In particular, the sublevel sets of the distance function are used in the computation of persistent homology—a backbone of the topological data analysis pipeline. Despite its stability to perturbations in the Hausdorff distance, persistent homology is highly sensitive to outliers. In this work, we develop a framework of statistical inference for persistent homology in the presence of outliers. Drawing inspiration from recent developments in robust statistics, we propose a *median-of-means* variant of the distance function (MoM Dist) and establish its statistical properties. In particular, we show that, even in the presence of outliers, the sublevel filtrations and weighted filtrations induced by MoM Dist are both consistent estimators of the true underlying population counterpart and exhibit near minimax-optimal performance in adversarial settings. Finally, we demonstrate the advantages of the proposed methodology through simulations and applications.

1. Introduction

Given a compact set $\mathbb{X} \subset \mathbb{R}^d$, its persistence diagram encodes the subtle geometric and topological features that underlie \mathbb{X} as a multiscale summary and forms the cornerstone of topological data analysis. Persistent homology serves as the backbone for computing persistence diagrams and encodes the homological features underlying \mathbb{X} at different resolutions. The computation of persistent homology is typically achieved by constructing a *filtration* $V_{\mathbb{X}}$, i.e., a nested sequence of topological spaces, which captures the evolution of geometric and topological features as the resolution varies. The persistent homology, which is encoded in its persistence module, $\mathbb{V}_{\mathbb{X}}$, extracts the homological information from the filtration $V_{\mathbb{X}}$. This is then summarized in a persistence diagram $\mathfrak{Dgm}(\mathbb{V}_{\mathbb{X}})$.

Broadly speaking, there are two different methods for obtaining filtrations. The first, and, arguably more classical method is obtained by examining the union of balls of radius r centered on the points of \mathbb{X} called the r -*offset* of \mathbb{X} , denoted $\mathbb{X}(r)$, for each resolution $r > 0$. The resulting filtration $V[\mathbb{X}] = \{\mathbb{X}(r) : r > 0\}$, depends only on the metric properties of \mathbb{X} . The second, and more general approach is based on constructing a *filter function* $f_{\mathbb{X}}$, which reflects the topological features underlying \mathbb{X} . The resulting filtration $V[f_{\mathbb{X}}]$, in this case, is obtained by probing the sublevel sets $f_{\mathbb{X}}^{-1}((-\infty, r])$ or the superlevel sets $f_{\mathbb{X}}^{-1}([r, \infty))$ associated with $f_{\mathbb{X}}$. While these two methods are vastly different, in principle, they both attempt to explore the topological features underlying \mathbb{X} .

In this context, the distance function $d_{\mathbb{X}}$ to the set \mathbb{X} plays a special role in topological data analysis, and satisfies the property that $V[\mathbb{X}] = V[d_{\mathbb{X}}]$. That is, the sublevel sets of the distance function encode the same topological information as the filtration from its offsets. The

*svishwanath@ucsd.edu

appeal of using the distance function in the computation of persistence diagrams comes from the celebrated stability of persistence diagrams (Chazal et al., 2016). In a nutshell, the stability result for persistence diagrams guarantees that (i) the persistence diagrams resulting from two compact sets \mathbb{X} and \mathbb{Y} are close whenever the sets themselves are close in the Hausdorff distance, and, (ii) the functional persistence diagrams resulting from two filter functions f and g are close whenever f and g are close w.r.t. the $\|\cdot\|_\infty$ metric.

In the statistical setting, one has access to \mathbb{X} only through samples $\mathbb{X}_n = \{\mathbf{X}_1, \dots, \mathbf{X}_n\}$ obtained using a probability distribution \mathbb{P} which is supported on the (unknown) set \mathbb{X} . The objective, in a statistical inference framework, is to use the samples \mathbb{X}_n to infer the true population persistence diagram $\mathfrak{Dgm}(\mathbb{V}_{\mathbb{X}})$. The offset $\mathbb{X}_n(r)$ and filter function f_n , constructed using the sample points, are themselves random quantities associated with their population counterparts $\mathbb{X}(r)$ and $f_{\mathbb{X}}$, respectively, and these may be used to construct a sample estimator $\mathfrak{Dgm}(\mathbb{V}_{\mathbb{X}_n})$. To this end, several existing works have studied the statistical properties of persistence diagrams from samples in a noiseless setting, e.g., constructing confidence bands and characterizing the convergence rate of $\mathfrak{Dgm}(\mathbb{V}_{\mathbb{X}_n})$ to $\mathfrak{Dgm}(\mathbb{V}_{\mathbb{X}})$ in the space of persistence diagrams (Fasy et al., 2014; Chazal et al., 2015a,b, 2017).

However, in practical settings, real-world data is likely subject to measurement errors and the presence of outliers. While some assumptions may be imposed on the noise and the outliers, in the most baneful settings, the given data may be subject to adversarial contamination. In this setting, for $m < n/2$, we assume that the samples \mathbb{X}_n , which we have access to, contain only $n - m$ points obtained from the probability distribution \mathbb{P} with $\text{supp}(\mathbb{P}) = \mathbb{X}$, and make no further assumptions on the remaining m points. In principle, the m outliers may be carefully chosen by an adversary after examining the remaining $n - m$ points. While the stability of persistence diagrams guarantees that small perturbations in the sample points induce only small changes in the resulting persistence diagrams, even a few outliers in the samples can lead to deleterious effects. This issue is further exacerbated in the adversarial setting, where the adversary is free to place the m points where it may drastically impact the resulting topological inference. The overarching objective of this paper is to construct an estimator of the (unknown) population quantity $\mathfrak{Dgm}(\mathbb{V}[\mathbb{X}])$ using the corrupted sample points \mathbb{X}_n which is, both, statistically consistent and computationally efficient.

1.1. Contributions

To this end, our contributions are as follows. First, we introduce **MoM Dist**, denoted by $\mathbf{d}_{n,Q}$, as an outlier-robust variant of the empirical distance function which is constructed using the median-of-means principle, and we establish its theoretical properties. Notably the **MoM Dist** relies on a tuning parameter Q which is easy to interpret, and, roughly speaking, reflects an estimate for the number of outliers in the observed sample. While the persistence diagram resulting from the sublevel filtration of $\mathbf{d}_{n,Q}$ is a valid candidate for statistical inference, it can be expensive to compute in practice. To overcome this, we use the weighted filtrations introduced by Buchet et al. (2016) and Anai et al. (2019) to construct $\mathbf{d}_{n,Q}$ -weighted filtrations, $V[\mathbb{X}_n, \mathbf{d}_{n,Q}]$, as computationally efficient estimators of $\mathfrak{Dgm}(V[\mathbb{X}])$. Our main contributions are the following:

- (I) We show that sublevel set persistence diagrams of $\mathbf{d}_{n,Q}$ are consistent estimators of the sublevel set persistence diagram of the true population counterpart $\mathbf{d}_{\mathbb{X}}$ even in the presence of outliers; we establish its convergence rate (Theorem 5.1) and show that it is near minimax optimal up to a $\log n$ factor (Theorem 3.1).
- (II) We establish a stability result for the the $\mathbf{d}_{n,Q}$ -weighted filtrations, $V[\mathbb{X}_n, \mathbf{d}_{n,Q}]$, and we show that they are stable w.r.t. adversarial contamination (Theorem 6.1).

- (III) Furthermore, we show that the persistence diagram $\mathfrak{Dgm}(V[\mathbb{X}_n, \mathbf{d}_{n,Q}])$ is both a computationally efficient and statistically near-optimal estimator of $\mathfrak{Dgm}(V[\mathbb{X}])$ (Theorem 6.2).
- (IV) Next, in a sensitivity analysis framework, we quantify the gain in robustness achieved when using the $\mathbf{d}_{n,Q}$ -weighted filtrations vis-à-vis its non-robust \mathbf{d}_n -weighted counterpart; (Theorem 7.1).
- (V) Lastly, we propose a data-driven procedure for adaptively selecting the tuning parameter Q using Lepski’s method. For the data-driven choice \hat{Q} , we show that the resulting estimator $\mathfrak{Dgm}\{V[\mathbb{X}_n, \mathbf{d}_{n,\hat{Q}}]\}$ is also minimax optimal up to a $\log n$ factor (Theorem 8.1).

1.2. Related Work

Several approaches have been proposed in existing literature to overcome the sensitivity of persistence diagrams to noise. The prevailing ideas in these approaches rely on constructing a filter function, $f_{\mathbb{P}}$, which reflects both the topological information and the distribution of mass underlying the support $\text{supp}(\mathbb{P}) = \mathbb{X}$. Replacing the population probability measure \mathbb{P} with the empirical measure \mathbb{P}_n associated with the samples \mathbb{X}_n results in an empirical estimator $f_{\mathbb{P}_n}$. Some notable examples include the distance-to-measure (Chazal et al., 2011), the kernel distance (Phillips et al., 2015), and kernel density estimators (Fasy et al., 2014; Vishwanath et al., 2020).

While these approaches mitigate, to some extent, the influence of noise on the resulting persistence diagrams, they are not without their drawbacks. For starters, while it may be argued that $\mathfrak{Dgm}(V[f_{\mathbb{P}_n}])$ is more resilient to noise, ultimately, this sample estimator corresponds to the population quantity $\mathfrak{Dgm}(V[f_{\mathbb{P}}])$, which may, nevertheless, omit some subtle geometric and topological features present in $\mathfrak{Dgm}(V[\mathbb{X}])$. Furthermore, from a statistical perspective, if \mathbb{X}_n comprises only $n - m$ points from \mathbb{P} and the remaining m points constitute outliers, then the sample estimator $V[f_{\mathbb{P}_n}]$, obtained using \mathbb{X}_n , will no longer be a valid estimator of the population quantity $\mathfrak{Dgm}(V[f_{\mathbb{P}}])$ which we wish to infer.

Lastly, the exact computation of these estimators can be prohibitively expensive, if not impossible in practice. For instance, the exact computation of the distance-to-measure requires computing an order- k Voronoi diagram. Moreover, in the general setting, the sublevel/superlevel filtrations arising from these approaches are computed using cubical homology, which relies on a (nuisance) grid resolution parameter. If this resolution is too coarse, then some subtle topological features are affected. On the flipside, if the resolution is too fine, then the accuracy is still impacted, as noted in Fasy et al. (2014). In the high-dimensional setting, cubical homology also falls victim to the curse of dimensionality, i.e., for a fixed grid resolution, the number of simplices in the resulting cubical complex grows exponentially with the dimension of the ambient space.

In order to overcome these computational drawbacks, Buchet et al. (2016) and Anai et al. (2019) propose weighted filtrations, $V[\mathbb{X}_n, f_{\mathbb{X}_n}]$, using power distances. While the weighted filtrations circumvent the need for constructing grid-based approximations, they come at the expense of exact inference, i.e., the weighted filtrations $V[\mathbb{X}_n, f_{\mathbb{X}_n}]$ only approximate $V[f_{\mathbb{X}_n}]$ and do not provide valid statistical inference, even in the absence of outliers.

In order to mitigate the effect of noise, Buchet et al. (2015) propose a method for estimating $V[f_{\mathbb{X}}]$ under a functional noise condition on $f_{\mathbb{X}_n}$ —which encompasses several commonly encountered noise scenarios, e.g., Wasserstein noise and additive Gaussian noise. In a more general setting, Buchet et al. (2018) propose a decluttering algorithm that uses the distance-to-measure to select a subset of the sample points \mathbb{X}_n which are representative of the underlying ground truth \mathbb{X} even when the sample contains outliers. Furthermore, the authors propose a parameter-free variant of the decluttering algorithm which can provably recover the ground truth under some weak-uniformity assumptions. A comprehensive study of these methods is outlined in the PhD thesis of Buchet (2014). Our proposed methodology can be seen as an analogue of the parameter-free decluttering algorithm, which comes with certifiable statistical

guarantees. In a similar vein, Br echeteau and Levrard (2020) propose a K -points approximation of the distance-to-measure, which produces a coresets of K points that can closely approximate the distance-to-measure of the original sample, and noticeably reduces the computational time when $K \ll n$. The authors also propose a trimmed heuristic that is resilient to noise. This is further extended by Br echeteau (2020) where the coresets of K -points approximates the sublevel sets of the distance-to-measure using unions of ellipsoids as opposed to isotropic balls.

On a similar note, Vishwanath et al. (2020) proposed robust persistence diagrams which are resilient to outliers using kernel density estimators (KDE), and also proposed a framework for characterizing the sensitivity to outliers using an analogue of influence functions. Although Vishwanath et al. (2020, Theorem 1) describes the gain in robustness by considering the robust KDE $f_{\rho,\sigma}^n$ using the persistence influence function, Theorems 2 & 3 of the same work establish that as $n \rightarrow \infty$ and $\sigma \rightarrow 0$, the persistence diagram $\mathfrak{Dgm}(f_{\rho,\sigma}^n)$ recovers the same information which underlies the sample points \mathbb{X}_n . However, if the underlying distribution is contaminated, e.g., $\mathbb{P} = (1 - \pi)\mathbb{P}^* + \pi\mathbb{Q}$, then the topological inference we hope to target is that of \mathbb{P}^* and not that of \mathbb{P} .

Finally, with a similar objective of mitigating the impact of noise in topological inference, recent approaches have considered multi-parameter persistent homology as a robust tool for inferring the topological features underlying \mathbb{X}_n (Carlsson and Zomorodian, 2009). While some recent results have demonstrated some promise (e.g., Vipond et al., 2021), they are, nevertheless, computationally infeasible for most applications, in addition to being hard to interpret (Otter et al., 2017; Bjerkevik et al., 2020).

On the statistical front, founded on the seminal works of Tukey (1960) and Huber (1964), robust statistics has witnessed renewed interest (Diakonikolas et al., 2017). In particular, the classical problem of mean and covariance estimation has been revisited in several works (Audibert and Catoni, 2011; Minsker, 2015; Devroye et al., 2016; Joly and Lugosi, 2016) with the objective of easing model assumptions to, either, the regularity of the data generating mechanism, or, the presence of outliers. See Lugosi and Mendelson (2019a) for a recent survey. In this regard, median-of-means (MoM) estimators—originally introduced by Nemirovskij and Yudin (1983)—and the broader median-of-means principle (Lecue and Lerasle, 2020) have emerged as powerful tools for "robustifying" existing estimators in near-linear time. Although this comes slightly at the expense of statistical optimality, median-of-means estimators are, nevertheless, easier to compute than statistically optimal *and* robust methods such as the tournament estimators introduced by (Lugosi and Mendelson, 2019b). Audibert and Catoni (2011) showed that, in the univariate setting, the MoM estimator achieves sub-Gaussian rates of convergence for heavy tailed data. Minsker (2015) and Devroye et al. (2016) extend these results to the multivariate setting by considering the geometric median. The MoM idea has subsequently been extended in several other directions, e.g., U-statistics Joly and Lugosi (2016), kernel mean embeddings Lerasle et al. (2019) and general M-estimators Lecue and Lerasle (2020) among others. Most importantly, these extensions move away from the heavy-tailed framework and provide significant insights on how MoM estimators can overcome the second relaxation, i.e., estimation in the presence of outlying contamination.

1.3. Organization

The remainder of this paper is organized as follows. In Section 2 we present the necessary background on persistent homology. We first introduce the proposed methodology in Section 4, and then present the main results in the remainder of the section. We establish the statistical properties of the proposed estimator in Section 5, and we present the influence analysis in Section 7. Numerical results supporting the theory are provided in Appendix 9. The proofs of all the results are collected in the Appendix B of the Supplementary Material.

2. Preliminaries

The following subsections introduce the essential ingredients used for the remaining of the paper.

2.1. Definitions and Notations

For $n \in \mathbb{Z}_+$, we use the notation $[n] = \{1, 2, \dots, n\}$, and for real-valued functions f and g we employ the notation $f(n) \lesssim g(n)$ if $f(n) = O(g(n))$. The closed ball of radius r centered at $\mathbf{x} \in \mathbb{R}^d$ is denoted $B(\mathbf{x}, r)$. For a compact set $\mathbb{X} \subset \mathbb{R}^d$, the r -offset of \mathbb{X} is given by

$$\mathbb{X}(r) = \bigcup_{\mathbf{x} \in \mathbb{X}} B(\mathbf{x}, r).$$

The distance function w.r.t. the compact set \mathbb{X} plays a central role in extracting the geometric and topological features underlying \mathbb{X} .

Definition 2.1 (Distance function). *For a compact set $\mathbb{X} \subseteq \mathbb{R}^d$, the distance function to the set \mathbb{X} , denoted as $d_{\mathbb{X}}$, is given by*

$$d_{\mathbb{X}}(\mathbf{y}) \doteq \inf_{\mathbf{x} \in \mathbb{X}} \|\mathbf{x} - \mathbf{y}\|, \quad \text{for all } \mathbf{y} \in \mathbb{R}^d.$$

For a finite collection of points \mathbb{X}_n , the distance function $d_{\mathbb{X}_n}$ is simply denoted as d_n . For two compact sets $\mathbb{X}, \mathbb{Y} \subset \mathbb{R}^d$ the *Hausdorff distance* between \mathbb{X} and \mathbb{Y} is given by

$$H(\mathbb{X}, \mathbb{Y}) \doteq \inf \left\{ \epsilon > 0 : \mathbb{X} \subseteq \mathbb{Y}(\epsilon), \mathbb{Y} \subseteq \mathbb{X}(\epsilon) \right\} = \|d_{\mathbb{X}} - d_{\mathbb{Y}}\|_{\infty},$$

and metrizes the space of all compact subsets of $(\mathbb{R}^d, \|\cdot\|)$. While results here should extend to general metric spaces (\mathcal{M}, ρ) with simple modifications along the lines of Chazal et al. (2015b) and Buchet et al. (2016), we assume that $(\mathcal{M}, \rho) = (\mathbb{R}^d, \|\cdot\|)$ throughout the paper.

$\mathcal{P}(\mathbb{X})$ denotes the set of Borel probability measures defined on \mathbb{R}^d with support $\mathbb{X} \subseteq \mathbb{R}^d$, and for $\mathbf{x} \in \mathbb{R}^d$, $\delta_{\mathbf{x}}$ is used to denote a Dirac measure at \mathbf{x} . A key assumption used throughout the paper is a regularity condition for the data-generating mechanism. For $a, b > 0$, the probability measure satisfies the (a, b) -standard condition if

$$\mathbb{P}\left(B(\mathbf{x}, r)\right) \geq 1 \wedge ar^b \quad \text{for all } r \geq 0, \text{ and for all } \mathbf{x} \in \text{supp}(\mathbb{X}). \quad (1)$$

We denote by $\mathcal{P}(\mathbb{X}, a, b)$ the subset of $\mathcal{P}(\mathbb{X})$ which satisfies the (a, b) -standard condition in Eq. (1) for $a, b > 0$. This regularity assumption is standard in the domain of geometric and topological inference (e.g., Cuevas and Rodríguez-Casal, 2004; Chazal et al., 2015b,a, 2017). For instance, if b is an integer and \mathbb{X} is a b -dimensional submanifold with positive reach, then $\mathcal{P}(\mathbb{X}, a, b)$ consists of probability measures supported on \mathbb{X} which admit a density with respect to the b -dimensional Hausdorff measure which is lower bounded by $O(a)$. Throughout the paper, we assume that the samples \mathbb{X}_n are obtained in an adversarial contamination setting (\mathcal{S}), as defined below.

Sampling Setting (\mathcal{S}). The data comprises of n samples $\mathbb{X}_n = \{\mathbf{X}_1, \dots, \mathbf{X}_n\}$, where for a collection $\mathcal{O} \subset [n]$ with $|\mathcal{O}| = m < n/2$, the samples $\mathbb{Y}_m = \{\mathbf{X}_i : i \in \mathcal{O}\}$ are contaminated with arbitrary outliers. No distributional assumption is made on these outliers. The remaining $n - m$ samples, $\mathbb{X}_{n-m}^* = \{\mathbf{X}_i : i \in \mathcal{O}^c\}$, are assumed to be observed i.i.d. from a distribution $\mathbb{P} \in \mathcal{P}(\mathbb{X}, a, b)$, for compact $\mathbb{X} \subset \mathbb{R}^d$ and $a, b > 0$.

A glossary of notations for additional definitions and notations introduced in the subsequent sections is provided in Table 3 of the Supplementary Material.

2.2. Background on Persistent Homology

In this section, we provide the necessary background on persistent homology. A detailed background is provided in Appendix A, and we refer the reader to Chazal and Michel (2017); Edelsbrunner and Harer (2010) for a comprehensive introduction.

Given a compact set \mathbb{X} , the building block of any topological data analysis pipeline to extract meaningful information from \mathbb{X} begins with a nested sequence of filtered topological spaces called a filtration, simply denoted by V . The sequence of spaces is parametrized by a resolution parameter t . There are several approaches for constructing filtrations using \mathbb{X} . One approach is to consider the collection of offsets built on top of \mathbb{X} , i.e., $V^t = V^t[\mathbb{X}] = \mathbb{X}(t)$. For $s < t$, the offsets are nested $V^s \subseteq V^t$, and $V[\mathbb{X}] \doteq \{V^t[\mathbb{X}] : t \in \mathbb{R}\}$ is a nested sequence of topological spaces and defines the filtration built using the offsets of \mathbb{X} .

The second approach to constructing a filtration is using a filter function $f_{\mathbb{X}} : \mathbb{R}^d \rightarrow \mathbb{R}$ which carries the topological information underlying \mathbb{X} . In this scenario, one typically constructs the filtration from the sublevel sets associated with $f_{\mathbb{X}}$, given by $V^t = f_{\mathbb{X}}^{-1}((-\infty, t])$ for each resolution t . Again, for $s < t$, $V^s[f_{\mathbb{X}}] \subseteq V^t[f_{\mathbb{X}}]$ and the sequence $V[f_{\mathbb{X}}] = \{V^t[f_{\mathbb{X}}] : t \in \mathbb{R}\}$ constitutes the sublevel filtration from $f_{\mathbb{X}}$. Mutatis mutandis a similar notion holds for the superlevel filtration.

In general, the filtration $V[\mathbb{X}]$ can be very different from $V[f_{\mathbb{X}}]$, although the prevailing objective is for $V[f_{\mathbb{X}}]$ to encode the same information as in $V[\mathbb{X}]$. In this context, the distance function $d_{\mathbb{X}}$ plays a special role owing to the fact that its sublevel filtration is the same filtration associated with the offsets, i.e., $V[d_{\mathbb{X}}] = V[\mathbb{X}]$. This fact plays an important role in motivating the MoM Dist estimator introduced in Section 4, and follows by noting that for every resolution $t > 0$, $d_{\mathbb{X}}^{-1}((-\infty, t]) = \{\mathbf{x} \in \mathbb{R}^d : d_{\mathbb{X}}(\mathbf{x}) \leq t\} = \bigcup_{\mathbf{x} \in \mathbb{X}} B(\mathbf{x}, t)$.

For general f , one can hope to get the best of both worlds by constructing f -weighted offsets as follows. For a *power parameter* $p \geq 1$, the f -weighted radius at \mathbf{x} is given by

$$r_{f,\mathbf{x}}(t) \doteq \begin{cases} (t^p - f(\mathbf{x})^p)^{1/p} & \text{if } t \geq f(\mathbf{x}) \\ -\infty & \text{if } t < f(\mathbf{x}), \end{cases} \quad (2)$$

and $B_f(\mathbf{x}, t) \doteq \{\mathbf{y} \in \mathbb{R}^d : \|\mathbf{x} - \mathbf{y}\| \leq r_{f,\mathbf{x}}(t)\}$ is the *weighted ball of resolution t at \mathbf{x}* . For a single resolution t , each $B_f(\mathbf{x}, t)$ is a Euclidean ball with a different radius determined by Eq. (2). The f -weighted offset at resolution t is then given by,

$$V^t[\mathbb{X}, f] \doteq \bigcup_{\mathbf{x} \in \mathbb{X}} B_f(\mathbf{x}, t).$$

See Figure 9 for an illustration. On the one hand, if $f(\mathbf{x}) = 0$ for all $\mathbf{x} \in \mathbb{X}$, as is the case with $d_{\mathbb{X}}$, then the f -weighted offsets reduce to the usual offsets $V^t[\mathbb{X}]$. On the other hand, if $\mathbb{X} = \mathbb{R}^d$, then the f -weighted offsets coincide with the sublevel sets $V^t[f]$.

Let $V = \{V^t : t \in \mathbb{R}\}$ denote a generic filtration. The set V^t encodes meaningful topological features at each resolution t , e.g., connected components, loops, holes, etc. Formally, this information is “stored” in the homology groups $\mathbb{V}^t = H_k(V^t)$, which are vector spaces. The basic idea of persistent homology is that as the resolution parameter t varies, the topological features evolve, and this evolution can be captured by examining the linear maps between vector spaces in \mathbb{V}^t . Roughly speaking, the collection $\mathbb{V} = \{\mathbb{V}^t : t \in \mathbb{R}\}$ constitutes a persistence module. See Figure 1. Imagine observing \mathbb{V}^t as t varies continuously; one of three things can happen: (1) the topology of \mathbb{V}^t is identical to that at t^+ and t^- , (2) at $t \equiv t_b$, \mathbb{V}^t contains an additional topological feature not present at t^- , or, (3) at $t \equiv t_d$, \mathbb{V}^t contains a feature which disappears at t^+ . In the last two cases, t_b and t_d are known as the birth/death times of a topological feature. A *persistence diagram*, given by

$$\mathfrak{Dgm}(\mathbb{V}) \doteq \{(t_b, t_d) \in \mathbb{R}^2 : \exists \text{ a feature born at } t_b \text{ and dies at } t_d\},$$

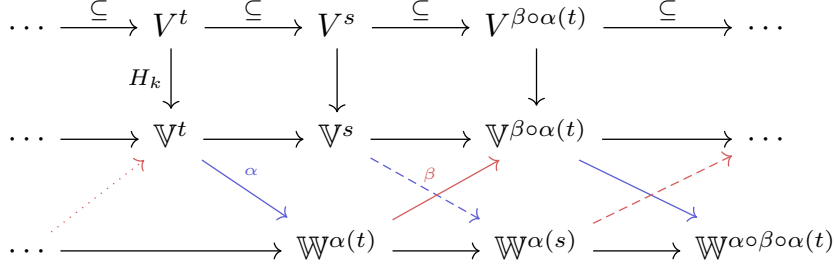


Figure 1: Informal illustration of interleaving of persistence modules. Here $s \leq t$ and $t \leq (\beta \circ \alpha)(s)$ for two nondecreasing maps α, β . See Appendix A.1 for a formal definition.

is obtained by pairing the birth/death times of all topological features in \mathbb{W} . Since $t_b < t_d$, persistence diagrams are multisets supported on the upper half-plane $\Omega = \{(x, y) : x \leq y\}$.

2.3. Interleaving and Bottleneck distance

Given persistence modules $\mathbb{V} = \{\mathbb{V}^t : t \in \mathbb{R}\}$ and $\mathbb{W} = \{\mathbb{W}^t : t \in \mathbb{R}\}$, there is a natural way to measure the similarity between them by considering two nondecreasing maps, $\alpha(t)$ and $\beta(t)$. In particular, if α and β form well-defined criss-crossing maps between \mathbb{V} and \mathbb{W} , as shown in Figure 1, for all $s \leq t$, then \mathbb{V} and \mathbb{W} are said to be (α, β) -interleaved.

When the interleaving maps α and β are *additive* and *identical*, i.e., $\alpha(t) = \beta(t) = t + \epsilon$, such maps induce a pseudometric on persistence modules and, from the isometry theorem (Chazal et al., 2016), a metric on persistence diagrams, referred to as the *bottleneck distance*,

$$W_\infty(\mathfrak{Dgm}(\mathbb{V}), \mathfrak{Dgm}(\mathbb{W})) \doteq \inf \left\{ \epsilon > 0 : \mathbb{V} \text{ and } \mathbb{W} \text{ are } (\alpha, \alpha)\text{-interleaved for } \alpha : t \mapsto t + \epsilon \right\}.$$

The bottleneck distance provides an avenue to study perturbations of persistence diagrams based on the input data, and is summarized in the following stability result. The stability of sublevel filtrations and unweighted offsets is due to Cohen-Steiner et al. (2007) and Chazal et al. (2016), whereas the stability of the f -weighted filtrations is due to Buchet et al. (2016) and Anai et al. (2019).

Proposition 2.1 (Stability of persistence diagrams). *For two compact sets $\mathbb{X}, \mathbb{Y} \subset \mathbb{R}^d$,*

$$W_\infty(\mathfrak{Dgm}(\mathbb{V}[\mathbb{X}]), \mathfrak{Dgm}(\mathbb{V}[\mathbb{Y}])) \leq H(\mathbb{X}, \mathbb{Y}).$$

Furthermore, given two filter functions $f, g : \mathbb{R}^d \rightarrow \mathbb{R}$,

$$W_\infty(\mathfrak{Dgm}(\mathbb{V}[\mathbb{X}, f]), \mathfrak{Dgm}(\mathbb{V}[\mathbb{X}, g])) \leq \|f - g\|_\infty.$$

Additionally, given $h : \mathbb{X} \cup \mathbb{Y} \rightarrow \mathbb{R}_+$, if h is L -Lipschitz and $H(\mathbb{X}, \mathbb{Y}) \leq \epsilon$, then

$$W_\infty(\mathbb{V}[\mathbb{X}, h], \mathbb{V}[\mathbb{Y}, h]) \leq \epsilon(1 + L^p)^{1/p}.$$

The stability of persistence diagrams guarantees that small changes in the function f or the underlying data \mathbb{X} result in small changes in the persistence diagrams, and is a key ingredient in establishing statistical guarantees. However, as noted in Section 1, stability is insufficient to guarantee robustness, and this will form the starting point for our analysis in Section 4.

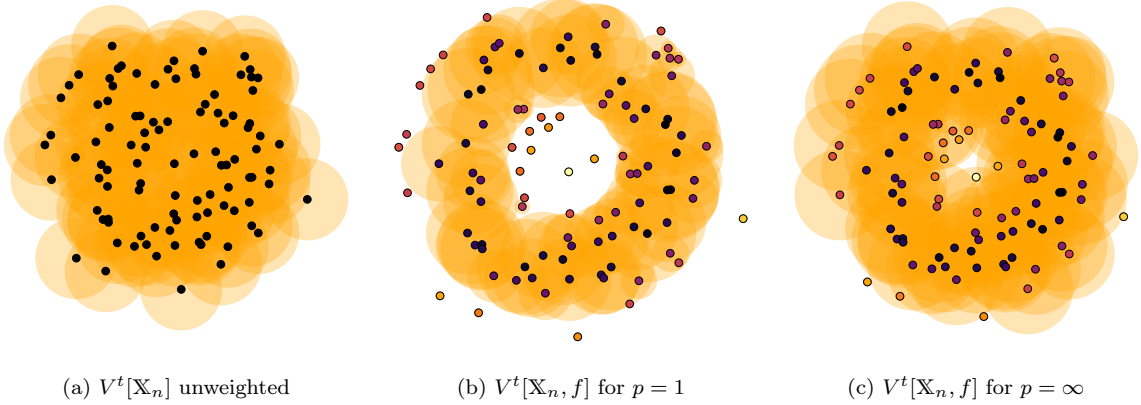


Figure 2: Illustration of offsets for $t = 0.5$ and $f(\mathbf{x}) = \inf_{\mathbf{y} \in S^1} \|\mathbf{x} - \mathbf{y}\|$.

3. Estimation thresholds under adversarial contamination

Let $\mathbb{X}_n = \{\mathbf{X}_1, \mathbf{X}_2, \dots, \mathbf{X}_n\} \subset \mathbb{R}^d$ be a sample of n observations. We assume that the samples are obtained under-sampling setting (\mathcal{S}). We emphasize that this setting encompasses the following scenarios:

- (a) The samples \mathbb{X}_n are obtained i.i.d. from $\mathbb{P} \in \mathcal{P}(\mathbb{X}, a, b)$ for compact $\mathbb{X} \subset \mathbb{R}^d$.
- (b) Samples $\{\mathbf{X}_1^*, \dots, \mathbf{X}_n^*\}$ are first obtained i.i.d. from $\mathbb{P} \in \mathcal{P}(\mathbb{X}, a, b)$, and for a collection $\mathcal{O} \subset [n]$ of size $|\mathcal{O}| = m < n/2$, an adversary is free to replace $\{\mathbf{X}_i^* : i \in \mathcal{O}\}$ with any points $\{\mathbf{Y}_i : i \in \mathcal{O}\}$ of their choice. Then, $\mathbb{X}_n = \{\mathbf{X}_i^* : i \in \mathcal{O}^c\} \cup \{\mathbf{Y}_i : i \in \mathcal{O}\}$ is shuffled and handed over to the topologist for inference, who has no prior knowledge of the original samples or the collection \mathcal{O} .

The central objective is to derive a statistically optimal and computationally efficient estimator of $\mathfrak{Dgm}(\mathbb{V}[\mathbb{X}])$ which is robust to the misspecification scenarios detailed above, using the samples \mathbb{X}_n . It is, therefore, instructive to first consider the estimation thresholds for persistence diagrams under adversarial contamination. To this end, we adopt the minimax framework. Specifically, given $\mathbb{X}_n = \mathbb{X}_{n-m}^* \cup \mathbb{Y}_m$ obtained under sampling setting (\mathcal{S}), i.e., \mathbb{X}_{n-m}^* is observed i.i.d. from $\mathbb{P} \in \mathcal{P} \equiv \mathcal{P}(\mathbb{X}, a, b)$ and \mathbb{Y}_m are the outliers, the minimax risk is given by

$$\mathfrak{R}_{n,m}(\mathcal{P}) = \inf_{\widehat{D}_n} \sup_{\mathbb{P} \in \mathcal{P}} \sup_{\mathbb{Y}_m} \mathbb{E}_{\mathbb{P}} \left[W_{\infty} \left(\widehat{D}_n, \mathfrak{Dgm}(\mathbb{V}[\mathbb{X}]) \right) \right], \quad (3)$$

where the infimum is taken over all persistence diagram estimators \widehat{D}_n based on the sample \mathbb{X}_n , and the expectation is taken over the randomness in $\mathbb{X}_{n-m}^* \sim \mathbb{P}$. The minimax risk $\mathfrak{R}_n(\mathcal{P})$ quantifies the best achievable performance of any estimator in estimating the target population quantity $\mathfrak{Dgm}(\mathbb{V}[\mathbb{X}])$ under the sampling setting (\mathcal{S}). The following result establishes a minimax lower bound for the estimation of persistence diagrams under adversarial contamination.

Theorem 3.1 (Minimax lower bound). *For $a > 0$ and $b \in [d]$, suppose $\mathbb{X}_n = \mathbb{X}_{n-m}^* \cup \mathbb{Y}_m$ is obtained under sampling setting (\mathcal{S}). Then,*

$$\mathfrak{R}_{n,m}(\mathcal{P}) \gtrsim \left(\frac{m}{2n-m} \right)^{1/b} \vee \left(\frac{\log n}{n} \right)^{1/b}. \quad (4)$$

Moreover, if $m \equiv m_n = cn^{\epsilon}$ for $0 < \epsilon < 1$ and $c > 0$, then

$$\mathfrak{R}_{n,m}(\mathcal{P}) \gtrsim \left(\frac{1}{n^{1-\epsilon}} \right)^{1/b}. \quad (5)$$

In other words, Theorem 3.1 establishes that the minimax rate of convergence roughly depends on the fraction of points from the true signal to the number of outliers, and, therefore, in the regime where $n, m \rightarrow \infty$ and $m = o(n)$, the rate of convergence is attenuated by a factor $\asymp (m/n)^{1/b}$. In the absence of outliers, i.e., when $m = 0$, and when b is an integer, Theorem 5 of Chazal et al. (2015b) shows that the minimax rate has a necessary $\log n$ factor, and we believe that the same should hold true in the presence of outliers in Eq. (5). In what follows, we present an estimator to obtain outlier robust persistence diagrams whose statistical performance is guaranteed to be minimax-optimal up to a logarithmic factor.

4. Empirical distance function using the Median-of-Means principle

In the following section, we present an estimator to obtain outlier robust persistence diagrams. Its statistical properties along with the influence analysis are presented in Sections 5–7. In Section 8 we present a method for adaptively calibrating the tuning parameter using a data-driven procedure. To this end, the MoM Distance (MoM Dist) function $\mathbf{d}_{n,Q}$ is defined as follows.

Definition 4.1 (MoM Dist). *Given a collection of points $\mathbb{X}_n \subset \mathbb{R}^d$ and $1 \leq Q \leq n$, let $\{S_1, S_2, \dots, S_Q\}$ be a partition of \mathbb{X}_n into Q disjoint blocks, such that each subset $S_q \subset \mathbb{X}_n$ comprises of $|S_q| = \lfloor n/Q \rfloor$ samples¹. The MoM distance function $\mathbf{d}_{n,Q} : \mathbb{R}^d \rightarrow \mathbb{R}_{\geq 0}$ is defined to be*

$$\mathbf{d}_{n,Q}(\mathbf{y}) \doteq \text{median} \left\{ \mathbf{d}_{n,S_q}(\mathbf{y}) : q \in [Q] \right\} = \text{median} \left\{ \inf_{\mathbf{x} \in S_q} \|\mathbf{x} - \mathbf{y}\| : q \in [Q] \right\}. \quad (6)$$

The proposed outlier robust persistence diagram $\mathfrak{Dgm}(V[\mathbb{X}_n, \mathbf{d}_{n,Q}])$ is then obtained using $\mathbf{d}_{n,Q}$ -weighted filtration $V[\mathbb{X}_n, \mathbf{d}_{n,Q}]$.

Remark 4.1. *Without loss of generality, and for convenience of the theoretical analysis we assume that Q is odd; in this case, the median in Eq. (6) is realized by a unique $q \in [Q]$. In practice, if Q is even, then, as per convention, the median can be taken as the average of the two middle values. Note that we recover the usual empirical distance function, i.e., $\mathbf{d}_{n,1} \equiv \mathbf{d}_n$ when $Q = 1$.*

Remark 4.2. *For each block S_q , distance function $\mathbf{d}_{n,q} \in \mathcal{F}(\mathbb{R}^d)$ can be viewed as the Kuratowski embedding of S_q (Lim et al., 2020, pg. 4). The most natural generalization of the multivariate median-of-means estimators proposed by Minsker (2015) and Lerasle et al. (2019) would suggest the following estimator as the natural candidate for MoM Dist:*

$$\tilde{\mathbf{d}}_{n,Q} = \arg \inf_{f \in \mathcal{F}(\mathbb{R}^d)} \sum_{q=1}^Q \|f - \mathbf{d}_{n,S_q}\|_{\infty},$$

where the median under consideration corresponds to the geometric median in $L_{\infty}(\mathbb{R}^d)$. Although $\tilde{\mathbf{d}}_{n,Q}$ has its appeal from a theoretical perspective, the computation of $\tilde{\mathbf{d}}_{n,Q}$ involves an infinite-dimensional optimization problem, making it infeasible in practice. In contrast, the proposed estimator in Definition 4.1, is a pointwise median-of-means estimator with a tractable computational cost. This has the promise of being highly modular, and widely applicable in many practical settings. The technical difficulty arises in showing that the pointwise estimator $\mathbf{d}_{n,Q}$ achieves an exponential concentration bound around $\mathbf{d}_{\mathbb{X}}$ in the $L_{\infty}(\mathbb{R}^d)$ metric.

Similar to the proposed methodology in Definition 4.1, the procedure of partitioning the data \mathbb{X}_n into smaller subsets, and then aggregating them as an estimator of persistent homology has been shown to satisfy several favorable properties by Solomon et al. (2021) and Gómez and Mémoli (2021), albeit in a different context. We argue that a similar principle, in our setting, also leads to provably robust estimators.

¹ Without loss of generality, we may assume that n is divisible by Q , so that $n/Q \in \mathbb{Z}_+$

Table 1: Comparison of computational complexity for robust weighted filtrations.

Method	Pre-processing	Evaluation	Provably robust?
$V[\mathbb{X}_n, \mathbf{d}_{n,Q}]$ (MoM Dist-filtration)	$O(n/Q \cdot \log(n/Q))$	$O(n \cdot (Q + \log n/Q))$	Yes
$V[\mathbb{X}_n, \delta_{n,k}]$ (Anai et al., 2019, DTM-filtration)	$O(n \log n)$	$O(kn \log n)$	Sometimes
$V[\mathbb{X}_n, f_\sigma^n]$ (Vishwanath et al., 2020, RKDE-filtration)	$O(n^2 \ell)$	$O(n^2)$	Sometimes
$V[\mathbb{X}_n, \mathbf{C}_K]$ (Bréchet et al., 2020, K -PDTM)	$O(nKL)$	$O(kK \log K)$	Sometimes

$n = \#$ samples, $Q = \#$ blocks, $k = \lfloor mn \rfloor =$ DTM parameter,
 $\ell = \#$ iterations of KIRWLS algorithm, $K = \#$ centroids, $L = \#$ iterations for K -PDTM.

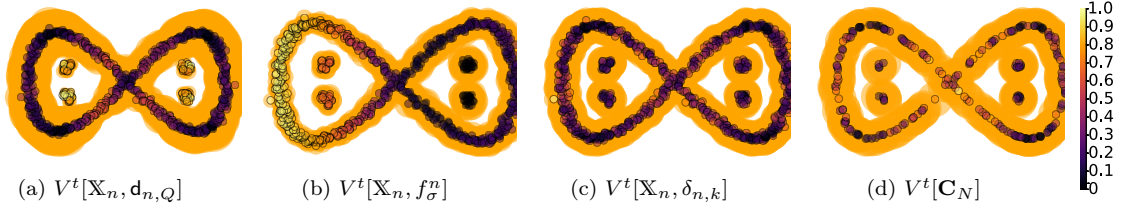


Figure 3: \mathbb{X}_n with $n = 620$ points from a Lemniscate with $m = 80$ outliers. Illustration of the robust weighted filtrations with $p = 1$ for MoM Dist $V^t[\mathbb{X}_n, \mathbf{d}_{n,Q}]$, RKDE $V^t[\mathbb{X}_n, f_\sigma^n]$, DTM $V^t[\mathbb{X}_n, \delta_{n,k}]$, and the K -PDTM $V^t[\mathbf{C}_N]$ filtration.

4.1. Computational considerations

The first step in constructing the f -weighted filtration involves estimating the weights for the sample points, $w_i = f(\mathbf{X}_i)$ for all $i \in [n]$. Once this is done, the complexity of constructing the filtration $V[\mathbb{X}_n, f]$ does not depend on the specific choice of f . Table 1 compares the complexities of four filtrations: (i) MoM Dist $\mathbf{d}_{n,Q}$, (ii) robust kernel density estimator f_σ^n (RKDE, Vishwanath et al., 2020), (iii) distance-to-measure $\delta_{n,k}$ (DTM, Anai et al., 2019), and (iv) K -Power Distance-to-measure $\delta_{n,k,K}$ (K -PDTM, Bréchet et al., 2020). For a test point $\mathbf{x} \in \mathbb{R}^d$, distances to blocks S_q are efficiently computed using a k -d tree with pre-processing time $O(|S_q| \log |S_q|)$ per block where $|S_q| = n/Q$. This operation can be parallelized, and the overall pre-processing can be achieved in $O(|S_q| \log |S_q|)$ time. Thereafter, $O(\log |S_q|)$ time is needed for a single query (Cormen et al., 2009, Chapter 10). The results for each block $q \in [Q]$ are then aggregated to compute the median, which takes an additional $O(Q)$ time per query. This results in a total evaluation time of $O(n \cdot (Q + \log |S_q|))$ for n samples.

The DTM with parameter m involves finding the k th nearest neighbor for $k = \lfloor mn \rfloor$, also optimized with a k -d tree, leading to a total complexity of $O(n \log n)$ for pre-processing and $O(n \cdot k \log n)$ for evaluation. The RKDE requires $O(n^2)$ time per iteration of the KIRWLS algorithm, with a total of $O(n^2 \ell)$ for ℓ iterations. Thereafter, the RKDE weights may be used to evaluate each query in $O(n)$ time. The K -PDTM constructs a quantized dataset via Lloyd’s algorithm, with each iteration requiring K comparisons to each of the N points, resulting in $O(nKL)$ time across L iterations, and outputs K points. Typically, $L = O(n)$ iterations suffice. The trimmed variant of the K -PDTM shares the same preprocessing cost and produces a subset of \mathbb{X}_n containing $n\alpha < n$ points, where $\alpha \in (0, 1)$ is a user-specified tuning parameter for the fraction of inliers. If $K \ll n$ or $\alpha \ll 1$, the K -PDTM and its trimmed variant offer significant speed-ups compared to weighted filtrations. The four filtrations are illustrated in Figure 3. A comparison of the computational and memory trade-offs are summarized in Table 2 for the experiment in Section 9.4.

We conclude this section with the following property of the MoM Dist function.

Lemma 4.1. *Given samples $\mathbb{X}_n = \{\mathbf{X}_1, \mathbf{X}_2, \dots, \mathbf{X}_n\}$ and $Q < n$,*

$$|\mathbf{d}_{n,Q}(\mathbf{x}) - \mathbf{d}_{n,Q}(\mathbf{y})| \leq \|\mathbf{x} - \mathbf{y}\|, \quad \text{for all } \mathbf{x}, \mathbf{y} \in \mathbb{R}^d.$$

In other words, the MoM Dist function $\mathbf{d}_{n,Q}$ is 1-Lipschitz — a key property for distance-like functions in geometric and topological inference (Boissonnat et al., 2018, Chapter 9).

5. Statistical properties of $\mathbb{V}[\mathbf{d}_{n,Q}]$

We begin our analysis by characterizing the persistence diagrams obtained using the sublevel filtration of $\mathbf{d}_{n,Q}$. The following result (proved in Section B.3), establishes that $\mathfrak{Dgm}(\mathbb{V}[\mathbf{d}_{n,Q}])$ is a statistically consistent estimator of target population quantity $\mathfrak{Dgm}(\mathbb{V}[\mathbb{X}])$ under sampling setting (S), and establishes its rate of convergence in the W_∞ metric.

Theorem 5.1 (Sublevel filtration). *Suppose $\mathbb{P} \in \mathcal{P}(\mathbb{X}, a, b)$ is a probability distribution with support \mathbb{X} satisfying the (a, b) -standard condition and \mathbb{X}_n is obtained under the sampling condition (S). For $2m < Q < n$ and for all $0 < \delta < e^{-(1+b)Q}$,*

$$\mathbb{P} \left\{ W_\infty \left(\mathfrak{Dgm}(\mathbb{V}[\mathbf{d}_{n,Q}]), \mathfrak{Dgm}(\mathbb{V}[\mathbb{X}]) \right) \leq 2\mathfrak{g}(n, Q, a, b) \right\} \geq 1 - \delta, \quad (7)$$

where

$$\mathfrak{g}(n, m, Q, a, b) = \left(\frac{Q \log(n/Q)}{an} + \frac{4Q \log(1/\delta)}{a(Q-2m)n} \right)^{1/b}. \quad (8)$$

Furthermore, if the number of outliers grows with n as $m = cn^\epsilon$ for $c > 0$ and $\epsilon \in [0, 1)$ then for all $Q = Cn^\epsilon$ where $C > 2c$,

$$\mathbb{E} \left[W_\infty \left(\mathfrak{Dgm}(\mathbb{V}[\mathbf{d}_{n,Q}]), \mathfrak{Dgm}(\mathbb{V}[\mathbb{X}]) \right) \right] \lesssim \left(\frac{\log n}{n^{1-\epsilon}} \right)^{1/b}. \quad (9)$$

Remark 5.1. *The following salient observations can be made from Theorem 5.1.*

- (i) *For the rate of convergence in Eq. (9), the dependence of Q with n is implicit through the dependence on m with n and the constraint that $2m < Q$. Given $m = cn^\epsilon$, the optimal choice of Q is obtained when $Q = 3cn^\epsilon$. On the other hand, if m is fixed relative to n , then choosing any fixed $Q > 2m$ yields a convergence rate of $(\log n/n)^{1/b}$, which coincides with the minimax rate for persistence diagram estimation in the absence of outliers (Theorem 3.1). In other words, in the regime where m is fixed relative to n , there is no price to pay for accommodating outliers in the data. Similarly, it becomes apparent that accommodating for more adverse noise conditions comes at the price of an attenuated rate of convergence.*
- (ii) *The two terms appearing in $\mathfrak{g}(n, m, Q, a, b)$ may be interpreted as follows: The first term is similar to the term appearing in Chazal et al. (2015b, Theorem 2) with an effective sample size of n/Q instead of n , which is a consequence of the Median-of-Means procedure. The second term incorporates the desired confidence level adaptive to the volume dimension $b > 0$, with an effective sample size of n/Q . Notably, as the number of outliers m increases, the number of blocks Q must also increase; thereby widening the resulting confidence band.*
- (iii) *The admissible confidence level δ for constructing the confidence band is implicitly dependent on the parameter Q . This phenomenon is unavoidable with estimators based on the median-of-means principle. We refer the reader to Lugosi and Mendelson (2019a, Section 2.4) for a discussion on how robustness must come at the price of the confidence level δ being restricted.*

The proof of Theorem 5.1 relies on Lemma C.1 (in the supplementary material) which allows us to control the deviation of a empirical processes arising from general classes of pointwise median-of-means estimators.

6. Statistical properties of $V[\mathbb{X}_n, \mathbf{d}_{n,Q}]$

In practice, the sublevel filtration $V[\mathbf{d}_{n,Q}]$ cannot be computed exactly, and one must rely on approximations using cubical homology. To this end, we now turn our attention to $\mathbf{d}_{n,Q}$ -weighted filtrations computed on the sample points directly. Before we study the statistical properties of the $\mathbf{d}_{n,Q}$ -weighted filtration, we state the following result which guarantees that the persistence module $\mathbb{V}[\mathbb{X}_n, \mathbf{d}_{n,Q}]$ is sufficiently regular and is amenable to the construction of a persistence diagram².

Lemma 6.1 (Regularity). *For \mathbb{X}_n obtained under sampling setting (S) and $\mathbf{d}_{n,Q}$ defined in Eq. (6), the persistence module $\mathbb{V}[\mathbb{X}_n, \mathbf{d}_{n,Q}]$ is q -tame and pointwise finite-dimensional.*

The proof of Lemma 6.1 is a direct consequence of Anai et al. (2019, Proposition 3.1), and ensures that the persistence diagram $\mathfrak{Dgm}(\mathbb{V}[\mathbb{X}_n, \mathbf{d}_{n,Q}])$ is well-defined. We now turn our attention to the $\mathbf{d}_{n,Q}$ -weighted filtration $V[\mathbb{X}_n, \mathbf{d}_{n,Q}]$. The following result, which establishes an analogue of the stability result for $\mathbf{d}_{n,Q}$ -weighted filtrations, but unlike the stability for the usual distance function \mathbf{d}_n , it is also robust to outliers.

Theorem 6.1 (Stability & robustness of $\mathbf{d}_{n,Q}$ -weighted filtrations). *Let $\mathbb{X}_n = \mathbb{X}_{n-m}^* \cup \mathbb{Y}_m$ be a collection of points obtained under the sampling condition (S). For $Q > 2m$ let $\mathbf{d}_{n,Q}$ be the MoM Dist function computed on the contaminated points \mathbb{X}_n and let \mathbf{d}_{n-m} be the distance function w.r.t. the inliers \mathbb{X}_{n-m}^* . Then*

$$W_\infty \left(\mathfrak{Dgm}(\mathbb{V}[\mathbb{X}_n, \mathbf{d}_{n,Q}]), \mathfrak{Dgm}(\mathbb{V}[\mathbb{X}_{n-m}^*, \mathbf{d}_{n-m}]) \right) \leq \sup_{\mathbf{x} \in \mathbb{X}_{n-m}^*} \mathbf{d}_{n,Q}(\mathbf{x}) + \|\mathbf{d}_{n,Q} - \mathbf{d}_{n-m}\|_\infty + \left(1 - \frac{1}{p}\right) t(\mathbb{X}_{n-m}^*),$$

where

$$t(\mathbb{X}_{n-m}^*) = \inf \left\{ t > 0 : \bigcap_{\mathbf{x} \in \mathbb{X}_{n-m}^*} B_{f,\rho}(\mathbf{x}, t) \neq \emptyset \right\}$$

is the filtration value t at which the inliers the $\mathbf{d}_{n,Q}$ -weighted balls of the inliers \mathbb{X}_{n-m}^* form a connected component. In particular, when $p = 1$ we have

$$W_\infty \left(\mathfrak{Dgm}(\mathbb{V}[\mathbb{X}_n, \mathbf{d}_{n,Q}]), \mathfrak{Dgm}(\mathbb{V}[\mathbb{X}_{n-m}^*, \mathbf{d}_{n-m}]) \right) \leq \sup_{\mathbf{x} \in \mathbb{X}_{n-m}^*} \mathbf{d}_{n,Q}(\mathbf{x}) + \|\mathbf{d}_{n,Q} - \mathbf{d}_{n-m}\|_\infty. \quad (10)$$

Remark 6.1. *The following observations follow from Theorem 6.1.*

- (i) *In contrast to what would follow from Lemma 2.1 (ii) for the standard unweighted filtration, the term appearing in the r.h.s. of Eq. (10) completely eliminates the dependence on the Hausdorff distance between \mathbb{X}_n and \mathbb{X}_{n-m}^* in the $\mathbf{d}_{n,Q}$ -filtration. More generally, the same bound in Theorem 6.1 holds even when $V[\mathbb{X}_n, \mathbf{d}_{n,Q}]$ is replaced by $V[\mathbb{M}, \mathbf{d}_{n,Q}]$ for any set $\mathbb{M} \supseteq \mathbb{X}_{n-m}^*$.*
- (ii) *Notably, $V[\mathbb{X}_n, \mathbf{d}_{n,Q}]$ remains resilient to outliers. To see this, observe that the first term appearing in the r.h.s. of Eq. (10) may be bounded as*

$$\sup_{\mathbf{x} \in \mathbb{X}_{n-m}^*} \mathbf{d}_{n,Q}(\mathbf{x}) = \sup_{\mathbf{x} \in \mathbb{X}_{n-m}^*} |\mathbf{d}_{n,Q}(\mathbf{x}) - \mathbf{d}_{\mathbb{X}}(\mathbf{x})| \leq \|\mathbf{d}_{n,Q} - \mathbf{d}_{\mathbb{X}}\|_\infty,$$

where the first equality follows from the fact that $\mathbf{d}_{\mathbb{X}}(\mathbf{x}) = 0$ for all $\mathbf{x} \in \mathbb{X}_{n-m}^*$. Therefore, from the proof of Theorem 5.1, the r.h.s. of Eq. (10) vanishes with high probability for sufficiently large sample sizes.

² q -tame and pointwise finite dimensional persistence modules result in persistence diagrams whose points in Ω are locally finite.

- (iii) For $p = 1$, a similar analysis for the DTM-filtrations appears in (Anai et al., 2019, Theorem 4.5) and the bottleneck distance is bounded above as

$$W_\infty \left(\mathfrak{Dgm}(V[\mathbb{X}_n, \delta_{n,k}]), \mathfrak{Dgm}(V[\mathbb{X}_{n-m}^*, \delta_{n-m,k}]) \right) \leq \sqrt{\frac{n}{k}} W_2(\mathbb{X}_{n-m}^*, \mathbb{X}_n) + \sup_{\mathbf{x} \in \mathbb{X}_{n-m}^*} \delta_{n-m,k}.$$

While the last term on the r.h.s. converges to the uncontaminated population analogue with high probability, the first term involving the Wasserstein distance $W_2(\mathbb{X}_{n-m}^*, \mathbb{X}_n)$ can be large even for a few extreme outliers. In contrast, the r.h.s. of Eq. (10) converges to zero with high probability with no assumptions on the outliers \mathbb{Y}_m .

- (iv) The power parameter p determines a computational vs. statistical trade-off in Theorem 6.1. When $p = 1$, the $\mathbf{d}_{n,Q}$ -weighted filtration, $V[\mathbb{X}_n, \mathbf{d}_{n,Q}]$, provides a provably good approximation of the underlying signal, $V[\mathbb{X}_{n-m}^*, \mathbf{d}_{n-m}]$. However, as p increases the number of non-trivial points in the filtration $V[\mathbb{X}_n, \mathbf{d}_{n,Q}]$ is non-increasing (Anai et al., 2019, Proposition 8). Therefore, the $\mathbf{d}_{n,Q}$ -weighted persistence diagrams obtained using $V[\mathbb{X}_n, \mathbf{d}_{n,Q}]$ for larger p are sparser than their counterpart when $p = 1$.
- (v) The proof of the result is based on a generalization of the ideas presented in Lemma 4.8 and Proposition 4.9 in Anai et al. (2019) for DTM-filtrations. Lemmas C.2 and C.3 in the supplementary material hold for general f -filtrations which satisfy a certain property, and the proof of Theorem 6.1 follows by showing that $\mathbf{d}_{n,Q}$ satisfies the required property.

With this background, we are now in a position to state our main result, which characterizes the rate of convergence for the $\mathbf{d}_{n,Q}$ -weighted filtration on the contaminated sample points $V[\mathbb{X}_n, \mathbf{d}_{n,Q}]$ to $V[\mathbb{X}]$.

Theorem 6.2 ($\mathbf{d}_{n,Q}$ -weighted filtration). *Let $p = 1$. Suppose $\mathbb{P} \in \mathcal{P}(\mathbb{X}, a, b)$ is a probability distribution with support \mathbb{X} satisfying the (a, b) -standard condition, and $\mathbb{X}_n = \mathbb{X}_{n-m}^* \cup \mathbb{Y}_m$ is obtained under sampling condition (S). Then, for $2m < Q < n$ and for all $\delta \in (0, 1)$,*

$$\mathbb{P} \left\{ W_\infty \left(V[\mathbb{X}_{n-m}^* \cup \mathbb{Y}_m, \mathbf{d}_{n,Q}], V[\mathbb{X}] \right) \leq 2f(n, m, Q, \delta_1, \delta_2) \right\} \geq 1 - \delta,$$

where

$$f(n, m, Q, \delta_1, \delta_2) \doteq 2 \left(\frac{Q \log(n/Q)}{an} + \frac{4Q \log(1/\delta_1)}{a(Q-2m)n} \right)^{1/b} + \left(\frac{\log(n-m)}{a(n-m)} + \frac{4 \log(1/\delta_2)}{a(n-m)} \right)^{1/b},$$

for $\delta_1, \delta_2 \in (0, 1)$ such that $\delta_1 \leq e^{-(1+b)Q}$ and $\delta_1 + \delta_2 = \delta$. In particular, if $m_n = cn^\epsilon$ for $0 \leq \epsilon < 1$, then for all $Q = Cn^\epsilon$ where $C > 2c$,

$$\mathbb{E} \left[W_\infty \left(V[\mathbb{X}_{n-m}^* \cup \mathbb{Y}_m, \mathbf{d}_{n,Q}], V[\mathbb{X}] \right) \right] \lesssim \left(\frac{\log n}{n^{1-\epsilon}} \right)^{1/b}. \quad (11)$$

Remark 6.2. We make the following observations from Theorem 6.2.

- (i) The term appearing in the r.h.s. of Eq. (11) is identical to the term appearing in the r.h.s. of Eq. (8) in Theorem 5.1. Therefore, the $\mathbf{d}_{n,Q}$ -weighted filtration and the $\mathbf{d}_{n,Q}$ sublevel filtration converge to the same population limit with identical convergence rates and match the minimax lower bound from Theorem 3.1 up to a $(\log n)^{1/b}$ factor.
- (ii) The uniform confidence band we obtain from Theorem 6.2 can, in principle, be computed for any confidence level $\delta \in (0, 1)$. However, the restriction on δ_1 makes the confidence band obtained using $V[\mathbb{X}_n, \mathbf{d}_{n,Q}]$ wider than that obtained using Theorem 5.1. This is, ultimately, the price we have to pay for choosing the computationally tractable $\mathbf{d}_{n,Q}$ -weighted filtration as the estimator as opposed to the $\mathbf{d}_{n,Q}$ sublevel filtration.

7. Influence analysis

The statistical analysis in the previous sections establishes that, even in the presence of outliers, as the number of samples increases we can eventually mitigate the effect of the outliers. In this section, we provide a more precise characterization for the influence the outliers have on the resulting $\mathbf{d}_{n,Q}$ -weighted filtrations, in contrast to the non-robust counterpart—the \mathbf{d}_n -weighted filtrations.

Given a probability measure $\mathbb{P} \in \mathcal{P}(\mathbb{X}, a, b)$, Vishwanath et al. (2020, Definition 4.1) characterized the influence an outlier at $\mathbf{x} \in \mathbb{R}^d$ has on a persistence diagram $\mathfrak{Dgm}(\mathbb{V}[f_{\mathbb{P}}])$ —obtained using the sublevel sets of $f_{\mathbb{P}}$ —using the *persistence influence* function

$$\Psi(f_{\mathbb{P}}; \mathbf{x}) \doteq \lim_{\epsilon \rightarrow 0} W_{\infty} \left(\mathfrak{Dgm}(\mathbb{V}[f_{\mathbb{P}^{\epsilon}}]), \mathfrak{Dgm}(\mathbb{V}[f_{\mathbb{P}}]) \right), \quad (12)$$

where $\mathbb{P}^{\epsilon} = (1 - \epsilon)\mathbb{P} + \epsilon\delta_{\mathbf{x}}$ is the perturbation curve w.r.t. \mathbf{x} in the space of probability measures. The persistence influence is a generalization of the influence function in robust statistics (Hampel et al., 2011) to general metric spaces. The analysis in this section is similar in spirit to the analysis based on the persistence influence but differs in two important aspects. First, the $\mathbf{d}_{n,Q}$ -weighted filtration is computed purely on the sample points—by partitioning the samples into Q disjoint blocks—and, therefore, the notion of persistence influence is adapted to the samples, in contrast to Eq. (12), which is based on the data-generating distribution \mathbb{P} . Additionally, unlike the case of the persistence influence function—where the influence of outliers in the resulting persistence diagram is quantified in terms of the bottleneck distance—here we directly examine the influence the outlying point has on the resulting persistence diagram itself. This provides a more tractable interpretation of how outliers impact the resulting topological inference.

With this background, we now introduce the empirical persistence influence framework. Suppose we are given a collection of observations \mathbb{X}_n , which is sampled i.i.d. from a probability distribution \mathbb{P} of interest. Let $\mathfrak{Dgm}(\mathbb{V}[\mathbb{X}_n, f_n])$ be its weighted-Rips persistence diagram, where the weight function f_n is constructed using the samples \mathbb{X}_n . Suppose \mathbb{X}_n is contaminated with $m < \frac{n}{2}$ outliers to obtain the contaminated dataset \mathbb{X}_{n+m} . In particular, we may assume that the m -points are placed at an outlying location \mathbf{x}_0 , i.e.,

$$\mathbb{X}_{n+m} = \mathbb{X}_n \cup \left\{ \bigcup_{j=1}^m \{\mathbf{x}_0\} \right\}, \quad (13)$$

such that the factor m and the location \mathbf{x}_0 together control the relative influence the outliers have. This is similar to the role played by the factor ϵ in the perturbation curve associated with the persistence influence. Note that when $m = 0$, the influence of the outliers is non-existent in the dataset.

Remark 7.1. *Note that, unlike the results in the preceding sections where we assumed that $\mathbb{X}_n = \mathbb{X}_{n-m} \cup \mathbb{Y}_m$ with $(n - m)$ points sampled from \mathbb{P} , here, for ease of exposition, we assume that $\mathbb{X}_{n+m} = \mathbb{X}_n \cup \mathbb{Y}_m$ where n points are sampled from the signal.*

Let $\mathfrak{Dgm}(\mathbb{V}[\mathbb{X}, f_{n+m}])$ be the f_{n+m} -weighted persistence diagram constructed on \mathbb{X}_{n+m} .

In a similar vein, we may characterize the influence the outliers have on the persistence diagrams resulting from the sublevel filtrations as

$$\tilde{\Psi}(W_{\infty}; \mathbb{X}_n, f_n, m, \mathbf{x}_0) = W_{\infty} \left(\mathfrak{Dgm}(\mathbb{V}[f_{n+m}]), \mathfrak{Dgm}(\mathbb{V}[f_n]) \right) \leq \|f_{n+m} - f_n\|_{\infty}. \quad (14)$$

Indeed, when $W_{\infty}(\mathfrak{Dgm}(\mathbb{V}[f_{n+m}]), \mathfrak{Dgm}(\mathbb{V}[f_n]))$ is small, it follows that the persistence diagram $\mathfrak{Dgm}(\mathbb{V}[\mathbb{X}_{n+m}, f_{n+m}])$ is more robust (and vice versa). The following result establishes that, under some mild conditions and with high probability, the $\mathbf{d}_{n,Q}$ -weighted persistence diagrams are more robust than their non-robust counterpart.

Theorem 7.1 (Influence analysis of $\mathbf{d}_{n,Q}$ -weighted filtrations). For \mathbb{X}_n observed i.i.d. from $\mathbb{P} \in \mathcal{P}(\mathbb{X}, a, b)$ and $\mathbf{x}_0 \in \mathbb{R}^d$, let \mathbb{X}_{n+m} be given by Eq. (13). For $2m < Q < n+m$, let \mathbf{d}_{n+m} and $\mathbf{d}_{n+m,Q}$ denote the distance and MoM distance function w.r.t. \mathbb{X}_{n+m} , and let $n_Q = (n+m)/Q$ and $c = \min \{a2^{-(1+2b)}, a2^{-3b}\}$. If

$$\varpi(\mathbf{x}_0) \doteq c \mathbf{d}_{\mathbb{X}}(\mathbf{x}_0)^b > \frac{\log n_Q}{n_Q} + \frac{4(1+b)Q}{n_Q}, \quad (\text{I})$$

then, for all $\delta \in (0, 1)$ satisfying

$$(1+b)Q \leq \log(2/\delta) \leq \frac{n_Q \varpi(\mathbf{x}_0) - \log n_Q}{4}, \quad (\text{II})$$

with probability greater than $1 - \delta$,

$$\|\mathbf{d}_{n+m} - \mathbf{d}_n\|_\infty - \|\mathbf{d}_{n+m,Q} - \mathbf{d}_n\|_\infty \geq \left(\frac{2 \log n_Q}{an_Q} + \frac{8 \log(2/\delta)}{an_Q} \right)^{1/b}.$$

Remark 7.2. The result from Theorem 7.1 may be interpreted as follows.

- (i) When conditions (I) and (II) hold, then with high probability, persistence diagrams obtained using $\mathbf{d}_{n,Q}$ are closer to the truth than those obtained using \mathbf{d}_n . Therefore, the interplay between n , m , and \mathbf{x}_0 is better understood by characterizing when conditions (I) and (II) hold.
- (ii) For fixed n observe that (I) is satisfied whenever $\mathbf{d}_{\mathbb{X}}(\mathbf{x}_0)$ is sufficiently large, i.e., \mathbf{x}_0 is sufficiently far away from the support. On the other hand, if \mathbf{x}_0 is fixed, then (I) is satisfied when $\log n_Q/n_Q$ is sufficiently small, i.e., n is sufficiently large. Together, this implies that for condition (I) to be satisfied, either (a) we need the outliers to be sufficiently well-separated from the support \mathbb{X} such that we are able to distinguish outliers \mathbf{x}_0 from the inliers \mathbb{X}_n , or (b) for outliers placed very close to the support \mathbb{X} we need sufficiently many inliers n for us to be able to distinguish them from the outliers. On the other hand, note that if n and m are fixed, then the r.h.s. of (I) is directly proportional to Q . Although Q can take any values between $2m < Q < (n+m)$, choosing a value of Q much larger than $2m+1$ will likely breach condition (I) for a fixed \mathbf{x}_0 . Equivalently, for a suboptimal choice of Q , we need the outliers to be sufficiently far away from the inliers in order to be able to distinguish them.
- (iii) The l.h.s. of (II) is equivalent to the constraint that $\delta \leq e^{-(1+b)Q}$, which appears in Theorems 5.1 and 6.2. The r.h.s. of (II) specifies a lower bound on the confidence level δ . Condition (I) guarantees that the admissible values of $\delta \in (0, 1)$ satisfying (II) is nonempty. For fixed m, Q and \mathbf{x}_0 , the r.h.s. of (II) is directly proportional to n , i.e., the lower bound vanishes as $n \rightarrow \infty$.
- (iv) When conditions (I) and (II) are satisfied, we have the following lower bound from the l.h.s. of (II):

$$\|\mathbf{d}_{n+m} - \mathbf{d}_n\|_\infty - \|\mathbf{d}_{n+m,Q} - \mathbf{d}_n\|_\infty \gtrsim \left(\frac{\log(n+m/Q)}{a(n+m)/Q} + \frac{Q}{(n+m)/Q} \right)^{1/b}. \quad (15)$$

In the regime when $n, m \rightarrow \infty$, and for the optimal choice of Q , i.e., $Q = km$ for $k > 2$, the r.h.s. of Eq. (15) is non-trivial when $m = \Omega(n^{1/2})$. Therefore, under conditions (I) and (II), when there are sufficiently many outliers, there is greater evidence to support the robustness of $\mathbf{d}_{n,Q}$.

8. Auto-tuning the parameter Q

The result in Theorem 6.2 relies on the crucial assumption that the number of outliers m^* is known *a priori*. While this assumption may hold in certain adversarial settings, in general, this information may be unavailable. In order to make Theorem 6.2 more useful in practical settings, we discuss two solutions for calibrating the parameter Q . The first procedure is based on Lepski's method (Lepski, 1991), which is a powerful data-driven method for adaptive parameter selection. In this case, we also provide theoretical guarantees for the adaptively tuned estimator. The second procedure—which is based on some heuristic observations regarding the sample estimator $\mathbb{V}[\mathbb{X}_n, \mathbf{d}_{n,Q}]$ —works well in practice, and may be used as a precursor to Lepski's method.

When the number of outliers m^* is known, choosing $Q^* = 2m^* + 1$ results in the rate of convergence in Theorem 6.2. However, without access to m^* , Lepski's method provides a systematic procedure for selecting a parameter \hat{Q} which provides the same error guarantees as Q^* (Birgé, 2001). The procedure is as follows. Let m_{\min} and m_{\max} be two coarse bounds on (unknown) m^* such that $m_{\min} \leq m^* \leq m_{\max}$. For a choice of $\theta > 1$, let $m(j) = \theta^j m_{\min}$ and define

$$\mathcal{J} \doteq \left\{ j \geq 1 : m_{\min} \leq m(j) < \theta m_{\max} \right\}.$$

For \mathbb{X}_n obtained under sampling condition (S), let $\mathbb{V}_n(j) = \mathbb{V}[\mathbb{X}_n, \mathbf{d}_{n,Q(j)}]$ be the persistence module obtained using the MoM Dist-weighted filtration with $Q(j) = 2m(j) + 1$.

For $\delta \in (0, 1)$ and $\delta_{\max} = \delta - e^{-(1+b)(2m_{\max}+1)}$, let $\mathfrak{h}(n, m, \delta)$ be defined as follows:

$$\begin{aligned} \mathfrak{h}(n, m, \delta) = & 4 \left(\frac{2m+1}{an} \mathcal{W}_0 \left(\frac{ne^{4(1+b)(2m_{\max}+1)}}{2m+1} \right) \right)^{1/b} \\ & + 2 \left(\frac{1}{a(n-m)} \mathcal{W}_0 \left((n-m)e^{4 \log(1/\delta_{\max})} \right) \right)^{1/b}, \end{aligned} \quad (16)$$

where for $z > 0$, $\mathcal{W}_0(z)$ is the Lambert \mathcal{W}_0 function given by the identity $\mathcal{W}_0(z)e^{\mathcal{W}_0(z)} = z$. With this background, let \hat{j} be the output of the following procedure:

$$\hat{j} \doteq \min \left\{ j \in \mathcal{J} : \mathcal{W}_\infty(\mathbb{V}_n(j), \mathbb{V}_n(j')) \leq 2\mathfrak{h}(n, m(j'), \delta) \quad \text{for all } j' \in \mathcal{J}, j' > j \right\}, \quad (17)$$

the resulting weighted persistence module $\hat{\mathbb{V}}_n = \mathbb{V}_n(\hat{j}) = \mathbb{V}[\mathbb{X}_n, \mathbf{d}_{n,Q(\hat{j})}]$ is the Lepski estimator for $\mathbb{V}[\mathbb{X}]$. The following result establishes that the adaptive selection of Q results in an estimator with the same convergence guarantees as in Theorem 6.2.

Theorem 8.1 (Adaptive $\mathbf{d}_{n,Q}$ -weighted filtration). *Suppose \mathbb{X}_n is obtained under sampling condition (S) for $\mathbb{P} \in \mathcal{P}(\mathbb{X}, a, b)$, and suppose m_{\min} and m_{\max} are known such that unknown number of outliers, m^* , such that $0 \leq m_{\min} \leq m^* \leq m_{\max} < n/2$. For a chosen $\theta > 1$ let \hat{j} be the output of data-driven procedure in Eq. (17) and let $\hat{\mathbb{V}}_n = \mathbb{V}_n(\hat{j})$. Then, for all $\delta \in (0, 1)$,*

$$\mathbb{P} \left(\mathcal{W}_\infty \left(\mathfrak{Dgm}(\hat{\mathbb{V}}_n), \mathfrak{Dgm}(\mathbb{V}[\mathbb{X}]) \right) \leq 3\mathfrak{h}(n, \theta m^*, \delta) \right) \geq 1 - \delta \log_\theta \left(\frac{\theta m_{\min}}{m_{\max}} \right).$$

Remark 8.1. *We make the following useful observations from Theorem 8.1.*

- (i) *We make the distinction that the output $\hat{\mathbb{V}}_n$ of Lepski's method does not necessarily correspond to the optimal choice \mathbb{V}_n^* if m^* were known. Instead, Theorem 8.1 guarantees that the error associated with $\hat{\mathbb{V}}_n$ is of the same order (up to constants) as that of \mathbb{V}_n^* .*

- (ii) While Lepski's method guarantees optimal errors for the adaptive estimator without any knowledge of the true m^* ; in practice, however, the empirical performance depends on several factors. Since the procedure in Theorem 8.1 is designed to match the guarantee of Theorem 6.2, the success of the procedure crucially depends on the tightness of the bound $\mathfrak{f}(n, m, Q, \delta_1, \delta_2)$ in Theorem 6.2. Furthermore, the implementation described in Eq. (17) requires knowledge of the parameters $a, b > 0$ arising from the (a, b) -standard condition. While the calibration of a and b in practice is more of an art and beyond the scope of the paper, we emphasize here that it is possible to construct a statistically consistent estimator of the true population quantity $\mathbb{V}[\mathbb{X}]$ in a purely data-adaptive fashion, even in the presence of adversarial contamination.
- (iii) Unlike a standard grid search, Lepski's method adapts to the true noise level m^* in an efficient manner. Given a reasonable estimate for m_{\min} and m_{\max} , Lepski's method has a computational cost of $O(\log_{\theta}^2(m_{\max}/m_{\min}))$. However, the choice of $\theta > 1$ must also be made judiciously, e.g., replacing θ with $\sqrt{\theta}$ for the procedure in Eq. (17) will require ~ 4 times more computational time.
- (iv) In the worst case, when there are no reasonable estimates for m_{\min} and m_{\max} , choosing $m_{\min} = 1$ and $m_{\max} = n/2$ requires $O(\log_{\theta}^2(n))$ computational time. Notably, more than just the additional computational price, a suboptimal choice of m_{\min} and m_{\max} leads to poor performance. To see this, note that the term $\mathfrak{h}(n, m, \delta)$ is a lower bound for the term $\mathfrak{f}(n, m, Q, \delta_1, \delta_2)$ in Theorem 6.2 when $Q = 2m + 1$ and $\delta_1 = e^{-(1+b)(2m_{\max}+1)} \leq e^{-(1+b)Q}$. Therefore, when the number of outliers grows with n as $m^* = cn^{\epsilon}$ for $c > 0$ and $\epsilon \in [0, 1)$, a similar analysis to that in Theorem 5.1 and Theorem 6.2 yields that

$$\mathbb{E} \left[\mathbb{W}_{\infty} \left(\mathfrak{Dgm}(\widehat{\mathbb{V}}_n), \mathfrak{Dgm}(\mathbb{V}[\mathbb{X}]) \right) \right] \lesssim \left(\frac{\log n}{n/m_{\max}} \right)^{1/b}.$$

Therefore, if the bound m_{\max} is not tight, i.e., $m_{\max} = Cn^{\beta}$ for $\epsilon < \beta$, then, asymptotically, the output of Lepski's method is not adaptive to the true noise m^* , and, instead, reflects the suboptimal choice of m_{\max} .

This method may also be used to adaptively select the parameter Q for the sublevel set persistence module. The following result outlines a data-driven procedure to obtain $\bar{j} \in \mathcal{J}$ such that the resulting sublevel persistence module $\bar{\mathbb{V}}_n = \mathbb{V}_n(\bar{j}) = \mathbb{V}[\mathfrak{d}_{n, Q(\bar{j})}]$ has the same convergence guarantee as Theorem 5.1.

Corollary 8.1 (Adaptive sublevel filtration). *For $\mathbb{P} \in \mathcal{P}(\mathbb{X}, a, b)$, suppose \mathbb{X}_n is obtained under sampling condition (S), and suppose m_{\min} and m_{\max} are known such that unknown number of outliers, m^* , is such that $0 \leq m_{\min} \leq m^* \leq m_{\max} < n/2$. Let $\mathbb{W}_n(j) = \mathbb{V}[\mathfrak{d}_{n, Q(j)}]$ be the sublevel persistence module obtained using $\mathfrak{d}_{n, Q(j)}$ with $Q(j) = 2m(j) + 1$ for all $j \in \mathcal{J}$. For a chosen $\theta > 1$, let \bar{j} be the output of data-driven procedure,*

$$\bar{j} = \min \left\{ j \in \mathcal{J} : \mathbb{W}_{\infty}(\mathbb{V}_n(j), \mathbb{V}_n(j')) \leq 2\mathfrak{p}(n, m(j'), \delta) \text{ for all } j' \in \mathcal{J}, j' > j \right\},$$

where

$$\mathfrak{p}(n, m, \delta) = \left(\frac{2m + 1}{an} \mathcal{W}_0 \left(\frac{ne^{(1+b)\log(1/\delta)}}{2m + 1} \right) \right)^{1/b}.$$

Then, for all $\delta \leq e^{-(1+b)(2m_{\max}+1)}$ and $\bar{\mathbb{V}}_n = \mathbb{V}_n(\bar{j})$,

$$\mathbb{P} \left\{ \mathbb{W}_{\infty} \left(\mathfrak{Dgm}(\bar{\mathbb{V}}_n), \mathfrak{Dgm}(\mathbb{V}[\mathbb{X}]) \right) \leq 3\mathfrak{h}(n, \theta m^*, \delta) \right\} \geq 1 - \delta \log_{\theta} \left(\frac{\theta m_{\min}}{m_{\max}} \right).$$

The proof is identical to that of Theorem 8.1, and is, therefore, omitted. The success of Lepski’s method depends on the tightness of the probabilistic bounds, knowledge of the (nuisance) parameters (i.e. a, b) appearing in these bounds, and a prudent choice for m_{\min} and m_{\max} . While the calibration of a is beyond the scope of this paper, in \mathbb{R}^d a conservative choice for b would be the dimension d of the ambient space. We refer the reader to Chazal et al. (2015b, Section 4) for further details.

To address the last bottleneck in Lepski’s method, we describe a heuristic method to select the parameter Q , which may be used to obtain reasonable choices for m_{\min} and m_{\max} .

The method is based on the observation that the blocks $\{S_q : q \in [Q]\}$ may be resampled by shuffling the sample points \mathbb{X}_n prior to partitioning it. The resulting estimator $\mathbb{V}[\mathbb{X}_n, \mathbf{d}_{n,Q}]$ is an unbiased estimator of the same population quantity when $2m < Q < n$. Therefore, we may choose the smallest value of Q for which the pairwise bottleneck distance over permutations of the data is minimized. Specifically, suppose $\mathbb{X}_n^\sigma = \{\mathbf{X}_{\sigma(1)}, \mathbf{X}_{\sigma(2)}, \dots, \mathbf{X}_{\sigma(n)}\}$ is a permutation of \mathbb{X}_n , then

$$\widehat{Q}_R = \arg \min_{Q \geq 1} \sum_{1 \leq i < j \leq N} W_\infty \left(\mathbb{V}[\mathbb{X}_n^{\sigma_i}, \mathbf{d}_{n,Q}], \mathbb{V}[\mathbb{X}_n^{\sigma_j}, \mathbf{d}_{n,Q}] \right),$$

where, for a chosen number of replicates N , σ_i, σ_j are permutations of $[n]$ for each $i, j \in [N]$. Furthermore, for $\widehat{m}_R = \lfloor \widehat{Q}_R / 2 \rfloor$ and for a constant $C > 1$, the bounds m_{\min} and m_{\max} may be taken to be $C^{-1}\widehat{m}_R$ and $C\widehat{m}_R$, respectively.

9. Experiments

In the following section, we supplement the theory through the illustration of the performance of the robust filtrations $\mathbb{V}[\mathbf{d}_{n,Q}]$ and $\mathbb{V}[\mathbb{X}_n, \mathbf{d}_{n,Q}]$ in synthetic experiments.

9.1. Adaptive calibration of Q

For $n = 500$, $K = 30$ replicates and for each $i \in [K]$, point clouds $\mathbb{X}_n^{(i)}$ are generated on a circle, and $m^{(i)} \sim \text{Unif}(50, 150)$ outliers added from a Matérn cluster process. This is illustrated in Figure 4 (a). Taking $m_{\min} = 20$, $m_{\max} = 200$ and $\theta = 1.07$, the adaptive estimate $\widehat{m}^{(i)}$ is computed using Lepski’s method, and $\widehat{m}_R^{(i)}$ is computed using the heuristic method described in Section 8 with $N = 50$. For a single replicate $i \in [K]$, Figure 4 (b) plots $\sum_{1 \leq i < j \leq N} W_\infty(\mathbb{V}[\mathbb{X}_n^{\sigma_i}, \mathbf{d}_{n,Q}], \mathbb{V}[\mathbb{X}_n^{\sigma_j}, \mathbf{d}_{n,Q}])$ vs. Q . In most cases, we have observed that the resampled bottleneck distance criterion stabilizes shortly before the optimal value of m . Figure 4 (c) shows a boxplot for the relative errors $\{\widehat{m}^{(i)} - m^{(i)} / m^{(i)} : i \in [K]\}$ and $\{\widehat{m}_R^{(i)} - m^{(i)} / m^{(i)} : i \in [K]\}$ for Lepski’s method and the heuristic procedure, respectively. Lepski’s method is fairly robust to the choice of the hyperparameters, and, consistently selects $\widehat{m}^{(i)} \geq m^{(i)}$. In contrast, since the resampled bottleneck distance from the heuristic procedure often stabilizes before $m^{(i)}$, we observe that $\widehat{m}_R^{(i)} < m^{(i)}$.

9.2. High dimensional topological inference

In this experiment, we illustrate the advantage of using $\mathbf{d}_{n,Q}$ -weighted filtrations for high dimensional topological inference. Points are uniformly sampled in \mathbb{R}^3 from two interlocked circles. Using a random rotation matrix $Q \in SO(100)$, the points are transformed to an arbitrary configuration in \mathbb{R}^{100} . The samples $\mathbb{X}_n \subset \mathbb{R}^{100}$ are obtained by replacing 12.5% of the points in \mathbb{R}^{100} with outliers sampled from $\text{Uniform}([-0.2, 0.2]^{100})$. A scatterplot for \mathbb{X}_n projected to 3 arbitrary coordinates is shown in Figure 5 (a). Since the point cloud is embedded in \mathbb{R}^{100} , computing sublevel filtrations using cubical homology with the same resolution as earlier requires $(10/0.5)^{100} \approx 10^{131}$ simplices to be stored in memory. In contrast, computing the $\mathbf{d}_{n,Q}$ -weighted

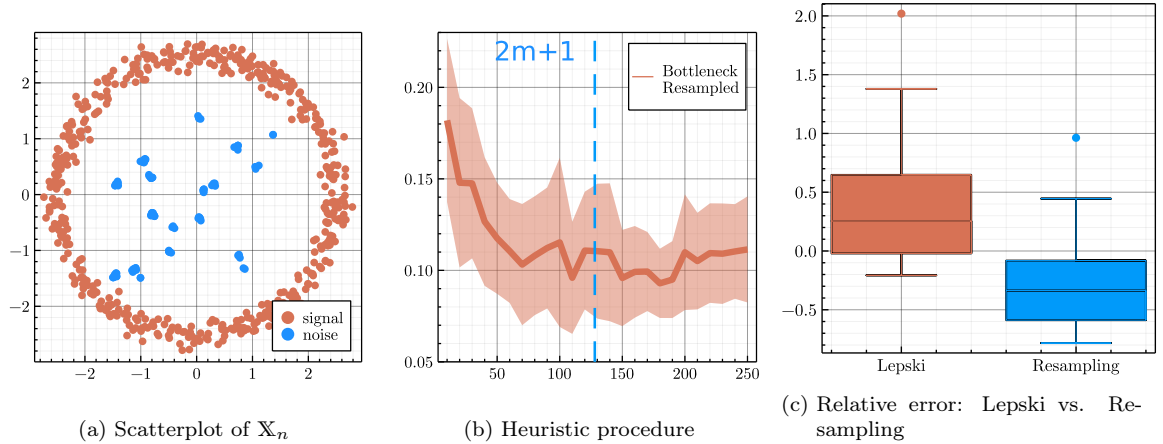


Figure 4: Comparison of Lepski's method and the heuristic procedure for selecting the parameter Q .

filtrations is less intensive. Figure 5 (b) shows the persistence diagram $\mathfrak{Dgm}(\widehat{V}_n)$ obtained using $d_{n,Q}$ -weighted filtrations, where the parameter Q is adaptively selected using Lepski's method. The two 1st order homological features underlying the interlocked circles are recovered. Figure 5 (c) illustrates the persistence diagram $\mathfrak{Dgm}(V[X_n, \delta_{n,k}])$ obtained using DTM-weighted filtrations where the parameter $k = 10$ was selected manually.

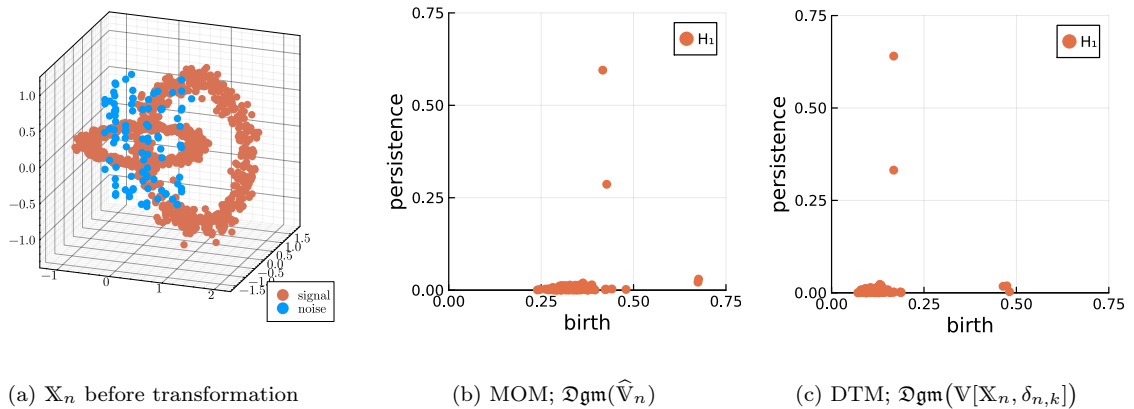


Figure 5: Robust persistence diagrams for interlocked circles in \mathbb{R}^{100} using $d_{n,Q}$ and $\delta_{n,k}$ weighted filtrations.

9.3. Recovering the true signal under adversarial contamination

In this experiment, we illustrate how $V[X_n, d_{n,Q}]$ can be used to recover the true topological features in the presence of adversarial contamination. In Figure 6 (a), we consider a 28×28 image for the digit “6” from the MNIST database (Deng, 2012). We consider the setting in which an adversary is allowed to manipulate 10% of the image by modifying the pixel intensities. Figure 6 (b) depicts the adversarially contaminated version of the image by transforming the “6” to an “8”.

For each pixel p with pixel intensity $\iota(p)$, we convert the image to a point cloud $X_n \subset \mathbb{R}^2$ by sampling $10 * \iota(p)$ points uniformly from the region enclosed by the pixel. Figures 6(d, e) illustrate the point clouds obtained from the true and contaminated images with $n - m \approx 1100$ and $n \approx 1300$, respectively. The persistence diagrams constructed using the distance function d_n for the two point clouds are reported in Figures 6(g, h). The persistence diagram in Figure 6 (h) indicates the presence of the additional loop introduced by the adversary. To account for the adversarial contamination, we compute the MoM Dist function $d_{n,Q}$ with the

parameter Q selected using the contamination budget, i.e., $Q = 1 + 2(1100 \times 10\%) = 221$. Figure 6(f) shows the adversarially contaminated point cloud with each point $\mathbf{x}_i \in \mathbb{X}_n$ colored by the value of $\mathbf{d}_{n,Q}(\mathbf{x}_i)$. The resulting $\mathbf{d}_{n,Q}$ -weighted persistence diagram $\mathfrak{Dgm}(\mathbb{V}[\mathbb{X}_n, \mathbf{d}_{n,Q}])$ is reported in Figure 6(f). We note that $\mathfrak{Dgm}(\mathbb{V}[\mathbb{X}_n, \mathbf{d}_{n,Q}])$ recovers the prominent features of Figure 6(g) up to a rescaling.

Additionally, for each pixel p we compute a rescaled version of $\mathbf{d}_{n,Q}$, given by

$$f_{n,Q}(p) = \frac{\max_x \mathbf{d}_{n,Q}(x) - \mathbf{d}_{n,Q}(p)}{\max_x \mathbf{d}_{n,Q}(x)},$$

as a proxy for the pixel intensity obtained using $\mathbf{d}_{n,Q}$. In Figure 6(c), we plot the level sets $\{p : f_{n,Q} = t\}$ on the original image for $t \geq 0.8$.

9.4. Comparison with existing methods

For this experiment, we examine the robustness of several filtrations as the sample size n grows and the number of outliers increases as $n = m^\epsilon$ for $\epsilon \in (0, 1)$. In particular, for each $n \in \{250, \dots, 2000\}$, $\mathbb{X}_{n-m}^* \subset \mathbb{R}^2$ is sampled from the unit circle with additive Gaussian noise with $\sigma = 0.1$, and compute the persistence diagram \mathbb{D}_n^* . Outliers \mathbb{Y}_m are sampled from a Matérn cluster process with $m = n^\epsilon$ for $\epsilon = 0.5$. For the composite sample $\mathbb{X}_n = \mathbb{X}_{n-m}^* \cup \mathbb{Y}_m$, persistence diagrams are constructed using the MoMDist, DTM, K -PDTM and the trimmed variant of the K -PDTM. For the MoMDist, we set $Q = 2m + 1$, and for the DTM we found that $k = 10$ worked best. This is in line with the recommendation from Bréchet and Levrard (2020, Section 4.1). For the K -PDTM, we set $N = n/5$ so as to not aggressively bias the K -point approximation, and for the trimmed version of the K -PDTM, we set $\alpha = (n - m)/n$ so that a total of $m = n(1 - \alpha)$ points are considered outliers and trimmed Bréchet and Levrard (2020, Section 4.2). The results are reported in Figure 8. For each persistence diagram \mathbb{D}_n we compare \mathbb{D}_n to \mathbb{D}_{n-m}^* in bottleneck distance $W_\infty(\mathbb{D}_n, \mathbb{D}_{n-m}^*)$. In addition, we also assess the quality of the signal in \mathbb{D}_n by computing

$$\Delta\text{-Lifetime}(\mathbb{D}_n, \mathbb{D}_{n-m}^*) := \frac{f(\mathbb{D}_n)}{f(\mathbb{D}_{n-m}^*)} \quad \text{where} \quad f(\mathbb{D}) = \frac{\text{pers}_{\max}(\mathbb{D}) - \text{pers}_{\max-1}(\mathbb{D})}{\text{pers}_{\max}(\mathbb{D})},$$

and $\text{pers}_{\max}(\mathbb{D})$ is the persistence of the longest bar in the first-order diagram of \mathbb{D} . Intuitively, $f(\mathbb{D})$ measures the excess persistence in the longest bar relative to the second longest bar in \mathbb{D} , and the ratio $\Delta\text{-Lifetime}(\mathbb{D}_n, \mathbb{D}_{n-m}^*)$ measures how closely this matches the $f(\mathbb{D}_{n-m}^*)$ in the signal. Ideally, we would like $\Delta\text{-Lifetime}(\mathbb{D}_n, \mathbb{D}_{n-m}^*)$ to be close to 1 as this would indicate that the longest bar in \mathbb{D}_n is separated from the second longest bar to the same extent as that in \mathbb{D}_{n-m}^* .

As corroborated by Theorem 6.2, when $m = o(n)$ the bottleneck distance $W_\infty(\mathbb{D}_n, \mathbb{D}_{n-m}^*)$ for the MoMDist is decreasing as seen in Figure 8(a), and \mathbb{D}_n recovers the signal for moderately large n as shown in Figure 8. On the other hand, the persistence diagrams for DTM, K -PDTM, and its trimmed variant are more influenced by the outliers. This can be attributed, to some extent, to the fact that the DTM is essentially inversely proportional to the density of the point cloud Biau et al. (2011); therefore, the clusters of outliers in \mathbb{Y}_m have a noticeable impact on the DTM. By virtue of this, the K -PDTM and its trimmed variant are also influenced by the outliers. Interestingly, in most cases, the quantized K -PDTM performed better than the trimmed K -PDTM, as seen in Figure 8(b). In essence, when the outliers are particularly troublesome, even a few outliers misclassified as signal points can have a significant impact on the trimmed K -PDTM. We also note that, unlike the MoMDist, under certain circumstances, e.g., when the noise \mathbb{Y}_m is uniformly distributed in the ambient space and the signal is (a, b) -standard, the K -PDTM remains robust to outliers even when $m > n/2$. We refer the readers to Bréchet and Levrard (2020, Section 4.3) for experiments in this setting.

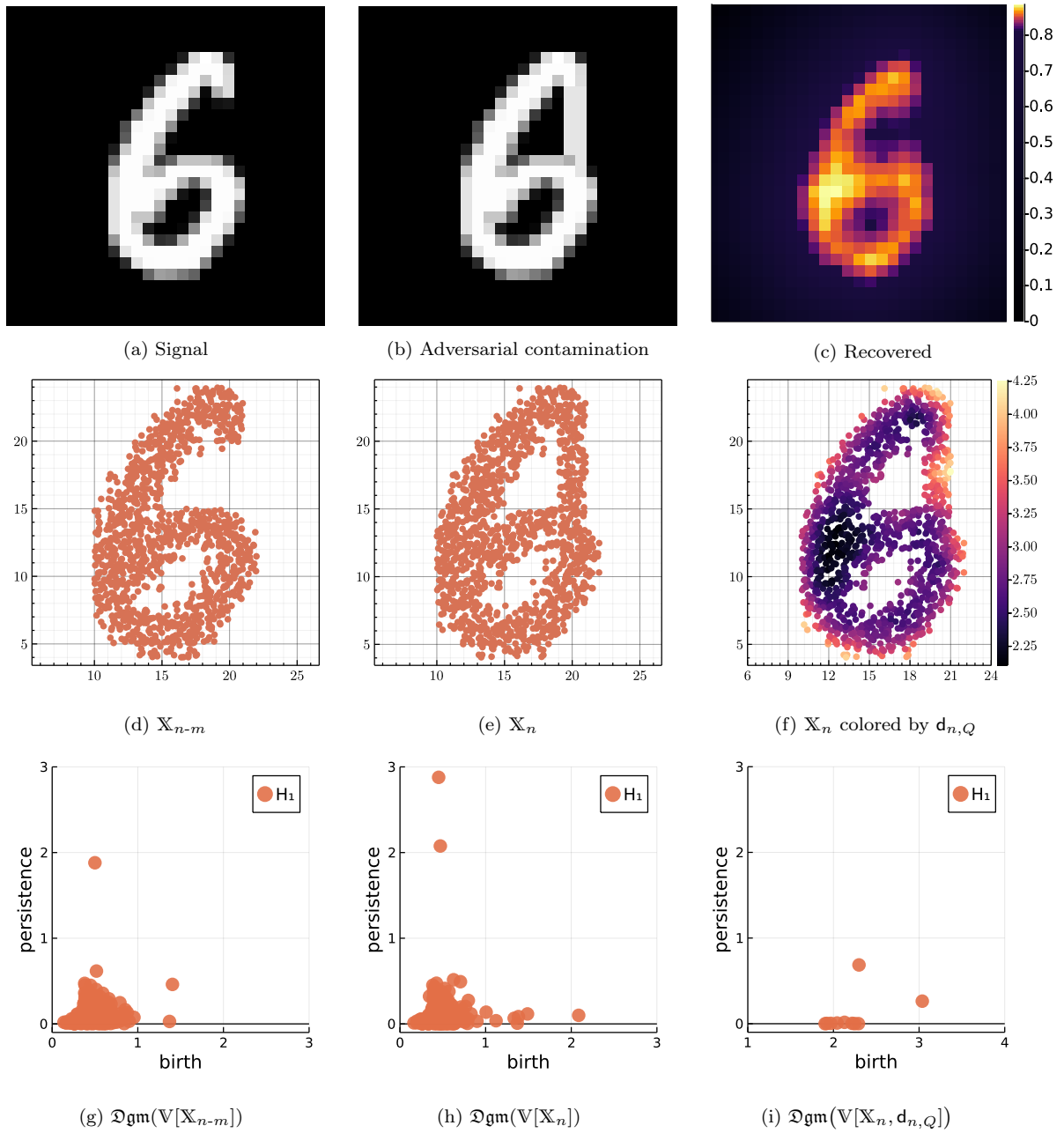


Figure 6: Recovering the topological information underlying the signal in the presence of adversarial contamination.

Table 2: Combined Summary of Time and Memory Usage

n	Time (seconds)					Memory (MB)				
	500	1000	1500	2000	2500	500	1000	1500	2000	2500
MoMDist	0.047	0.237	0.570	1.166	2.105	30.94	109.79	221.43	426.67	649.88
DTM	0.054	0.240	0.593	1.373	2.177	29.61	106.99	190.41	419.92	634.20
K -PDTM	0.539	0.577	2.523	5.755	5.838	558.03	2806.43	5511.02	14882.10	21109.80
RKDE	0.178	1.216	1.873	3.961	7.074	93.49	368.59	659.98	1202.16	1968.14

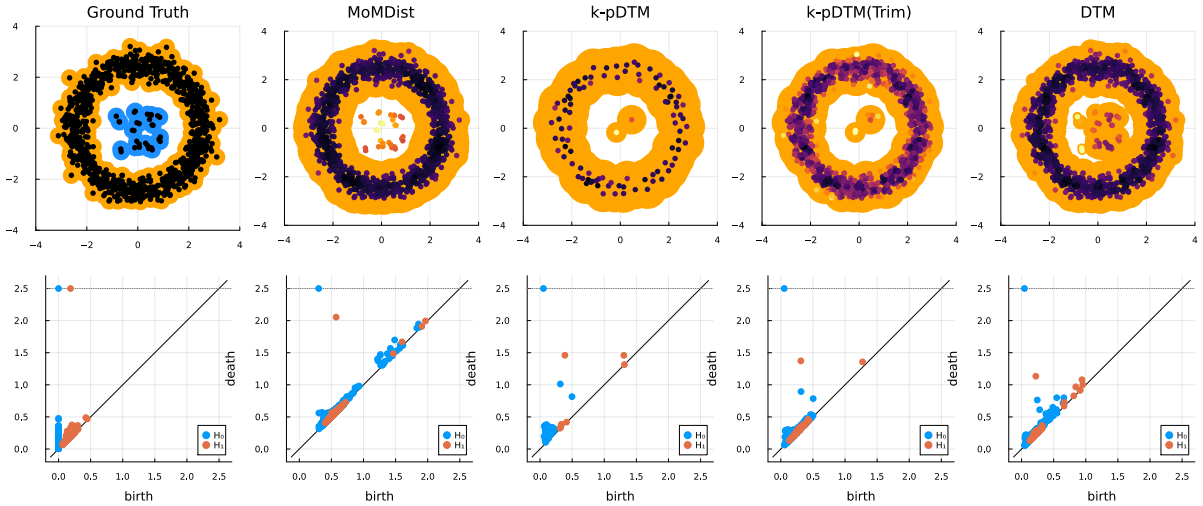


Figure 7: Illustration of the offsets V_{n+m}^t and the persistence diagrams D_{n+m} for the MoMDist, K -PDTM, the trimmed K -PDTM, and the DTM filtration, where $n-m$ points are sampled from a circle with additive Gaussian noise and m outliers are sampled from a Matérn cluster process.

Lastly, in Table 2, we provide a summary of the time and memory usage for the MoMDist, DTM, RKDE, and the K -PDTM for the same setup. We exclude the trimmed K -PDTM from the summary since it always takes longer than K -PDTM. In all cases, we use the publicly available implementation.³ We note that MoMDist and DTM are significantly faster and use less memory despite the fact that the K -PDTM constructs persistence diagrams using a smaller number of quantized points. The main computational bottleneck for the K -PDTM stems from the preprocessing step which uses a variant of Lloyd’s algorithm, and is likely to be more efficient in settings where n is very large.

10. Conclusion & Discussion

In this paper, we introduce a methodology for constructing filtrations that are computationally efficient, provably robust, and statistically (near) optimal even in the presence of outliers.

To elaborate, we introduced MoM Dist, $d_{n,Q}$, as a computationally efficient and outlier-robust variant of the distance function based on the median-of-means principle, and established some of its theoretical properties. In particular, when the samples contain outliers in the adversarial contamination setting, we (i) showed that the $d_{n,Q}$ -weighted filtrations are statistically (near) optimal estimators of the true (uncontaminated) population counterpart, (ii) characterized its convergence rate in the bottleneck metric, and (iii) provided uniform confidence bands in the space of persistence diagrams. Furthermore, we used an empirical influence analysis framework to quantify the robustness of the $d_{n,Q}$ -filtrations, and provide a framework for selecting the parameter Q .

³<https://github.com/GUDHI/TDA-tutorial/blob/master/Tuto-GUDHI-kPDTM-kPLM.ipynb>

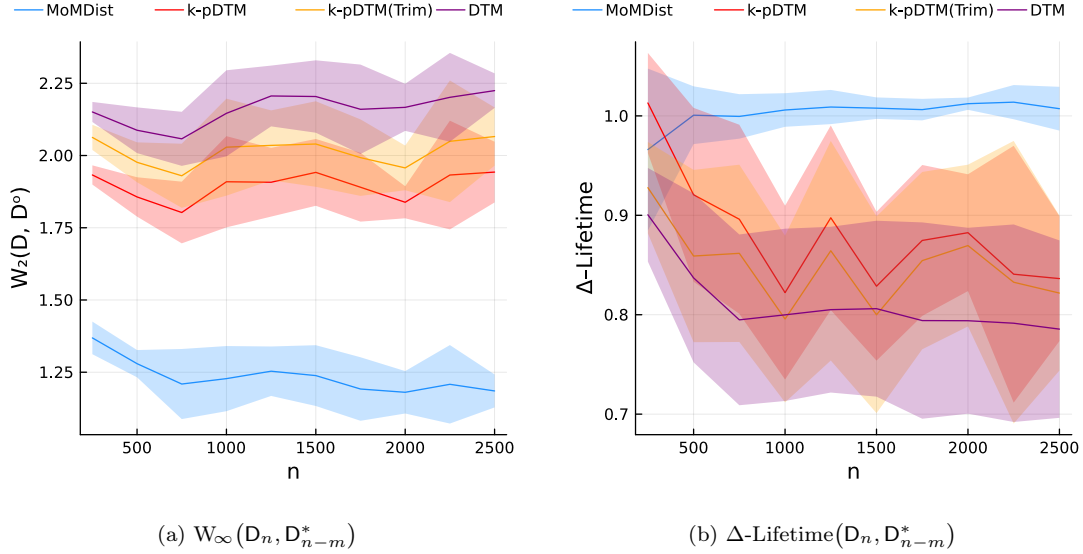


Figure 8: Comparison of MoMDist, DTM, K -PDTM and the trimmed K -PDTM for the experiment in Section 9.4.

Topological inference in the presence of outliers is a topic that has received considerable attention in recent years and with good reason. We would like to highlight that the objective of this paper has been to develop a framework of topological inference in which the population target is the persistence diagram $\mathfrak{Dgm}(\mathbb{V}[\mathbb{X}])$. Therefore, the proposed methodology disregards, to a large extent, the distribution of mass on the support. As a future direction, we would like to explore a framework of inference that incorporates information from, both, the geometry of the underlying space and the structure of the probability measure generating the data. As noted in Anai et al. (2019, Section 5), their results follow only from a few simple properties of the distance-to-measure. We build off their foundation to provide some useful generalizations which we hope will be useful in the analysis of other estimators using this framework.

Acknowledgements

BKS is partially supported by the National Science Foundation (NSF) CAREER Award DMS-1945396. SK is partially supported by JSPS KAKENHI Grant Number 21H03403. KF and SK are supported by JST, CREST Grant Number JPMJCR15D3, Japan.

References

- Hirokazu Anai, Frédéric Chazal, Marc Glisse, Yuichi Ike, Hiroya Inakoshi, Raphaël Tinarrage, and Yuhei Umeda. DTM-based filtrations. In *SoCG 2019-35th International Symposium on Computational Geometry*, 2019.
- Jean-Yves Audibert and Olivier Catoni. Robust linear least squares regression. *The Annals of Statistics*, 39(5):2766–2794, 2011.
- Amir-Hossein Bateni and Arnak S Dalalyan. Confidence regions and minimax rates in outlier-robust estimation on the probability simplex. *Electronic Journal of Statistics*, 14:2653–2677, 2020.
- Gérard Biau, Frédéric Chazal, David Cohen-Steiner, Luc Devroye, and Carlos Rodriguez. A weighted k -nearest neighbor density estimate for geometric inference. *Electronic Journal of Statistics*, 5:204–237, 2011.

- Lucien Birgé. An alternative point of view on Lepski’s method. *State of the Art in Probability and Statistics: Festschrift for Willem R. Van Zwet*, 36:114, 2001.
- Håvard Bakke Bjerkevik, Magnus Bakke Botnan, and Michael Kerber. Computing the interleaving distance is NP-hard. *Foundations of Computational Mathematics*, 20(5):1237–1271, 2020.
- Jean-Daniel Boissonnat, Frédéric Chazal, and Mariette Yvinec. *Geometric and Topological Inference*, volume 57. Cambridge University Press, 2018.
- Claire Brécheteau. Robust anisotropic power-functions-based filtrations for clustering. In Sergio Cabello and Danny Z. Chen, editors, *36th International Symposium on Computational Geometry (SoCG 2020)*, volume 164, pages 23:1–23:15, 2020.
- Claire Brécheteau and Clément Levrard. A k -points-based distance for robust geometric inference. *Bernoulli*, 26(4):3017 – 3050, 2020.
- Peter Bubenik, Vin De Silva, and Jonathan Scott. Metrics for generalized persistence modules. *Foundations of Computational Mathematics*, 15(6):1501–1531, 2015.
- Mickaël Buchet. *Topological Inference from Measures*. PhD thesis, Université Paris Sud-Paris XI, 2014.
- Mickaël Buchet, Frédéric Chazal, Tamal K Dey, Fengtao Fan, Steve Y Oudot, and Yusu Wang. Topological analysis of scalar fields with outliers. In *31st International Symposium on Computational Geometry (SoCG 2015)*, 2015.
- Mickaël Buchet, Frédéric Chazal, Steve Y Oudot, and Donald R Sheehy. Efficient and robust persistent homology for measures. *Computational Geometry*, 58:70–96, 2016.
- Mickaël Buchet, Tamal K Dey, Jiayuan Wang, and Yusu Wang. Declutter and resample: Towards parameter free denoising. *Journal of Computational Geometry*, 9(2):21–46, 2018.
- Gunnar Carlsson and Afra Zomorodian. The theory of multidimensional persistence. *Discrete & Computational Geometry*, 42(1):71–93, 2009.
- Frédéric Chazal and Bertrand Michel. An introduction to topological data analysis: Fundamental and practical aspects for data scientists. *arXiv preprint arXiv:1710.04019*, 2017.
- Frédéric Chazal, David Cohen-Steiner, and Quentin Mérigot. Geometric inference for probability measures. *Foundations of Computational Mathematics*, 11(6):733–751, 2011.
- Frédéric Chazal, Brittany Fasy, Fabrizio Lecci, Bertrand Michel, Alessandro Rinaldo, and Larry Wasserman. Subsampling methods for persistent homology. In *International Conference on Machine Learning*, pages 2143–2151. PMLR, 2015a.
- Frédéric Chazal, Marc Glisse, Catherine Labruere, and Bertrand Michel. Convergence rates for persistence diagram estimation in topological data analysis. *Journal of Machine Learning Research*, 16:3603–3635, 2015b.
- Frédéric Chazal, Vin De Silva, Marc Glisse, and Steve Oudot. *The Structure and Stability of Persistence Modules*. Springer, 2016.
- Frédéric Chazal, Brittany Fasy, Fabrizio Lecci, Bertrand Michel, Alessandro Rinaldo, and Larry Wasserman. Robust topological inference: Distance to a measure and kernel distance. *Journal of Machine Learning Research*, 18(1):5845–5884, 2017.

- Mengjie Chen, Chao Gao, and Zhao Ren. Robust covariance and scatter matrix estimation under Huber’s contamination model. *The Annals of Statistics*, 46(5):1932–1960, 2018.
- Xi Chen and Wen-Xin Zhou. Robust inference via multiplier bootstrap. *The Annals of Statistics*, 48(3):1665–1691, 2020.
- David Cohen-Steiner, Herbert Edelsbrunner, and John Harer. Stability of persistence diagrams. *Discrete & Computational Geometry*, 37(1):103–120, 2007.
- Thomas H Cormen, Charles E Leiserson, Ronald L Rivest, and Clifford Stein. *Introduction to Algorithms*. MIT press, 2009.
- Antonio Cuevas and Alberto Rodríguez-Casal. On boundary estimation. *Advances in Applied Probability*, pages 340–354, 2004.
- Li Deng. The MNIST database of handwritten digit images for machine learning research. *IEEE Signal Processing Magazine*, 29(6):141–142, 2012.
- Luc Devroye, Matthieu Lerasle, Gabor Lugosi, and Roberto I Oliveira. Sub-gaussian mean estimators. *The Annals of Statistics*, 44(6):2695–2725, 2016.
- Ilias Diakonikolas, Gautam Kamath, Daniel M Kane, Jerry Li, Ankur Moitra, and Alistair Stewart. Being robust (in high dimensions) can be practical. In *International Conference on Machine Learning*, pages 999–1008. PMLR, 2017.
- David L Donoho. Statistical estimation and optimal recovery. *The Annals of Statistics*, 22(1):238–270, 1994.
- Herbert Edelsbrunner and John Harer. *Computational Topology: An Introduction*. American Mathematical Society, 2010.
- Brittany Terese Fasy, Fabrizio Lecci, Alessandro Rinaldo, Larry Wasserman, Sivaraman Balakrishnan, and Aarti Singh. Confidence sets for persistence diagrams. *The Annals of Statistics*, 42(6):2301–2339, 2014.
- Mario Gómez and Facundo Mémoli. Curvature sets over persistence diagrams. *arXiv preprint arXiv:2103.04470*, 2021.
- Torben Hagerup and Christine Rüb. A guided tour of Chernoff bounds. *Inf. Process. Lett.*, 33:305–308, 1990.
- Frank R Hampel, Elvezio M Ronchetti, Peter J Rousseeuw, and Werner A Stahel. *Robust Statistics: The Approach Based on Influence Functions*, volume 196. John Wiley & Sons, 2011.
- Mehdi Hassani. Approximation of the Lambert W function. *Research report collection*, 8(4), 2005.
- Wassily Hoeffding. Probability inequalities for sums of bounded random variables. *Journal of the American Statistical Association*, 58(301):13–30, 1963.
- Peter J Huber. Robust estimation of a location parameter. *The Annals of Mathematical Statistics*, pages 73–101, 1964.
- Pierre Humbert, Batiste Le Bars, Ludovic Minvielle, and Nicolas Vayatis. Robust kernel density estimation with median-of-means principle. *arXiv preprint arXiv:2006.16590*, 2020.

- Emilien Joly and Gábor Lugosi. Robust estimation of U-statistics. *Stochastic Processes and their Applications*, 126(12):3760–3773, 2016.
- Guillaume Lecué and Matthieu Lerasle. Robust machine learning by median-of-means: Theory and practice. *Annals of Statistics*, 48(2):906–931, 2020.
- Oleg V. Lepski. On a problem of adaptive estimation in Gaussian white noise. *Theory of Probability & Its Applications*, 35(3):454–466, 1991.
- Matthieu Lerasle, Zoltán Szabó, Timothée Mathieu, and Guillaume Lecué. MONK: Outlier-robust mean embedding estimation by median-of-means. In *International Conference on Machine Learning*, pages 3782–3793. PMLR, 2019.
- Sunhyuk Lim, Facundo Memoli, and Osman Berat Okutan. Vietoris-Rips persistent homology, injective metric spaces, and the filling radius. *arXiv preprint arXiv:2001.07588*, 2020.
- Gábor Lugosi and Shahar Mendelson. Mean estimation and regression under heavy-tailed distributions: A survey. *Foundations of Computational Mathematics*, 19(5):1145–1190, 2019a.
- Gabor Lugosi and Shahar Mendelson. Risk minimization by median-of-means tournaments. *Journal of the European Mathematical Society*, 22(3):925–965, 2019b.
- Yuriy Mileyko, Sayan Mukherjee, and John Harer. Probability measures on the space of persistence diagrams. *Inverse Problems*, 27(12):124007, 2011.
- Stanislav Minsker. Geometric median and robust estimation in Banach spaces. *Bernoulli*, 21(4):2308–2335, 2015.
- Stanislav Minsker. Sub-Gaussian estimators of the mean of a random matrix with heavy-tailed entries. *The Annals of Statistics*, 46(6A):2871–2903, 2018.
- Arkadij Semenovič Nemirovskij and David Borisovich Yudin. *Problem Complexity and Method Efficiency in Optimization*. Wiley-Interscience, 1983.
- Nina Otter, Mason A Porter, Ulrike Tillmann, Peter Grindrod, and Heather A Harrington. A roadmap for the computation of persistent homology. *EPJ Data Science*, 6:1–38, 2017.
- Jeff M Phillips, Bei Wang, and Yan Zheng. Geometric inference on kernel density estimates. In *31st International Symposium on Computational Geometry*, volume 34, pages 857–871, 2015.
- Elchanan Solomon, Alexander Wagner, and Paul Bendich. From geometry to topology: Inverse theorems for distributed persistence. *arXiv preprint arXiv:2101.12288*, 2021.
- Alexandre B. Tsybakov. *Introduction to Nonparametric Estimation*. Springer Publishing Company, Incorporated, 1st edition, 2008. ISBN 0387790519.
- John W Tukey. A survey of sampling from contaminated distributions. *Contributions to Probability and Statistics*, pages 448–485, 1960.
- Katharine Turner, Yuriy Mileyko, Sayan Mukherjee, and John Harer. Fréchet means for distributions of persistence diagrams. *Discrete & Computational Geometry*, 52(1):44–70, 2014.
- Matija Čufar. Ripsrerer.jl: Flexible and efficient persistent homology computation in Julia. *Journal of Open Source Software*, 5(54):2614, 2020.
- Oliver Vipond, Joshua A Bull, Philip S Macklin, Ulrike Tillmann, Christopher W Pugh, Helen M Byrne, and Heather A Harrington. Multiparameter persistent homology landscapes identify immune cell spatial patterns in tumors. *Proceedings of the National Academy of Sciences*, 118(41), 2021.

Appendix

A. Background on Persistent Homology

Given a compact set \mathbb{X} , the building block of any topological data analysis pipeline to extract meaningful information from \mathbb{X} begins with a nested sequence of filtered topological spaces called a filtration, simply denoted by V . The sequence of spaces is parametrized by a resolution parameter t . There are several approaches for constructing a filtration using \mathbb{X} . One approach is to consider the collection of offsets built on top of \mathbb{X} , i.e., $V^t = V^t[\mathbb{X}] = \mathbb{X}(t)$. For $s < t$, the offsets are nested $V^s \subseteq V^t$, and $V[\mathbb{X}] \doteq \{V^t[\mathbb{X}] : t \in \mathbb{R}\}$ is a nested sequence of topological spaces and defines the filtration built using the offsets of \mathbb{X} .

The second approach to constructing a filtration is using a filter function $f_{\mathbb{X}} : \mathbb{R}^d \rightarrow \mathbb{R}$ which carries the topological information underlying \mathbb{X} . In this scenario, one typically constructs the filtration from the sublevel sets associated with $f_{\mathbb{X}}$, given by $V^t = f_{\mathbb{X}}^{-1}((-\infty, t])$ for each resolution t . Again, for $s < t$, $V^s[f_{\mathbb{X}}] \subseteq V^t[f_{\mathbb{X}}]$ and the sequence $V[f_{\mathbb{X}}] = \{V^t[f_{\mathbb{X}}] : t \in \mathbb{R}\}$ constitutes the sublevel filtration from $f_{\mathbb{X}}$. Mutatis mutandis a similar notion holds for the superlevel filtration.

In general, the filtration $V[\mathbb{X}]$ can be very different from $V[f_{\mathbb{X}}]$, although the prevailing objective is for $V[f_{\mathbb{X}}]$ to encode the same information as in $V[\mathbb{X}]$. In this context, the distance function $d_{\mathbb{X}}$ plays a special role owing to the fact that its sublevel filtration is the same filtration associated with the offsets, i.e., $V[d_{\mathbb{X}}] = V[\mathbb{X}]$. This fact plays an important role in motivating the MoM Dist estimator introduced in Section 4, and follows by noting that for every resolution $t > 0$,

$$d_{\mathbb{X}}^{-1}((-\infty, t]) = \left\{ \mathbf{x} \in \mathbb{R}^d : d_{\mathbb{X}}(\mathbf{x}) \leq t \right\} = \bigcup_{\mathbf{x} \in \mathbb{X}} B(\mathbf{x}, t).$$

Let $V = \{V^t : t \in \mathbb{R}\}$ denote a generic filtration and let $\iota_s^t : V^s \hookrightarrow V^t$ denote the inclusion map between the filtered spaces at resolutions $s < t$. For each resolution t , let $\mathbb{V}^t = H_*(V^t; \mathbf{F})$ be the homology⁴ of V^t with coefficients in a field \mathbf{F} . As the resolution t varies, the evolution of topological features is captured by V . Roughly speaking, new cycles (i.e., connected components, loops, holes, and higher dimensional analogues) are born, or existing cycles can disappear. The collection of cycles in V^t at each resolution t is encoded as a vector space in \mathbb{V}^t . The inclusion maps $\iota_s^t : V^s \hookrightarrow V^t$ induce linear maps $\phi_s^t : \mathbb{V}^s \rightarrow \mathbb{V}^t$ between the vector spaces \mathbb{V}^s and \mathbb{V}^t .

As such, the collection V can be described more succinctly as the *category* $V = \{V^t, \iota_s^t : s \leq t\}$ with the inclusion maps ι_s^t representing the morphisms for $s \leq t$. The image of V under the *homology functor* $\mathbf{Hom}_* : V \mapsto \mathbb{V}$, gives us the *persistence module*

$$\mathbb{V} \doteq \left\{ \mathbb{V}^t, \phi_s^t : s \leq t \right\},$$

where the induced maps $\phi_s^t : \mathbb{V}^s \rightarrow \mathbb{V}^t$ are homomorphisms between two vector spaces. For $r < s < t$, the persistence module can equivalently be represented as

$$\dots \longrightarrow \mathbb{V}^r \xrightarrow{\phi_r^s} \mathbb{V}^s \xrightarrow{\phi_s^t} \mathbb{V}^t \longrightarrow \dots$$

⁴Where, as per convention, the order of homology, denoted by $*$, is an arbitrary non-negative integer.

Informally, a new topological feature is born at resolution $b \in \mathbb{R}$ if the cycle associated with that feature is not present in $\mathbb{V}^{b-\epsilon}$ for all $\epsilon > 0$. The same feature is said to die at resolution $d > b$ if the cycle associated with this feature disappears from $\mathbb{V}^{d+\epsilon}$ for all $\epsilon > 0$, resulting in the (ordered) persistence pair (b, d) . By collecting all the persistence pairs, the persistence module \mathbb{V} may be succinctly represented by a *persistence diagram*,

$$\mathfrak{Dgm}(\mathbb{V}) \doteq \{(b, d) \in \mathbb{R}^2 : b \leq d \leq \infty\}.$$

A.1. Interleaving of Persistence Modules

Given two persistence modules $\mathbb{V} = \{\mathbb{V}^t, \phi_s^t\}_{s \leq t}$ and $\mathbb{W} = \{\mathbb{W}^t, \psi_s^t\}_{s \leq t}$, they are said to be equivalent (or isomorphic) if there exists a family of linear maps $\{\xi_t\}_{t \in \mathbb{R}}$ such that each $\xi^t : \mathbb{V}^t \rightarrow \mathbb{W}^t$ is an isomorphism. This notion can be extended to define two collections of maps $\{\alpha_t : t \in \mathbb{R}\}$ and $\{\beta_t : t \in \mathbb{R}\}$ which weave the two persistence modules together.

Definition A.1 (Interleaving of persistence modules). *Given two persistence modules \mathbb{V} and \mathbb{W} , and two monotone increasing maps $\alpha, \beta : \mathbb{R} \rightarrow \mathbb{R}$, \mathbb{V} and \mathbb{W} are said to be (α, β) -interleaved if the following diagrams commute for all $s \leq t$*

$$\begin{array}{ccc}
 \mathbb{V}^s & \xrightarrow{\phi_s^t} & \mathbb{V}^t \\
 \searrow \alpha_s & & \searrow \alpha_t \\
 \mathbb{W}^{\alpha(s)} & \xrightarrow{\psi_{\alpha(s)}^{\alpha(t)}} & \mathbb{W}^{\alpha(t)}
 \end{array}
 \qquad
 \begin{array}{ccc}
 & \mathbb{V}^{\beta(s)} & \xrightarrow{\phi_{\beta(s)}^{\beta(t)}} & \mathbb{V}^{\beta(t)} \\
 \beta_s \nearrow & & \searrow \beta_t & \\
 \mathbb{W}^s & \xrightarrow{\psi_s^t} & \mathbb{W}^t &
 \end{array}$$

$$\begin{array}{ccc}
 & \mathbb{V}^{\beta(t)} & \searrow \alpha_{\beta(t)} \\
 \beta_t \nearrow & & \\
 \mathbb{W}^t & \xrightarrow{\psi_t^{\alpha \circ \beta(t)}} & \mathbb{W}^{\alpha \circ \beta(t)}
 \end{array}
 \qquad
 \begin{array}{ccc}
 \mathbb{V}^t & \xrightarrow{\phi_t^{\beta \circ \alpha(t)}} & \mathbb{V}^{\beta \circ \alpha(t)} \\
 \searrow \alpha_t & & \nearrow \beta_{\alpha(t)} \\
 & \mathbb{W}^{\alpha(t)} &
 \end{array}$$

Remark A.1. *The persistence modules \mathbb{V} and \mathbb{W} are purely algebraic objects, and their underlying filtrations V and W are not necessarily compatible. However, when the filtrations V and W arise as filtered subsets of the same underlying space (e.g., \mathbb{R}^d), we can similarly define an (α, β) -interleaving between the filtrations V and W by replacing all linear maps in Definition A.1 by inclusion maps.*

The resulting persistence diagrams $\mathfrak{Dgm}(\mathbb{V})$ and $\mathfrak{Dgm}(\mathbb{W})$ are elements of the space of persistence diagrams $\Omega = \{(x, y) : x \leq y\}$ endowed with the family of q -Wasserstein metrics $W_q(\cdot, \cdot)$ for $1 \leq q \leq \infty$. We refer the reader to Edelsbrunner and Harer (2010); Mileyko et al. (2011) for more details. In the special case of $q = \infty$, the resulting metric W_∞ is commonly referred to as the *bottleneck distance*, and is given as follows.

Definition A.2 (Bottleneck distance). *Given two persistence diagrams $D_1, D_2 \in \Omega$, the bottleneck distance is given by*

$$W_\infty(D_1, D_2) \doteq \inf_{\gamma \in \Gamma} \sup_{p \in D_1 \cup \Delta} \|p - \gamma(p)\|_\infty,$$

where $\Gamma = \{\gamma : D_1 \cup \Delta \rightarrow D_2 \cup \Delta\}$ is the set of all multi-bijections from D_1 to D_2 including the diagonal $\Delta = \{(x, y) : x = y\}$ with infinite multiplicity⁵.

⁵In order to ensure that both persistence diagrams have the same cardinality.

Although the space of persistence diagrams (Ω, W_q) , together with the q -Wasserstein distance, presents a challenging mathematical structure for refined statistical analyses (Mileyko et al., 2011; Turner et al., 2014), the stability of persistence diagrams (Cohen-Steiner et al., 2007; Chazal et al., 2016) provides a handle on this space by allowing us to directly work on the space generating the filtrations.

Lemma A.1 (Stability of persistence diagrams). *Given two compact sets $\mathbb{X}, \mathbb{Y} \subset \mathbb{R}^d$,*

$$W_\infty\left(\mathfrak{Dgm}(\mathbb{V}[\mathbb{X}]), \mathfrak{Dgm}(\mathbb{V}[\mathbb{Y}])\right) \leq H(\mathbb{X}, \mathbb{Y}).$$

Alternatively, for two filter functions $f, g : \mathbb{R}^d \rightarrow \mathbb{R}$,

$$W_\infty\left(\mathfrak{Dgm}(\mathbb{V}[f]), \mathfrak{Dgm}(\mathbb{V}[g])\right) \leq \|f - g\|_\infty.$$

Remark A.2. *Given two persistence modules \mathbb{V} and \mathbb{W} and their associated persistence diagrams $\mathfrak{Dgm}(\mathbb{V})$ and $\mathfrak{Dgm}(\mathbb{W})$, the following relationships hold:*

- (i) *When the interleaving maps (α, β) are additive, i.e., of the form $\alpha : t \mapsto t + \epsilon$ and $\beta : t \mapsto t + \delta$, then persistence diagrams $\mathfrak{Dgm}(\mathbb{V})$ and $\mathfrak{Dgm}(\mathbb{W})$ obtained from the persistence modules satisfy the following relationships:*

$$\mathfrak{Dgm}(\mathbb{V}) \in \mathfrak{Dgm}(\mathbb{W}) \oplus [-\delta, \epsilon]^2 \quad \text{and} \quad \mathfrak{Dgm}(\mathbb{W}) \in \mathfrak{Dgm}(\mathbb{V}) \oplus [-\epsilon, \delta]^2,$$

where \oplus denotes the Minkowski sum in \mathbb{R}^2 . A coarser bound is obtained from the stability theorem, which guarantees that

$$W_\infty(\mathfrak{Dgm}(\mathbb{V}), \mathfrak{Dgm}(\mathbb{W})) \leq \max\{\epsilon, \delta\}.$$

- (ii) *Furthermore, when the interleaving maps are identical, i.e., $\alpha \equiv \beta : t \mapsto t + \epsilon$, this notion can be extended to define an interleaving pseudo-distance between persistence modules,*

$$d_{\mathcal{I}}(\mathbb{V}, \mathbb{W}) \doteq \inf \left\{ \epsilon > 0 : \mathbb{V} \text{ and } \mathbb{W} \text{ are } (\alpha, \alpha)\text{-interleaved for } \alpha : t \mapsto t + \epsilon \right\}.$$

From the isometry theorem (Chazal et al., 2016) the interleaving distance is identical to the bottleneck distance, i.e., $W_\infty(\mathfrak{Dgm}(\mathbb{V}), \mathfrak{Dgm}(\mathbb{W})) = d_{\mathcal{I}}(\mathbb{V}, \mathbb{W})$. Therefore, with a slight abuse of notation, for the proofs in Appendix B we use $W_\infty(\mathbb{V}, \mathbb{W})$ to denote the interleaving distance between the persistence modules \mathbb{V} and \mathbb{W} . In such cases, it is equivalent to say that \mathbb{V} and \mathbb{W} are (α, α) -interleaved or $d_{\mathcal{I}}(\mathbb{V}, \mathbb{W}) \leq \epsilon$. Similarly, for filtrations V and W comprising of subsets of \mathbb{R}^d ,

$$d_{\mathcal{I}}(V, W) \doteq \inf \left\{ \epsilon > 0 : V^t \subseteq W^{t+\epsilon} \quad \text{and} \quad W^t \subseteq V^{t+\epsilon} \right\}. \quad (18)$$

Moreover, $d_{\mathcal{I}}(V, W) \leq \epsilon \implies d_{\mathcal{I}}(\mathbb{V}, \mathbb{W}) \leq \epsilon \implies W_\infty(\mathfrak{Dgm}(\mathbb{V}), \mathfrak{Dgm}(\mathbb{W})) \leq \epsilon$.

A.2. Weighted Rips Filtrations

In practice, given a compact set $\mathbb{X} \subset \mathbb{R}^d$ or a filter function f , the persistence modules $\mathbb{V}[\mathbb{X}]$ and $\mathbb{V}[f]$ are computed using simplicial complexes. In particular:

- (i) For each $t \in \mathbb{R}$, one may use the Čech or Alpha complex to compute the nerve of the cover, $\text{nerve}\{B(\mathbf{x}, t) : \mathbf{x} \in \mathbb{X}\}$. Since the Nerve lemma (Edelsbrunner and Harer, 2010) guarantees that $V^t[\mathbb{X}] \cong \text{nerve}\{B(\mathbf{x}, t) : \mathbf{x} \in \mathbb{X}\}$, the resulting persistence module $\mathbb{V}[\mathbb{X}]$ may be computed exactly using simplicial homology.

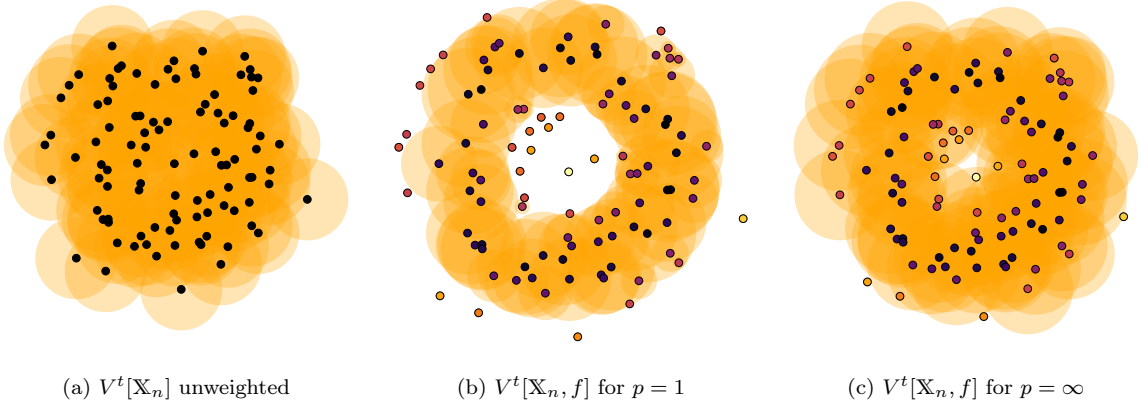


Figure 9: Illustration of offsets for $t = 0.5$ and $f(\mathbf{x}) = \inf_{\mathbf{y} \in S^1} \|\mathbf{x} - \mathbf{y}\|$.

- (ii) In the case of $\mathbb{V}[f]$, this is typically achieved by choosing a grid resolution parameter ϵ , and constructing a cubical complex \mathcal{K}_ϵ on the underlying space. The function $f : \mathbb{R}^d \rightarrow \mathbb{R}$ may be extended to define $f : \mathcal{K}_\epsilon \rightarrow \mathbb{R}$, and at each resolution $t \in \mathbb{R}$, the sublevel sets $V^t[f_{\mathbb{X}}]$ can be approximated using the lower-star filtration $\mathcal{K}_\epsilon^t = \{\sigma \in \mathcal{K}_\epsilon : \max_{\mathbf{x} \in \sigma} f(\mathbf{x}) \leq t\}$. Therefore, the filtration $\mathbb{V}[f]$ can be approximated by the filtration $\{\mathcal{K}_\epsilon^t : t \in \mathbb{R}\}$, and the resulting persistence module is computed using cubical homology.

Note that (i) is able to compute the exact persistence module in practice, but is unable to weight points according to f . On the other hand, (ii) is only an approximate computation and depends on the nuisance parameter ϵ . Furthermore, the size of the cubical complex is $|\mathcal{K}_\epsilon| = O(\epsilon^{-d})$, making it scale poorly in high dimensions. To overcome this limitation, Buchet et al. (2016) proposed the f -weighted filtrations, which was subsequently generalized by Anai et al. (2019).

Given a non-negative *weight function* $f : \mathbb{R}^d \rightarrow \mathbb{R}_{\geq 0}$ and *power* $1 \leq p \leq \infty$, the *weighted radius function* of resolution $t > 0$ at \mathbf{x} is given by

$$r_{f,\mathbf{x}}(t) \doteq \begin{cases} (t^p - f(\mathbf{x})^p)^{1/p} & \text{if } t \geq f(\mathbf{x}) \\ -\infty & \text{if } t < f(\mathbf{x}). \end{cases}$$

Consequently, $B_{f,\rho}(\mathbf{x}, t)$ is the *weighted ball of resolution t at \mathbf{x}* w.r.t. the metric ρ , which is illustrated in Figure 9, and is given by

$$B_{f,\rho}(\mathbf{x}, t) \doteq B_\rho(\mathbf{x}, r_{f,\mathbf{x}}(t)) = \left\{ \mathbf{y} \in \mathbb{R}^d : \rho(\mathbf{x}, \mathbf{y}) \leq r_{f,\mathbf{x}}(t) \right\}.$$

Given $\mathbb{X} \subseteq \mathbb{R}^d$, the collection of weighted balls $\mathcal{V}^t[\mathbb{X}, f] = \{B_f(\mathbf{x}, t) : \mathbf{x} \in \mathbb{X}\}$, is called the *weighted cover* of \mathbb{X}_n . The f -weighted offset at resolution t is given by the union of balls in $\mathcal{V}^t[\mathbb{X}, f]$,

$$V^t[\mathbb{X}, f] \doteq \bigcup_{\mathbf{x} \in \mathbb{X}} B_f(\mathbf{x}, t).$$

Together with the inclusion maps $\iota_s^t : V^s[\mathbb{X}, f] \hookrightarrow V^t[\mathbb{X}, f]$, the f -weighted filtration is given by

$$V[\mathbb{X}, f] \doteq \{V^t[\mathbb{X}, f], \iota_s^t : s \leq t\}.$$

The image of $V[\mathbb{X}, f]$ under the *homology functor* $\mathbf{Hom}_* : V[\mathbb{X}, f] \mapsto \mathbb{V}[\mathbb{X}, f]$, results in the *weighted persistence module* $\mathbb{V}[\mathbb{X}, f] \doteq \{\mathbb{V}^t[\mathbb{X}, f], \phi_s^t : s \leq t\}$, where the induced maps

$\phi_s^t : \mathbb{V}^s[\mathbb{X}, f] \rightarrow \mathbb{V}^t[\mathbb{X}, f]$ are linear maps between vector spaces. The weighted-simplicial complexes

$$\mathcal{C}^t[\mathbb{X}, f] = \text{nerve}\{\mathcal{V}^t[\mathbb{X}, f]\} \quad \text{and} \quad \mathcal{R}^t[\mathbb{X}, f] = \text{Rips}\{\mathcal{V}^t[\mathbb{X}, f]\}$$

denote the weighted-Čech complex and weighted-Rips complex associated with the weighted cover $\mathcal{V}^t[\mathbb{X}, f]$ respectively. Without loss of generality $\mathbb{V}^t[\mathbb{X}, f] = \mathbb{H}_*(V^t[\mathbb{X}, f])$ is the homology of the offset $V^t[\mathbb{X}, f]$, which, by the nerve lemma, is the same as the homology of the weighted-Čech complex. Furthermore, if $f(\mathbf{x}) \equiv 0$ for all $\mathbf{x} \in \mathbb{R}^d$ then the resulting filtrations are the usual unweighted filtrations. In particular, $V[\mathbb{X}_n] \cong \mathcal{C}[\mathbb{X}_n, f]$ and $\mathcal{R}[\mathbb{X}_n, f]$ correspond to Čech and Rips filtrations, respectively. The following structural results appear in Anai et al. (2019), and serve as analogues of the stability result for f -weighted filtrations.

Lemma A.2 (Anai et al., 2019, Propositions 3.2 & 3.3). *Given $\mathbb{X} \subset \mathbb{R}^d$ and $f, g : \mathbb{X} \rightarrow \mathbb{R}$*

- (i) $\mathbb{V}[\mathbb{X}, f]$ and $\mathbb{V}[\mathbb{X}, g]$ are (α, α) -interleaved for $\alpha : t \mapsto t + \|f - g\|_\infty$.

Additionally, given $\mathbb{Y} \subset \mathbb{R}^d$ and $h : \mathbb{X} \cup \mathbb{Y} \rightarrow \mathbb{R}_+$, if h is L -Lipschitz and $\mathbb{H}(\mathbb{X}, \mathbb{Y}) \leq \epsilon$, then

- (ii) $\mathbb{V}[\mathbb{X}, h]$ and $\mathbb{V}[\mathbb{Y}, h]$ are (β, β) -interleaved for $\beta : t \mapsto t + \epsilon(1 + L^p)^{1/p}$.

Table 3: Glossary of Notation

NOTATION	DESCRIPTION
$\mathbb{H}_\rho(\mathbb{X}, \mathbb{Y})$	Hausdorff distance between $\mathbb{X} \subseteq \mathcal{M}$ and $\mathbb{Y} \subseteq \mathcal{M}$ measured w.r.t. metric ρ .
$V^t[f]$	Sublevel set of f at level t given by $\{\mathbf{x} \in \mathbb{R}^d : f(\mathbf{x}) \leq t\}$
$V[f]$ and $\mathbb{V}[f]$	Sublevel filtration $\{V^t[f] : t \in \mathbb{R}\}$ and its persistence module $\mathbf{Hom}(V[f])$
$r_{f,\mathbf{x}}(t)$	The f -weighted radius function of resolution t at \mathbf{x} . $r_{f,\mathbf{x}}(t) = (t^p - f(\mathbf{x})^p)^{\frac{1}{p}}$
$B_{f,\rho}(\mathbf{x}, t)$	f -weighted ball at \mathbf{x} with radius $r_{f,\mathbf{x}}(t)$ w.r.t the metric ρ .
$V^t[\mathbb{X}, f]$	The f -weighted offset of \mathbb{X} at resolution t given by $V^t[\mathbb{X}, f] = \bigcup_{\mathbf{x} \in \mathbb{X}} B_{f,\rho}(\mathbf{x}, t)$
$V[\mathbb{X}, f]$	f -weighted filtration $\{V^t[\mathbb{X}, f] : t \in \mathbb{R}\}$ s.t. $V^s[\mathbb{X}, f] \subseteq V^t[\mathbb{X}, f]$ for all $s \leq t$.
$\mathbb{V}[\mathbb{X}, f]$	f -weighted persistence module, i.e., $\mathbb{V}[\mathbb{X}, f] = \{\mathbb{V}^t[f], \phi_s^t : s \leq t\}$ for linear maps ϕ_s^t .
$\mathcal{D}\mathbf{gm}(\mathbb{V})$	Persistence diagram associated with the persistence module \mathbb{V}
$\hat{\theta}_{n,Q}$	MoM-estimator, median $\{\hat{\theta}_1, \dots, \hat{\theta}_Q\}$, where $\hat{\theta}_q$ is the estimator from block S_q .
$\mathbf{d}_{n,Q}$	MoM Dist function given by $\mathbf{d}_{n,Q}(\mathbf{x}) = \text{median}\{\inf_{\mathbf{y} \in S_q} \ \mathbf{x} - \mathbf{y}\ : q \in [Q]\}$
$\mathbf{d}_{\mathbb{X}}$	Distance function to a compact set \mathbb{X} given by $\mathbf{d}_{\mathbb{X}}(\mathbf{y}) = \inf_{\mathbf{x} \in \mathbb{X}} \ \mathbf{x} - \mathbf{y}\ $

B. Proofs

Notation. We adopt the notations introduced in the main text. A glossary of notation is provided in Table 3 for the reader's convenience. In the proofs, we use $\text{id} : b \mapsto b$ to denote the identity map, and we also use $a \lesssim b$, equivalently $b \gtrsim a$, if there exists a constant $C > 0$ such that $a \leq Cb$. Throughout, we use C, c, C_1, C_2, \dots to denote constants whose values may change from line to line, but are independent of the other parameters of the problem. With a slight abuse of notation and in the interest of brevity, we use $W_\infty(\mathbb{V}, \mathbb{W})$ to denote $W_\infty(\mathcal{D}\mathbf{gm}(\mathbb{V}), \mathcal{D}\mathbf{gm}(\mathbb{W}))$ which is equivalent to the interleaving distance between the persistence modules \mathbb{V} and \mathbb{W} from Remark A.2 (ii).

B.1. Proof for Theorem 3.1

Notation. First, we introduce some notation in order to simplify the presentation of the proof. Fix $\mathcal{P} = \mathcal{P}(\mathbb{X}, a, b)$ and $\pi \doteq m/n$, and for samples $\mathbb{X}_n = \{\mathbf{X}_1, \dots, \mathbf{X}_n\}$, let \mathbb{P}_n denote its empirical distribution. Let $\mathcal{M}^{HC}(\mathcal{P}, \pi)$ denote the set of all empirical distributions satisfying

the Huber contamination model (Eq. (55) in Appendix D) with fraction π , i.e., $\mathbb{P}_n \in \mathcal{M}^{\text{HC}}(\mathcal{P}, \pi)$ if there exists $\mathbb{P} \in \mathcal{P}$ and a probability distribution \mathbb{Q} such that

$$\{\mathbf{X}_i : i \in [n]\} \stackrel{\text{iid}}{\sim} \mathbb{P}_{\pi, \mathbb{Q}} \quad \text{where} \quad \mathbb{P}_{\pi, \mathbb{Q}} = (1 - \pi)\mathbb{P} + \pi\mathbb{Q}. \quad (19)$$

Following Bateni and Dalalyan (2020, Section 2.2), let $\mathcal{M}^{\text{HDC}}(\mathcal{P}, \pi)$ denote the set of all empirical distributions satisfying the *Huber deterministic contamination* model, where $\mathbb{P}_n \in \mathcal{M}^{\text{HDC}}(\mathcal{P}, \pi)$ if there exists $\mathbb{P} \in \mathcal{P}$, a distribution \mathbb{Q} , and a set $\mathcal{O} \subset [n]$ such that

$$|\mathcal{O}| = n\pi, \quad \mathbf{X}_{n-m}^* = \{\mathbf{X}_i : i \in \mathcal{O}^c\} \stackrel{\text{iid}}{\sim} \mathbb{P}, \quad \text{and} \quad \mathbf{Y}_m = \{\mathbf{X}_i : i \in \mathcal{O}\} \stackrel{\text{iid}}{\sim} \mathbb{Q}. \quad (20)$$

Finally, let $\mathcal{M}^{\mathcal{S}}(\mathcal{P}, \pi)$ denote the set of all empirical distributions satisfying sampling setting (\mathcal{S}) , where $\mathbb{P}_n \in \mathcal{M}^{\mathcal{S}}(\mathcal{P}, \pi)$ if there exists $\mathbb{P} \in \mathcal{P}$ and a set $\mathcal{O} \subset [n]$ such that

$$|\mathcal{O}| = n\pi, \quad \mathbf{X}_{n-m}^* = \{\mathbf{X}_i : i \in \mathcal{O}^c\} \stackrel{\text{iid}}{\sim} \mathbb{P}, \quad \text{and} \quad \mathbf{Y}_m = \{\mathbf{X}_i : i \in \mathcal{O}\} \sim \mathbb{Q}_{\mathcal{O}}, \quad (21)$$

where $\mathbb{Q}_{\mathcal{O}}$ is an arbitrary joint distribution on \mathbf{Y}_m . Let $\widehat{\mathbf{D}}_n$ be an estimator of the persistence diagram based on the sample \mathbf{X}_n , and let $\mathfrak{R}(\widehat{\mathbf{D}}_n, \mathcal{M}(\mathcal{P}, \pi))$ be the worst-case risk under the contamination model $\mathcal{M}(\mathcal{P}, \pi)$, given by

$$\mathfrak{R}(\widehat{\mathbf{D}}_n, \mathcal{M}(\mathcal{P}, \pi)) \doteq \sup_{\mathbb{P}_n \in \mathcal{M}(\mathcal{P}, \pi)} \mathbb{E}_{\mathbb{P}} \left[W_{\infty} \left(\widehat{\mathbf{D}}_n, \mathfrak{Dgm}(\mathbb{V}[\mathbf{X}]) \right) \right].$$

Note that $\mathfrak{R}_{n,m}(\mathcal{P}) = \inf_{\widehat{\mathbf{D}}_n} \mathfrak{R}(\widehat{\mathbf{D}}_n, \mathcal{M}^{\mathcal{S}}(\mathcal{P}, \pi))$. The proof of Theorem 3.1 requires the following bound on the minimax risk under the Huber contamination model.

Lemma B.1. *For $\pi \in (0, 1)$ and $\mathcal{P} = \mathcal{P}(\mathbb{X}, a, b)$, let $\mathcal{M}^{\text{HC}}(\mathcal{P}, \pi)$ be the Huber contamination model in Eq. (19). Then, there exist absolute constants $C, c > 0$ such that*

$$\inf_{\widehat{\mathbf{D}}_n} \sup_{\mathbb{P}_n \in \mathcal{M}^{\text{HC}}(\mathcal{P}, \frac{\pi}{2})} \mathbb{P} \left\{ W_{\infty} \left(\widehat{\mathbf{D}}_n, \mathfrak{Dgm}(\mathbb{V}[\mathbf{X}]) \right) \geq C \left(\left(\frac{\pi}{2 - \pi} \right)^{1/b} \vee \left(\frac{\log n}{n} \right)^{1/b} \right) \right\} \geq c. \quad (22)$$

The proof of Lemma B.1 is deferred to Appendix B.1.1. We now proceed with the proof of Theorem 3.1.

Proof. Let $\mathfrak{R}_n^{\circ}(\mathcal{P}) = \mathfrak{R}_{n,0}(\mathcal{P})$ be the minimax lower bound in the absence of any contamination, i.e., when $m = 0$. From Theorem 4 and Theorem 5 of Chazal et al. (2015b),

$$\mathfrak{R}_n^{\circ}(\mathcal{P}) \gtrsim \left(\frac{\log n}{n} \right)^{1/b}. \quad (23)$$

For the claim in Eq. (4), we want to show that

$$\mathfrak{R}_{n,m}(\mathcal{P}) \gtrsim \left(\frac{\pi}{2 - \pi} \right)^{1/b} \vee \left(\frac{\log n}{n} \right)^{1/b} =: r_n(\pi). \quad (24)$$

We first note that it suffices to show Eq. (24) holds for all $\pi > \log n/n$. Indeed, if $\pi \leq \log n/n$, then

$$\frac{\pi}{2 - \pi} \leq \frac{\log n}{2n - \log n} \leq \frac{\log n}{n}. \quad (25)$$

Moreover, since the sampling setting (\mathcal{S}) encompasses the scenario where the samples \mathbf{X}_n are obtained i.i.d. from $\mathbb{P} \in \mathcal{P}$ (i.e., $\{\mathbf{X}_i : i \in \mathcal{O}\} \sim \mathbb{P}$), when $\pi \leq \log n/n$, the bound in Eq. (24) follows trivially from Eq. (23) and Eq. (25), i.e.,

$$\mathfrak{R}_{n,m}(\mathcal{P}) \gtrsim \mathfrak{R}_n^{\circ}(\mathcal{P}) \gtrsim \left(\frac{\log n}{n} \right)^{1/b} = r_n(\pi). \quad (26)$$

Therefore, we assume $\log n/n < \pi < 1/2$ in the remainder of the proof.

From Eq. (20) and Eq. (21) it is clear that $\mathcal{M}^{\text{HDC}}(\mathcal{P}, \pi) \subseteq \mathcal{M}^{\text{s}}(\mathcal{P}, \pi)$, and

$$\mathfrak{R}_{n,m}(\mathcal{P}) = \inf_{\widehat{\mathcal{D}}_n} \mathfrak{R}(\widehat{\mathcal{D}}_n, \mathcal{M}^{\text{s}}(\mathcal{P}, \pi)) \geq \inf_{\widehat{\mathcal{D}}_n} \mathfrak{R}(\widehat{\mathcal{D}}_n, \mathcal{M}^{\text{HDC}}(\mathcal{P}, \pi)).$$

Furthermore, from Proposition 1 of Bateni and Dalalyan (2020), for all $r > 0$ we have

$$\inf_{\widehat{\mathcal{D}}_n} \mathfrak{R}(\widehat{\mathcal{D}}_n, \mathcal{M}^{\text{HDC}}(\mathcal{P}, \pi)) \geq \left(\inf_{\widehat{\mathcal{D}}_n} \sup_{\mathbb{P}_n \in \mathcal{M}^{\text{HC}}(\mathcal{P}, \frac{\pi}{2})} r \mathbb{P} \left\{ W_\infty(\widehat{\mathcal{D}}_n, \mathfrak{Dgm}(\mathbb{V}[\mathbb{X}])) > r \right\} \right) - r e^{-n\pi/6}, \quad (27)$$

Note that first term on the right hand side of Eq. (27) is lower bounded by Lemma B.1. Therefore, setting $r = Cr_n(\pi)$ in Eq. (27) we get

$$\mathfrak{R}_{n,m}(\mathcal{P}) \geq Cr_n(\pi) \left(c - e^{-n\pi/6} \right) \geq Cr_n(\pi) \left(c - e^{-\log n/6} \right), \quad (28)$$

where the final inequality follows by noting that $e^{-n\pi/6} \leq e^{-\log n/6}$ for $\pi > \log n/n$. For sufficiently large⁶ n , it follows that

$$\mathfrak{R}_{n,m}(\mathcal{P}) \geq \frac{C}{2} \cdot r_n(\pi) = \frac{C}{2} \cdot \left(\frac{\pi}{2-\pi} \right)^{1/b} \vee \left(\frac{\log n}{n} \right)^{1/b}. \quad (29)$$

Combining the bound in Eq. (26) for $\pi \leq \log n/n$ and the bound in Eq. (29) for $\pi > \log n/n$ gives the desired lower bound in Eq. (24).

For the bound in Eq. (5), note that when $m = cn^\epsilon$ for $0 < \epsilon < 1$ and $c > 0$, we have $2n - m \gtrsim n$, from which it follows that $m/(2n - m) \lesssim (1/n)^{1-\epsilon}$. Therefore, for $\epsilon > 0$ we have $(1/n)^{1-\epsilon} \gg \log n/n$, and

$$\mathfrak{R}_{n,m}(\mathcal{P}) \gtrsim \left(\frac{1}{n^{1-\epsilon}} \right)^{1/b}. \quad (30)$$

This completes the proof of Theorem 3.1. ■

B.1.1. Proof of Lemma B.1

Proof. From Theorem 5.1 of Chen et al. (2018) (see Theorem D.1 in Appendix D), there exist absolute constants $C > 0$ and $c \in (0, 1)$ such that

$$\inf_{\widehat{\mathcal{D}}_n} \sup_{\mathbb{P}_n \in \mathcal{M}^{\text{HC}}(\mathcal{P}, \frac{\pi}{2})} \mathbb{P} \left\{ W_\infty(\widehat{\mathcal{D}}_n, \mathfrak{Dgm}(\mathbb{V}[\mathbb{X}])) \gtrsim r_n(0) \vee \omega(\pi/2, \mathcal{P}, W_\infty) \right\} \geq c, \quad (31)$$

where $r_n(0)$ is the minimax rate of convergence in the absence of any contamination, and $\omega(\pi/2, \mathcal{P}, W_\infty)$ is the total-variation modulus of continuity of the bottleneck distance W_∞ , given by

$$\omega(\pi/2, \mathcal{P}, W_\infty) = \sup \left\{ W_\infty(\mathfrak{Dgm}(\mathbb{X}_1), \mathfrak{Dgm}(\mathbb{X}_2)) : \text{TV}(\mathbb{P}_1, \mathbb{P}_2) \leq \frac{\pi/2}{1 - \pi/2} \right\},$$

for $\mathbb{X}_i = \text{supp}(\mathbb{P}_i)$. See, also, Definition D.1. From Eq. (23) and by standard protocol for reduction of the minimax risk using Markov's inequality (see, e.g., Chapter 2.2 of Tsybakov, 2008), we have $r_n(0) = \mathfrak{R}_n^{\text{o}}(\mathcal{P}) \gtrsim (\log n/n)^{1/b}$, and it remains to establish a lower bound for $\omega(\pi/2, \mathcal{P}, W_\infty)$.

⁶It suffices for $n \geq (2/c)^6$.

To this end, for $b \leq d$ let $B_b(r)$ denote the b -dimensional closed ball of radius r embedded in \mathbb{R}^d and centered at the origin, i.e.,

$$B_b(0, r) = \left\{ \mathbf{x} = (\mathbf{y}, \mathbf{0}_{d-b}) \in \mathbb{R}^d : \|\mathbf{y}\| \leq r \right\}.$$

Further, let $\mathbb{P}_1 = \text{Unif}(B_b(1))$ and $\mathbb{P}_2 = \text{Unif}(B_b(1) \setminus B_b(r))$ for some $r \in (0, 1)$, i.e., \mathbb{P}_2 is the uniform distribution on the spherical shell. The total variation distance between \mathbb{P}_1 and \mathbb{P}_2 is given by

$$\begin{aligned} \text{TV}(\mathbb{P}_1, \mathbb{P}_2) &= \int_{B_b(1)} \left| \frac{\mathbf{1}\{\mathbf{x} \in B_b(1)\}}{\text{vol}(B_b(1))} - \frac{\mathbf{1}\{\mathbf{x} \in B_b(1) \setminus B_b(r)\}}{\text{vol}(B_b(1) \setminus B_b(r))} \right| d\mathbf{x} \\ &= r^b \cdot |1 - 0| + (1 - r^b) \cdot \left| \frac{1}{1 - r^b} - 1 \right| = r^b. \end{aligned}$$

Moreover, by construction, $\mathbb{X}_2 = B_b(1) \setminus B_b(0)$ has a b -dimensional hole of radius r in the center whereas $\mathbb{X}_1 = B_b(1)$ has trivial order- b homology. In other words, the b -th order persistence diagram $\mathfrak{Dgm}_b(\mathbb{X}_1)$ is empty and $\mathfrak{Dgm}_b(\mathbb{X}_2)$ has a single point at $(0, r)$, and,

$$W_\infty(\mathfrak{Dgm}_b(\mathbb{X}_1), \mathfrak{Dgm}_b(\mathbb{X}_2)) = r.$$

Therefore,

$$\omega(\pi/2, \mathcal{P}, W_\infty) = \sup \left\{ r : r^b \leq \frac{\pi/2}{1 - \pi/2} \right\} = \left(\frac{\pi/2}{1 - \pi/2} \right)^{1/b} = \left(\frac{\pi}{2 - \pi} \right)^{1/b}.$$

■

B.2. Proof for Lemma 4.1

We begin by noting that for each $q \in [Q]$, the distance function \mathbf{d}_{n, S_q} associated with the block S_q is 1-Lipschitz (Boissonnat et al., 2018, Chapter 9.1). Thus, for each $q \in [Q]$ and for all $\mathbf{x}, \mathbf{y} \in \mathbb{R}^d$ we have that

$$0 \leq \mathbf{d}_{n, q}(\mathbf{x}) \leq \mathbf{d}_{n, q}(\mathbf{y}) + \|\mathbf{x} - \mathbf{y}\|,$$

and, therefore, it follows that

$$\text{median}\{\mathbf{d}_{n, q}(\mathbf{x}) : q \in [Q]\} \leq \text{median}\{\mathbf{d}_{n, q}(\mathbf{y}) : q \in [Q]\} + \|\mathbf{x} - \mathbf{y}\|.$$

As a result, we obtain that $\mathbf{d}_{n, Q}(\mathbf{x}) \leq \mathbf{d}_{n, Q}(\mathbf{y}) + \|\mathbf{x} - \mathbf{y}\|$. Exchanging \mathbf{x} and \mathbf{y} in the steps above yields the desired result. ■

B.3. Proof of Theorem 5.1

For the sake of brevity, we use $\mathfrak{Dgm}(f)$ to denote $\mathfrak{Dgm}(\mathbb{V}[f])$. First, we note from the stability of persistence diagrams that,

$$\mathbb{P} \left\{ W_\infty \left(\mathfrak{Dgm}(\mathbf{d}_{n, Q}), \mathfrak{Dgm}(\mathbf{d}_{\mathbb{X}}) \right) > 2t \right\} \leq \mathbb{P} \left\{ \|\mathbf{d}_{n, Q} - \mathbf{d}_{\mathbb{X}}\|_\infty > 2t \right\}. \quad (32)$$

Therefore, it suffices to control the probability of the event $\{\|\mathbf{d}_{n, Q} - \mathbf{d}_{\mathbb{X}}\|_\infty > 2t\}$. To this end, let $A = \{q \in [Q] : S_q \cap \mathbb{Y}_m = \emptyset\}$ be the blocks which contain no outliers. From the assumption on Q , i.e., $2m < Q < n$, it follows that, and $|A| > Q/2$. For $q \in [Q]$, let $\xi_q(2t; n, Q)$ be given by

$$\xi_q(2t; n, Q) = \mathbf{1} \left(\|\mathbf{d}_{n, q} - \mathbf{d}_{\mathbb{X}}\|_\infty > 2t \right).$$

On application of Lemma C.1 to the estimator $\mathbf{d}_{n,Q}$, it follows that

$$\mathbb{P}\left\{\|\mathbf{d}_{n,Q} - \mathbf{d}_{\mathbb{X}}\|_{\infty} > 2t\right\} \leq \mathbb{P}\left(\sum_{q \in A} \xi_q(2t; n, Q) > \frac{Q}{2} - m\right). \quad (33)$$

Since $S_q \subseteq \mathbb{X}_{n-m}^*$ for all $q \in A$, it follows that $\{\xi_q(2t; n, Q) : q \in A\}$ are i.i.d. $\text{Ber}(p(2t; n, Q))$ random variables, where

$$p(2t; n, Q) = \mathbb{E}(\xi_q(2t; n, Q)) = \mathbb{P}\left(\|\mathbf{d}_{n,q} - \mathbf{d}_{\mathbb{X}}\|_{\infty} > 2t\right).$$

For the remainder of the proof we need two key ingredients: (i) we need an upper bound for $\mathbb{E}(\xi_q(2t; n, Q))$, and (ii) we need a tight bound for the binomial tail probability in Eq. (33).

Bound for $p(2t; n, Q)$. From Chazal et al. (2015b, Theorem 2), under the (a, b) -standard condition it follows that

$$p(2t; n, Q) \leq \frac{2^b}{at^b} \exp\left(-\frac{n}{Q}at^b\right) = \exp\left(-\frac{n}{Q}at^b - \log(at^b) + b \log 2\right). \quad (34)$$

Binomial tail probability bound. For $0 < \epsilon < 1$, using the Chernoff-Hoeffding bound from Lemma D.2 yields,

$$\mathbb{P}\left(\frac{1}{|A|} \sum_{q \in A} \xi_q(2t; n, Q) > \epsilon\right) \leq \exp\left(|A| \left(\frac{2}{e} + \epsilon \log p(2t; n, Q)\right)\right).$$

Using the bound for $p(2t; n, Q)$ from Eq. (34), we obtain

$$\begin{aligned} \mathbb{P}\left(\frac{1}{|A|} \sum_{q \in A} \xi_q(2t; n, Q) > \epsilon\right) &\leq \exp\left(|A| \left(\frac{2}{e} + b\epsilon \log 2 - \epsilon \frac{n}{Q}at^b - \epsilon \log(at^b)\right)\right) \\ &\leq \exp\left(|A| \left(1 + b\epsilon - \epsilon \frac{n}{Q}at^b - \epsilon \log(at^b)\right)\right) \\ &\leq \exp\left(|A| \left(1 + b\epsilon - \epsilon \Omega(t, n/Q)\right)\right), \end{aligned}$$

where, in the last line we use $\Omega(t, n/Q) \doteq (n/Q)at^b + \log(at^b)$ for brevity. When t satisfies the condition that

$$\Omega(t, n/Q) \geq \frac{2(1+b\epsilon)}{\epsilon}, \quad (35)$$

then it implies that

$$1 + b\epsilon - \epsilon \Omega(t, n/Q) \leq -\frac{\epsilon}{2} \Omega(t, n/Q),$$

and we get

$$\mathbb{P}\left(\frac{1}{|A|} \sum_{q \in A} \xi_q(2t; n, Q) > \epsilon\right) \leq \exp\left(-\frac{|A|\epsilon}{2} \Omega(t, n/Q)\right).$$

By setting δ equal to the r.h.s. of the inequality above, we obtain

$$\Omega(t, n/Q) = \frac{2 \log(1/\delta)}{|A|\epsilon}. \quad (36)$$

When $\delta \leq e^{-(1+b)Q}$, using the fact that $Q > |A|$ and $0 < \epsilon < 1$, it follows that

$$\Omega(t, n/Q) = \frac{2 \log(1/\delta)}{|A|\epsilon} \geq \frac{2(1+b)Q}{|A|\epsilon} \geq \frac{2(1+b\epsilon)}{\epsilon},$$

and, therefore, the condition in Eq. (35) is satisfied. Consequently, for $\delta \leq e^{-(1+b)Q}$, on rearranging the terms in Eq. (36) we obtain

$$\mathbb{P} \left(\sum_{q \in A} \xi_q(2t; n, Q) > \frac{2 \log(1/\delta)}{\Omega(t, n/Q)} \right) \leq \delta. \quad (37)$$

Comparing Eq. (33) with Eq. (37) we conclude that

$$\mathbb{P} \left(\sum_{q \in A} \xi_q(2t; n, Q) > \frac{Q-2m}{2} \right) = \mathbb{P} \left(\sum_{q \in A} \xi_q(2t; n, Q) > \frac{2 \log(1/\delta)}{\Omega(t, n/Q)} \right) \leq \delta,$$

by setting

$$\frac{2 \log(1/\delta)}{\Omega(t, n/Q)} = \frac{Q-2m}{2} \iff \Omega(t, n/Q) = \frac{4 \log(1/\delta)}{Q-2m}.$$

Since $\Omega(t, n/Q) = \frac{n}{Q} at^b + \log(at^b)$, this is equivalent to

$$\exp\left(\frac{n}{Q} at^b\right) \frac{n}{Q} at^b = \frac{n}{Q} \exp\left(\frac{4 \log(1/\delta)}{Q-2m}\right).$$

Moreover, using the fact that the Lambert \mathcal{W}_0 function satisfies $\mathcal{W}_0(x)e^{\mathcal{W}_0(x)} = x$ (Hassani, 2005), we obtain that

$$t = \left(\frac{Q}{an} \mathcal{W}_0 \left(\frac{n}{Q} \exp \left\{ \frac{4 \log(1/\delta)}{Q-2m} \right\} \right) \right)^{1/b}. \quad (38)$$

Therefore, from Eq. (32) and (33), for t satisfying Eq. (38) and for all $\tau \geq t$ we have

$$\mathbb{P} \left\{ \mathcal{W}_\infty \left(\mathfrak{Dgm}(d_{n,Q}), \mathfrak{Dgm}(d_X) \right) > 2\tau \right\} \leq \mathbb{P} \left\{ \mathcal{W}_\infty \left(\mathfrak{Dgm}(d_{n,Q}), \mathfrak{Dgm}(d_X) \right) > 2t \right\} \leq \delta. \quad (39)$$

Since $\delta \leq e^{-(1+b)Q}$, observe that

$$\frac{4 \log(1/\delta)}{Q-2m} \geq \frac{4(1+b)Q}{Q-2m} \geq 4(1+b) > 1.$$

Furthermore, using the fact that $\mathcal{W}_0(z) \leq \log(z)$ for $z > e$ (Hassani, 2005), we may take τ to be

$$\begin{aligned} t &= \left(\frac{Q}{an} \mathcal{W}_0 \left(\frac{n}{Q} \exp \left\{ \frac{4 \log(1/\delta)}{Q-2m} \right\} \right) \right)^{1/b} \leq \left(\frac{Q}{an} \log \left(\frac{n}{Q} \exp \left\{ \frac{4 \log(1/\delta)}{Q-2m} \right\} \right) \right)^{1/b} \\ &= \left(\frac{Q \log(n/Q)}{an} + \frac{4Q \log(1/\delta)}{a(Q-2m)n} \right)^{1/b} \doteq \tau. \end{aligned}$$

Plugging this into Eq. (39), we obtain the desired result.

For the second claim in the theorem, by inverting the relationship between t and δ in Eq. (38) and using the fact that $\mathcal{W}_0(z)$ is an increasing function for $z > 0$, observe that the constraint on δ equivalently specifies a constraint on t , i.e.,

$$\delta \leq e^{-(1+b)Q} \iff t \geq \left(\frac{Q}{an} \mathcal{W}_0 \left(\frac{n}{Q} \exp \left\{ \frac{4(1+b)Q}{Q-2m} \right\} \right) \right)^{1/b}.$$

A sufficient condition for this to hold is that

$$t \geq t(n, Q) \doteq \left(\frac{Q \log(n/Q)}{an} + \frac{4(1+b)Q^2}{a(Q-2m)n} \right)^{1/b}.$$

Therefore, from Eq. (39) we have that for all $t \geq t(n, Q)$

$$\mathbb{P} \left\{ \mathcal{W}_\infty \left(\mathfrak{Dgm}(d_{n,Q}), \mathfrak{Dgm}(d_{\mathbb{X}}) \right) > 2t \right\} \leq \exp \left(- \left(\frac{Q-2m}{4} \right) \Omega(t, n/Q) \right).$$

By taking $\mathbb{P} \left\{ \mathcal{W}_\infty \left(\mathfrak{Dgm}(d_{n,Q}), \mathfrak{Dgm}(d_{\mathbb{X}}) \right) > 2t \right\}$ to be its maximum value of 1 in the interval $[0, 2t(n, Q)]$ we have

$$\begin{aligned} \mathbb{E} \left[\mathcal{W}_\infty \left(\mathfrak{Dgm}(d_{n,Q}), \mathfrak{Dgm}(d_{\mathbb{X}}) \right) \right] &= 2 \int_0^\infty \mathbb{P} \left\{ \mathcal{W}_\infty \left(\mathfrak{Dgm}(d_{n,Q}), \mathfrak{Dgm}(d_{\mathbb{X}}) \right) > 2t \right\} dt \\ &\leq 2t(n, Q) + 2 \int_{2t(n, Q)}^\infty \exp \left(- \left(\frac{Q-2m}{4} \right) \Omega(t, n/Q) \right) dt. \\ &\leq 2t(n, Q) + 2 \int_{2t(n, Q)}^\infty \exp \left(- \frac{\Omega(t, n/Q)}{4} \right) dt. \end{aligned}$$

Let $w = \Omega(t, n/Q)$, i.e., $t = \left(\frac{Q}{an} \mathcal{W}_0 \left(\frac{n}{Q} e^w \right) \right)^{1/b}$. By noting that $\Omega'(t, n/Q) = b(w+1)/t$, and that $t \geq 2t(n, Q)$ implies that $w = \Omega(t, n/Q) \geq 8(1+b)/(Q-2m)$ by Eq. (40), the change of variables from t to w in the integral gives

$$\begin{aligned} \int_{t \geq 2t(n, Q)} \exp \left(- \frac{\Omega(t, n/Q)}{4} \right) dt &\leq \int_{w \geq \frac{8(1+b)}{Q-2m}} e^{-w/4} \cdot \frac{\left(\frac{Q}{an} \mathcal{W}_0 \left(\frac{n}{Q} e^w \right) \right)^{1/b}}{b(w+1)} dw \\ &\lesssim \left(\frac{Q}{n} \right)^{1/b} \int_{r_n}^\infty \frac{e^{-w/4} \left(\mathcal{W}_0 \left(\frac{n}{Q} e^w \right) \right)^{1/b}}{w+1} dw, \end{aligned} \quad (40)$$

where $r_n \doteq 8(1+b)/(Q-2m)$ and the factor $ba^{1/b}$ is absorbed into the symbol \lesssim . Therefore, we have that

$$\begin{aligned} \mathbb{E} \left[\mathcal{W}_\infty \left(\mathfrak{Dgm}(d_{n,Q}), \mathfrak{Dgm}(d_{\mathbb{X}}) \right) \right] &\lesssim t(n, Q) + \left(\frac{Q}{n} \right)^{1/b} \int_{r_n}^\infty \frac{e^{-w/4} \left(\mathcal{W}_0 \left(\frac{n}{Q} e^w \right) \right)^{1/b}}{w+1} dw \end{aligned}$$

$$\stackrel{\text{(ii)}}{\lesssim} t(n, Q) + \underbrace{\left(\frac{\log(n/Q)}{n/Q}\right)^{1/b} \int_{r_n}^{\infty} \frac{e^{-w/4}}{w+1} dw}_{\text{(a)}} + \underbrace{\left(\frac{Q}{n}\right)^{1/b} \int_{r_n}^{\infty} \frac{e^{-w/4} w^{1/b}}{w+1} dw}_{\text{(b)}}, \quad (41)$$

where (ii) follows from the fact that $W_0(z) \leq \log(z)$ for $z > e$ together with, either, an application of Lemma D.1 (iii) when $b \geq 1$, or Lemma D.1 (i) with the additional factor $2^{1/b-1}$ being absorbed in the symbol \lesssim when $b < 1$. The term (a) can be bounded above using the incomplete Γ function as,

$$\text{(a)} = \int_{r_n}^{\infty} \frac{e^{-w/4}}{w+1} dw = e^{1/4} \int_{(r_n+1)/4}^{\infty} v^{-1} e^{-v} dv = e^{1/4} \Gamma(0, (r_n+1)/4) < \infty.$$

Similarly, using the fact that $w+1 > 1$, the term (b) may be bounded above as,

$$\text{(b)} = \int_{r_n}^{\infty} \frac{e^{-w/4} w^{1/b}}{w+1} dw \leq \int_{r_n}^{\infty} e^{-w/4} w^{1/b} dw \leq \int_0^{\infty} e^{-w/4} w^{1/b} dw \leq \frac{\Gamma(1+b^{-1})}{4^{1+1/b}} < \infty,$$

Therefore, the inequality in Eq. (41) becomes

$$\mathbb{E}\left[W_{\infty}\left(\mathfrak{Dgm}(d_{n,Q}), \mathfrak{Dgm}(d_{\mathbf{X}})\right)\right] \lesssim \left(\frac{\log(n/Q)}{n/Q} + \frac{Q^2}{(Q-2m)n}\right)^{1/b} + \left(\frac{Q}{n}\right)^{1/b}.$$

When the number of outliers grows with n as $m_n = cn^{\epsilon}$ where $0 \leq \epsilon < 1$, let the number of blocks be $Q_n = 3cn^{\beta}$, where $\epsilon \leq \beta < 1$. Therefore,

$$\begin{aligned} \mathbb{E}\left[W_{\infty}\left(\mathfrak{Dgm}(d_{n,Q}), \mathfrak{Dgm}(d_{\mathbf{X}})\right)\right] &\lesssim \inf_{\epsilon \leq \beta < 1} \left(\frac{\log(n/n^{\beta})}{n/n^{\beta}} + \frac{n^{2\beta}}{(3n^{\beta} - 2n^{\epsilon})n}\right)^{1/b} + \left(\frac{n^{\beta}}{n}\right)^{1/b} \\ &\lesssim \left(\frac{\log n}{n^{1-\epsilon}}\right)^{1/b}, \end{aligned}$$

which gives us the desired result when $Q_n = 3cn^{\epsilon}$. ■

B.4. Proof of Theorem 6.1

We begin by establishing the following result:

$$W_{\infty}\left(\mathbb{V}[\mathbf{X}_n, d_{n,Q}], \mathbb{V}[\mathbf{X}_{n-m}^*, d_{n,Q}]\right) \leq \sup_{\mathbf{x} \in \mathbf{X}_{n-m}^*} d_{n,Q}(\mathbf{x}) + \left(1 - \frac{1}{p}\right) t(\mathbf{X}_{n-m}^*).$$

Observe that from Lemma C.2 and Lemma C.3, it suffices to show that for every $\mathbf{y} \in \mathbb{Y}_m$ the MoM-Dist function $d_{n,Q}$ satisfies the property that

$$\inf_{\mathbf{x} \in \mathbf{X}_{n-m}^*} \|\mathbf{x} - \mathbf{y}\| \leq d_{n,Q}(\mathbf{y}).$$

To this end, let $A = \{q \in [Q] : S_q \cap \mathbb{Y}_m = \emptyset\}$ be the blocks containing no outliers. For $\mathbf{y} \in \mathbb{Y}_m$ and every $q \in A$, we have that $S_q \subseteq \mathbf{X}_{n-m}^*$, and therefore

$$\inf_{\mathbf{x} \in \mathbf{X}_{n-m}^*} \|\mathbf{x} - \mathbf{y}\| \leq \inf_{\mathbf{x} \in S_q} \|\mathbf{x} - \mathbf{y}\| = d_{n,q}(\mathbf{y}).$$

Since this holds for every $q \in A$, taking the infimum on the right-hand side over A yields

$$\inf_{\mathbf{x} \in \mathbb{X}_{n-m}^*} \|\mathbf{x} - \mathbf{y}\| \leq \inf_{q \in A} \mathbf{d}_{n,q}(\mathbf{y}).$$

Since $2m < Q$ by assumption, using the pigeonhole principle we further have that

$$\inf_{q \in A} \mathbf{d}_{n,q}(\mathbf{y}) \leq \text{median} \left\{ \mathbf{d}_{n,q}(\mathbf{y}) : q \in [Q] \right\},$$

which implies that $\inf_{\mathbf{x} \in \mathbb{X}_{n-m}^*} \|\mathbf{x} - \mathbf{y}\| \leq \mathbf{d}_{n,Q}(\mathbf{y})$ for every $\mathbf{y} \in \mathbb{Y}_m$. Therefore, taking $a = 0$ in Lemma C.2 and Lemma C.3 we obtain

$$W_\infty \left(\mathbb{V}[\mathbb{X}_n, \mathbf{d}_{n,Q}], \mathbb{V}[\mathbb{X}_{n-m}^*, \mathbf{d}_{n,Q}] \right) \leq \sup_{\mathbf{x} \in \mathbb{X}_{n-m}^*} \mathbf{d}_{n,Q}(\mathbf{x}) + \left(1 - \frac{1}{p}\right) t(\mathbb{X}_{n-m}^*). \quad (42)$$

Turning our attention to the quantity appearing in the statement of the theorem, note that an application of the triangle inequality yields

$$\begin{aligned} W_\infty \left(\mathbb{V}[\mathbb{X}_n, \mathbf{d}_{n,Q}], \mathbb{V}[\mathbb{X}_{n-m}^*, \mathbf{d}_{n-m}] \right) &\leq W_\infty \left(\mathbb{V}[\mathbb{X}_n, \mathbf{d}_{n,Q}], \mathbb{V}[\mathbb{X}_{n-m}^*, \mathbf{d}_{n,Q}] \right) \\ &\quad + W_\infty \left(\mathbb{V}[\mathbb{X}_{n-m}^*, \mathbf{d}_{n,Q}], \mathbb{V}[\mathbb{X}_{n-m}^*, \mathbf{d}_{n-m}] \right) \\ &\stackrel{(*)}{\leq} \sup_{\mathbf{x} \in \mathbb{X}_{n-m}^*} \mathbf{d}_{n,Q}(\mathbf{x}) + \left(1 - \frac{1}{p}\right) t(\mathbb{X}_{n-m}^*) + \|\mathbf{d}_{n,Q} - \mathbf{d}_{n-m}\|_\infty, \end{aligned}$$

where the first term in $(*)$ follows from Eq. (42) and the last term follows from Proposition 2.1. This gives us the desired result. Furthermore, when $p = 1$ note that $1 - 1/p = 0$, giving us the tighter bound in this case. \blacksquare

B.5. Proof of Theorem 6.2

We begin by noting that $\mathbb{V}[\mathbb{X}] = \mathbb{V}[\mathbb{X}, \mathbf{d}_\mathbb{X}]$. Indeed, the distance function $\mathbf{d}_\mathbb{X}(\mathbf{x}) = 0$ for all $\mathbf{x} \in \mathbb{X}$. We may further conclude that

$$\sup_{\mathbf{x} \in \mathbb{X}} \mathbf{d}_\mathbb{X}(\mathbf{x}) = 0. \quad (43)$$

The bottleneck distance between $\mathbb{V}[\mathbb{X}_{n-m}^* \cup \mathbb{Y}_m, \mathbf{d}_{n,Q}]$ and $\mathbb{V}[\mathbb{X}]$ may be bounded above as

$$\begin{aligned} W_\infty \left(\mathbb{V}[\mathbb{X}_{n-m}^* \cup \mathbb{Y}_m, \mathbf{d}_{n,Q}], \mathbb{V}[\mathbb{X}] \right) &\leq W_\infty \left(\mathbb{V}[\mathbb{X}_{n-m}^* \cup \mathbb{Y}_m, \mathbf{d}_{n,Q}], \mathbb{V}[\mathbb{X}_{n-m}^*, \mathbf{d}_{n,Q}] \right) &= \textcircled{a} \\ &\quad + W_\infty \left(\mathbb{V}[\mathbb{X}_{n-m}^*, \mathbf{d}_{n,Q}], \mathbb{V}[\mathbb{X}_{n-m}^*, \mathbf{d}_\mathbb{X}] \right) &= \textcircled{b} \\ &\quad + W_\infty \left(\mathbb{V}[\mathbb{X}_{n-m}^*, \mathbf{d}_\mathbb{X}], \mathbb{V}[\mathbb{X}, \mathbf{d}_\mathbb{X}] \right). &= \textcircled{c} \end{aligned}$$

When $p = 1$, the terms $\textcircled{b} \leq \|\mathbf{d}_{n,Q} - \mathbf{d}_\mathbb{X}\|_\infty$ and $\textcircled{c} \leq H(\mathbb{X}_{n-m}^*, \mathbb{X})$ using Proposition 2.1. The term \textcircled{a} is bounded above by taking $p = 1$ in Eq. (42) (from the proof of Theorem 6.1) to give

$$\begin{aligned} \textcircled{a} &= \sup_{\mathbf{x} \in \mathbb{X}_{n-m}^*} \mathbf{d}_{n,Q}(\mathbf{x}) \\ &\stackrel{(*)}{\leq} \sup_{\mathbf{x} \in \mathbb{X}} \mathbf{d}_{n,Q}(\mathbf{x}) \\ &\stackrel{(\dagger)}{\leq} \|\mathbf{d}_{n,Q} - \mathbf{d}_\mathbb{X}\|_\infty + \sup_{\mathbf{x} \in \mathbb{X}} \mathbf{d}_\mathbb{X}(\mathbf{x}) \end{aligned}$$

$$\stackrel{(\ddagger)}{=} \|\mathbf{d}_{n,Q} - \mathbf{d}_{\mathbb{X}}\|_{\infty},$$

where (\star) follows from the fact $\mathbb{X}_{n-m}^* \subset \mathbb{X}$, (\dagger) uses the identity $f(\mathbf{x}) \leq \|f - g\|_{\infty} + g(\mathbf{x})$ for all $\mathbf{x} \in \mathbb{X}$, and (\ddagger) follows from Eq. (43). Plugging in the bounds for the bottleneck distance we obtain

$$W_{\infty} \left(\mathbb{V}[\mathbb{X}_{n-m}^* \cup \mathbb{Y}_m, \mathbf{d}_{n,Q}], \mathbb{V}[\mathbb{X}] \right) \leq 2\|\mathbf{d}_{n,Q} - \mathbf{d}_{\mathbb{X}}\|_{\infty} + \mathbf{H}(\mathbb{X}_{n-m}^*, \mathbb{X}).$$

By noting that the Hausdorff distance $\mathbf{H}(\mathbb{X}_{n-m}^*, \mathbb{X}) = \|\mathbf{d}_{n-m} - \mathbf{d}_{\mathbb{X}}\|_{\infty}$, for t_1, t_2 such that $t_1 + t_2 = t$ we may bound the tail probability for the bottleneck distance as follows.

$$\mathbb{P} \left\{ W_{\infty} \left(\mathbb{V}[\mathbb{X}_{n-m}^* \cup \mathbb{Y}_m, \mathbf{d}_{n,Q}], \mathbb{V}[\mathbb{X}] \right) > 2t \right\} \quad (44)$$

$$\begin{aligned} &\leq \mathbb{P} \left(2\|\mathbf{d}_{n,Q} - \mathbf{d}_{\mathbb{X}}\|_{\infty} > 2t_1 \right) + \mathbb{P} \left(\|\mathbf{d}_{n-m} - \mathbf{d}_{\mathbb{X}}\|_{\infty} > 2t_2 \right) \\ &\leq \delta_1 + \delta_2 = \delta, \end{aligned} \quad (45)$$

where the relationship between δ_1, δ_2 and t_1, t_2 is given by Eq. (38), i.e., $\delta_1 \leq e^{-(1+b)Q}$ from the condition in Theorem 5.1, $\delta_2 = \delta - \delta_1$,

$$t_1 = 2 \left(\frac{Q}{an} \mathcal{W}_0 \left(\frac{n}{Q} \exp \left\{ \frac{4 \log(1/\delta_1)}{Q - 2m} \right\} \right) \right)^{1/b}, \quad \text{and} \quad t_2 = \left(\frac{1}{an - m} \mathcal{W}_0 \left(n - me^{4 \log(1/\delta_2)} \right) \right)^{1/b}. \quad (46)$$

Furthermore, using the bound for the Lambert \mathcal{W}_0 function $\mathcal{W}_0(z) \leq \log z$ for $z > e$, we have

$$t_1 \leq 2 \left(\frac{Q \log(n/Q)}{an} + \frac{4Q \log(1/\delta_1)}{a(Q - 2m)n} \right)^{1/b}, \quad t_2 \leq \left(\frac{\log(n - m)}{a(n - m)} + \frac{4 \log(1/\delta_2)}{a(n - m)} \right)^{1/b},$$

and $t = t_1 + t_2 \leq \mathbf{f}(n, m, Q, \delta_1, \delta_2)$. Therefore, the bound in Eq. (45) yields

$$\begin{aligned} &\mathbb{P} \left\{ W_{\infty} \left(\mathbb{V}[\mathbb{X}_{n-m}^* \cup \mathbb{Y}_m, \mathbf{d}_{n,Q}], \mathbb{V}[\mathbb{X}] \right) \leq 2\mathbf{f}(n, m, Q, a, b) \right\} \\ &\geq \mathbb{P} \left\{ W_{\infty} \left(\mathbb{V}[\mathbb{X}_{n-m}^* \cup \mathbb{Y}_m, \mathbf{d}_{n,Q}], \mathbb{V}[\mathbb{X}] \right) \leq 2t_1 + 2t_2 \right\} \geq 1 - \delta, \end{aligned}$$

which gives the desired result. The second part of the theorem follows directly using the identical procedure as that used in the proof of Theorem 5.1 in Appendix B.3. \blacksquare

Remark B.1. *The result in Theorem 6.2 holds when $p = 1$. For $p \geq 1$, from (Anai et al., 2019, Proposition 3.6) it follows that the number of points in the 0th persistence diagram $\mathfrak{Dgm}(\mathbb{V}[\mathbb{X}_n])$ is non-increasing in p , i.e., choosing $p > 1$ leads to sparser persistence diagrams, and has an appeal from a computational perspective. The following result characterizes the error incurred when using $\mathbb{V}[\mathbb{X}_n, \mathbf{d}_{n,Q}]$ to approximate the sublevel filtration $\mathbb{V}[\mathbf{d}_{n,Q}]$ for $p \geq 1$. In light of Remark 6.1 (ii), the approximation error vanishes with increasing sample size. In contrast, the approximation error for the DTM-filtration is non-vanishing (Anai et al., 2019, Proposition 4.6).*

Proposition B.1. *Let $p \geq 1$. For $\mathbb{X}_n = \mathbb{X}_{n-m}^* \cup \mathbb{Y}_m$ under sampling setting (\mathcal{S}) and $2m < Q < n$, the filtrations $\mathbb{V}[\mathbf{d}_{n,Q}]$ and $\mathbb{V}[\mathbb{X}_n, \mathbf{d}_{n,Q}]$ are (η, ξ) -interleaved, where*

$$\eta(t) = 2^{\frac{p-1}{p}} t + \sup_{\mathbf{x} \in \mathbb{X}_{n-m}^*} \mathbf{d}_{n,Q}(\mathbf{x}) \quad \text{and} \quad \xi(t) = 2^{\frac{p-1}{p}} \eta(t).$$

Proof. We begin by noting from Lemma C.4 that the filtrations $V[\mathbf{d}_{n,Q}]$ and $V[\mathbb{R}^d, \mathbf{d}_{n,Q}]$ are (id, α) -interleaved for $\alpha : t \mapsto 2^{\frac{p-1}{p}} t$. Furthermore, consider the intermediate filtrations $V[\mathbb{X}_{n-m}^*, \mathbf{d}_{n,Q}]$. From Theorem 6.1 and Lemma C.2 we have that $V[\mathbb{R}^d, \mathbf{d}_{n,Q}]$ and $V[\mathbb{X}_{n-m}^*, \mathbf{d}_{n,Q}]$ are (η, id) -interleaved for

$$\eta : t \mapsto 2^{\frac{p-1}{p}} t + \sup_{\mathbf{x} \in \mathbb{X}_{n-m}^*} \mathbf{d}_{n,Q}(\mathbf{x}).$$

Using an identical argument, but reversing the order, we have that $V[\mathbb{X}_{n-m}^*, \mathbf{d}_{n,Q}]$ and $V[\mathbb{X}_n, \mathbf{d}_{n,Q}]$ are (id, η) -interleaved. We can now apply the “*triangle inequality*” for generalized interleavings (Bubenik et al., 2015, Proposition 3.11) to obtain that $V[\mathbf{d}_{n,Q}]$ and $V[\mathbb{X}_n, \mathbf{d}_{n,Q}]$ are $(\text{id} \circ \eta \circ \text{id}, \alpha \circ \text{id} \circ \eta)$ -interleaved. On simplifying the interleaving maps, we obtain that for

$$\xi(t) = \alpha \circ \eta(t) = 2^{\frac{p-1}{p}} \eta(t),$$

the two filtrations are (η, ξ) -interleaved. ■

B.6. Proof of Theorem 7.1

We begin by observing that $\|\mathbf{d}_{n+m} - \mathbf{d}_n\|_\infty$ can be bounded from below as follows:

$$\begin{aligned} \|\mathbf{d}_{n+m} - \mathbf{d}_n\|_\infty &\geq \mathbf{d}_n(\mathbf{x}_0) - \mathbf{d}_{n+m}(\mathbf{x}_0) \\ &= \mathbf{d}_n(\mathbf{x}_0) - 0 \\ &= \inf_{\mathbf{x} \in \mathbb{X}_n} \|\mathbf{x} - \mathbf{x}_0\| \\ &\geq \inf_{\mathbf{x} \in \mathbb{X}} \|\mathbf{x} - \mathbf{x}_0\| = \mathbf{d}_{\mathbb{X}}(\mathbf{x}_0). \end{aligned}$$

Furthermore, for $\delta/2 \leq e^{-(1+b)Q}$ and $k \doteq \max\{1, 2^{\frac{b-1}{b}}\}$, with probability greater than $1 - \delta$,

$$\begin{aligned} &\|\mathbf{d}_{n+m,Q} - \mathbf{d}_n\|_\infty \\ &\stackrel{(i)}{\leq} \|\mathbf{d}_{n+m,Q} - \mathbf{d}_{\mathbb{X}}\|_\infty + \|\mathbf{d}_n - \mathbf{d}_{\mathbb{X}}\|_\infty \\ &\stackrel{(ii)}{\leq} 2 \left[\frac{1}{an_Q} \mathcal{W}_0 \left(n_Q \exp \left\{ \frac{4 \log(2/\delta)}{Q-2m} \right\} \right) \right]^{1/b} + 2 \left[\frac{1}{an} \mathcal{W}_0(n \exp \{4 \log(2/\delta)\}) \right]^{1/b} \\ &\stackrel{(iii)}{\leq} \frac{2k}{a^{1/b}} \left[\frac{1}{n_Q} \mathcal{W}_0 \left(n_Q \exp \left\{ \frac{4 \log(2/\delta)}{Q-2m} \right\} \right) + \frac{1}{n} \mathcal{W}_0(n \exp \{4 \log(2/\delta)\}) \right]^{1/b} \\ &\stackrel{(iv)}{\leq} \frac{2k}{a^{1/b}} \left[\frac{\log n_Q}{n_Q} + \frac{\log n}{n} + 4 \log(2/\delta) \left(\frac{1}{n_Q(Q-2m)} + \frac{1}{n} \right) \right]^{1/b} \\ &\stackrel{(v)}{\leq} \frac{2k2^{1/b}}{a^{1/b}} \left(\frac{\log n_Q + 4 \log(2/\delta)}{n_Q} \right)^{1/b} \doteq \eta(n, m, Q, \delta), \end{aligned}$$

where, for $n_Q = (n+m)/Q$, (i) is a consequence of the triangle inequality and (ii) follows from the proofs of Theorem 5.1 and Theorem 6.2, (iii) uses Lemma D.1, (iv) follows from the fact that $\mathcal{W}_0(z) < \log(z)$ for $z > e$, and (v) uses the fact that $n_Q < n$ and $(Q-2m)^{-1} \leq 1$ for $Q > 2m$.

Observe that if $2\eta(n, m, Q, \delta) \leq \mathbf{d}_{\mathbb{X}}(\mathbf{x}_0)$, then with probability greater than $1 - \delta$,

$$\|\mathbf{d}_{n+m} - \mathbf{d}_n\|_\infty - \|\mathbf{d}_{n+m,Q} - \mathbf{d}_n\|_\infty \geq \mathbf{d}_{\mathbb{X}}(\mathbf{x}_0) - \eta(n, m, Q, \delta) \geq \eta(n, m, Q, \delta), \quad (47)$$

and the result follows. Therefore, in order to establish the claim for the second part it suffices to check that $2\eta(n, m, Q, \delta) \leq \mathbf{d}_{\mathbb{X}}(\mathbf{x}_0)$ under conditions (I) and (II). To this end, note that

$$\mathbf{d}_{\mathbb{X}}(\mathbf{x}_0) \geq 2\eta(n, m, Q, \delta) \iff \varpi(\mathbf{x}_0) \geq \frac{\log n_Q + 4 \log(2/\delta)}{n_Q},$$

which is satisfied whenever δ satisfies the r.h.s. of condition (II), i.e.,

$$\log(2/\delta) \leq \frac{n_Q \varpi(\mathbf{x}_0) - \log n_Q}{4}.$$

Furthermore, the l.h.s. of condition (II), i.e., $\delta \leq 2e^{-(1+b)Q}$, is satisfied only when

$$(1+b)Q \leq \frac{n_Q \varpi(\mathbf{x}_0) - \log n_Q}{4},$$

or, equivalently, when condition (I) is satisfied:

$$\varpi(\mathbf{x}_0) \geq \frac{\log n_Q}{n_Q} + \frac{4(1+b)Q}{n_Q}.$$

The result now follows from Eq. (47). ■

B.7. Proof of Theorem 8.1

Let $j^* = \min \{j \in \mathcal{J} : m(j) \geq m^*\}$. By definition of \mathcal{J} we have that $|\mathcal{J}| \leq 1 + \log_\theta(m_{\max}/m_{\min})$ and $m(j^*) < \theta m^*$ for $\theta > 1$. The outline of the proof is as follows. First, we show that $\mathfrak{h}(n, m, \delta)$ is non-decreasing in m , from which it follows that $\mathfrak{h}(n, m(j), \delta) \leq \mathfrak{h}(n, m(j+1), \delta)$. Next, we show that the event $\{\hat{j} \leq j^*\}$ contains the event \mathcal{E} given by

$$\mathcal{E} = \bigcap_{\{j \in \mathcal{J} : j \geq j^*\}} \left\{ \mathbb{W}_\infty(\mathbb{V}_n(j), \mathbb{V}[\mathbb{X}]) \leq \mathfrak{h}(n, m(j), \delta) \right\}.$$

Then, using a standard procedure for obtaining the Lepski bound (e.g., Theorem 5.1 of Minsker 2018 and Theorem 3.1 of Chen and Zhou 2020), we show that the event \mathcal{E} , and, therefore the event $\{\hat{j} \leq j^*\}$, holds with probability at least $1 - \delta \log_\theta(m_{\max}/m_{\min})$. Lastly, we use the bound on the event $\{\hat{j} \leq j^*\}$ to obtain the desired result.

1. Monotonicity of $\mathfrak{h}(n, m, \delta)$ in m . Consider the function $f(z; \alpha, \beta) = \alpha \mathbb{W}_0(\beta z)/z$ for fixed constants $\alpha, \beta > 0$. The derivative of f is given by

$$\begin{aligned} f'(z; \alpha, \beta) &= \frac{d}{dz} \left(\frac{\alpha}{z} \mathbb{W}_0(\beta z) \right) = \alpha \left(\frac{\beta}{z} \mathbb{W}'_0(\beta z) - \frac{1}{z^2} \mathbb{W}_0(\beta z) \right) \\ &\stackrel{(i)}{=} \alpha \left(\frac{\beta}{z} \left\{ \frac{\mathbb{W}_0(\beta z)}{\beta z (1 + \mathbb{W}_0(\beta z))} \right\} - \frac{1}{z^2} \mathbb{W}_0(\beta z) \right) \\ &= -\frac{\alpha \mathbb{W}_0(\beta z)^2}{z^2 (1 + \mathbb{W}_0(\beta z))} < 0 \quad \text{for all } z > 0. \end{aligned}$$

Note that in (i) we have used the fact that the derivative of the Lambert \mathbb{W}_0 function is given by $\mathbb{W}'_0(z) = \mathbb{W}_0(z)/z(1 + \mathbb{W}_0(z))$. Therefore, it follows that f is non-increasing in z . The claim follows by noting that the function \mathfrak{h} is given by

$$\mathfrak{h}(n, m, \delta) = f(n/(2m+1); \alpha_1, \beta_1)^{1/b} + f(n-m; \alpha_2, \beta_2)^{1/b},$$

for constants $\alpha_1, \beta_1, \alpha_2, \beta_2 > 0$ not depending on n or m .

2. \mathcal{E} is a subset of $\{\hat{j} \leq j^*\}$. We begin by noting that since $m^* \leq m(j^*)$, it follows that $2m^* < Q(j) = 2m(j) + 1$ for all $j \geq j^*$ and satisfies the first condition for Theorem 6.2. By taking

$$\delta_1 = e^{-2(1+b)(2m_{\max}+1)} \leq e^{-2(1+b)Q(j)},$$

and $\delta_2 = \delta - \delta_1$, note that $\mathfrak{h}(n, m(j), \delta) = 2t_1 + 2t_2$ for the two terms, t_1, t_2 , appearing in Eq. (46) from the proof of Theorem 6.2 by taking $m = m(j)$ and $Q = Q(j) = 2m(j) + 1$. Therefore, we may use Theorem 6.2 to obtain

$$\mathbb{P}\left(\mathbb{W}_\infty(\mathbb{V}_n(j), \mathbb{V}[\mathbb{X}]) > \mathfrak{h}(n, m(j), \delta)\right) < \delta \quad \text{for all } j \geq j^*. \quad (48)$$

Furthermore, by definition of \hat{j} , it follows that for all $j < \hat{j}$, there exists at least one $i > j$ such that $\mathbb{W}_\infty(\mathbb{V}_n(i), \mathbb{V}_n(j)) > 2\mathfrak{h}(n, m(i), \delta)$. Therefore,

$$\begin{aligned} \{\hat{j} > j^*\} &\subseteq \bigcup_{\{j \in \mathcal{J}: j > j^*\}} \left\{ \mathbb{W}_\infty(\mathbb{V}_n(j), \mathbb{V}_n(j^*)) > 2\mathfrak{h}(n, m(j), \delta) \right\} \\ &\stackrel{\text{(ii)}}{\subseteq} \bigcup_{\{j \in \mathcal{J}: j > j^*\}} \left\{ \mathbb{W}_\infty(\mathbb{V}_n(j), \mathbb{V}[\mathbb{X}]) > \mathfrak{h}(n, m(j), \delta) \right\} \cup \left\{ \mathbb{W}_\infty(\mathbb{V}_n(j^*), \mathbb{V}[\mathbb{X}]) > \mathfrak{h}(n, m(j^*), \delta) \right\} \\ &= \bigcup_{\{j \in \mathcal{J}: j \geq j^*\}} \left\{ \mathbb{W}_\infty(\mathbb{V}_n(j), \mathbb{V}[\mathbb{X}]) > \mathfrak{h}(n, m(j), \delta) \right\} \doteq \mathcal{E}^c, \end{aligned}$$

where, in (ii) we have used the fact that $\mathfrak{h}(n, m(j^*), \delta) \leq \mathfrak{h}(n, m(j), \delta)$ for all $j > j^*$, and

$$\begin{aligned} &\left\{ \mathbb{W}_\infty(\mathbb{V}_n(j), \mathbb{V}[\mathbb{X}]) \leq \mathfrak{h}(n, m(j), \delta) \right\} \cap \left\{ \mathbb{W}_\infty(\mathbb{V}_n(j^*), \mathbb{V}[\mathbb{X}]) \leq \mathfrak{h}(n, m(j^*), \delta) \right\} \\ &\subseteq \left\{ \mathbb{W}_\infty(\mathbb{V}_n(j), \mathbb{V}_n(j^*)) \leq 2\mathfrak{h}(n, m(j), \delta) \right\}. \end{aligned}$$

By inverting the above inclusion we get the inclusion in (ii). Therefore, we obtain $\mathcal{E} \subseteq \{\hat{j} \leq j^*\}$.

3. Tail bound for the event \mathcal{E} . Applying a union bound to (34), we obtain

$$\begin{aligned} \mathbb{P}(\mathcal{E}^c) &= \mathbb{P}\left(\bigcup_{\{j \in \mathcal{J}: j \geq j^*\}} \left\{ \mathbb{W}_\infty(\mathbb{V}_n(j), \mathbb{V}[\mathbb{X}]) > \mathfrak{h}(n, m(j), \delta) \right\}\right) \\ &\leq \sum_{\{j \in \mathcal{J}: j \geq j^*\}} \mathbb{P}\left(\mathbb{W}_\infty(\mathbb{V}_n(j), \mathbb{V}[\mathbb{X}]) > \mathfrak{h}(n, m(j), \delta)\right) \\ &\stackrel{\text{(iv)}}{\leq} \sum_{\{j \in \mathcal{J}: j \geq j^*\}} \delta \\ &\stackrel{\text{(v)}}{\leq} \delta \log_\theta \left(\frac{\theta m_{\max}}{m_{\min}} \right), \end{aligned}$$

where (iv) follows from Eq. (48) and (v) uses the fact that $|\mathcal{J}| \leq 1 + \log_\theta(m_{\max}/m_{\min})$.

4. Bound for $\mathbb{W}_\infty(\mathbb{V}_n(\hat{j}), \mathbb{V}[\mathbb{X}])$. We begin by noting that when the event \mathcal{E} holds, we have that

$$\begin{aligned} \mathbb{W}_\infty(\mathbb{V}_n(\hat{j}), \mathbb{V}[\mathbb{X}]) &\leq \mathbb{W}_\infty(\mathbb{V}_n(\hat{j}), \mathbb{V}_n(j^*)) + \mathbb{W}_\infty(\mathbb{V}_n(j^*), \mathbb{V}[\mathbb{X}]) \\ &\stackrel{\text{(vi)}}{\leq} 2\mathfrak{h}(n, m(j^*), \delta) + \mathfrak{h}(n, m(j^*), \delta) \\ &\stackrel{\text{(vii)}}{\leq} 3\mathfrak{h}(n, \theta m^*, \delta), \end{aligned}$$

where the first term in (vi) follows from the definition of \hat{j} , which is guaranteed to hold because $\mathcal{E} \subseteq \{\hat{j} \leq j^*\}$, and the second term in (vi) follows from the definition of \mathcal{E} . The inequality in (vii) uses the fact that $m(j^*) < \theta m^*$ and the fact that $\mathfrak{h}(n, m, \delta)$ is non-decreasing in m . Therefore, we have the inclusion

$$\mathcal{E} \subseteq \left\{ \mathbb{W}_\infty(\mathbb{V}_n(\hat{j}), \mathbb{V}[\mathbb{X}]) \leq 3\mathfrak{h}(n, \theta m^*, \delta) \right\}.$$

Using the tail bound on \mathcal{E} we obtain

$$\mathbb{P}\left(W_\infty(\mathbb{V}_n(\hat{j}), \mathbb{V}[\mathbb{X}]) \leq 3\mathfrak{h}(n, \theta m^*, \delta)\right) \geq \mathbb{P}(\mathcal{E}) \geq 1 - \delta \log_\theta \left(\frac{\theta m_{\max}}{m_{\min}}\right),$$

which is the desired result. \blacksquare

C. Technical Lemmas for Appendix B

The proof of Theorem 5.1 relies on the following lemma, which allows us to control the deviation of a pointwise median-of-means estimator from its uncontaminated population counterpart in terms of a Binomial tail probability.

Lemma C.1. *Suppose $\mathbb{P} \in \mathcal{P}(\mathbb{X})$ for $\mathbb{X} \subset \mathbb{R}^d$ and $\mathbb{X}_n = \mathbb{X}_{n-m}^* \cup \mathbb{Y}_m$ is obtained under sampling condition (S) with \mathbb{X}_{n-m}^* observed i.i.d. from \mathbb{P} . Let \mathbb{P}_n denote the empirical measure associated with \mathbb{X}_n and for $2m < Q < n$, let \mathbb{P}_q be the empirical measure associated with the block S_q for all $q \in [Q]$. Given a statistical functional $T : \mathcal{P}(\mathbb{R}^d) \rightarrow \mathcal{F}(\mathbb{R}^d)$, let $T_Q(\mathbb{P}_n) \in \mathcal{F}(\mathbb{R}^d)$ be the pointwise MoM estimator given by*

$$T_Q(\mathbb{P}_n)(\mathbf{x}) = \text{median}\left\{T(\mathbb{P}_q)(\mathbf{x}) : q \in [Q]\right\}, \quad \text{for all } \mathbf{x} \in \mathbb{R}^d.$$

Then, for $t > 0$

$$\mathbb{P}\left(\|T_Q(\mathbb{P}_n) - T(\mathbb{P})\|_\infty > t\right) \leq \mathbb{P}\left(\sum_{q \in A} \xi_q(t; n, Q) > \frac{Q - 2m}{2}\right),$$

where $A = \{q \in [Q] : S_q \cap \mathbb{Y}_m = \emptyset\}$ are the indices for the blocks containing no outliers, and

$$\xi_q(t; n, Q) \doteq \mathbb{1}\left(\|T(\mathbb{P}_q) - T(\mathbb{P})\|_\infty > t\right) \quad \text{for all } q \in A.$$

The proof is provided in Appendix C.1. The statement of Lemma C.1 holds for empirical processes arising from general classes of pointwise median-of-means estimators. In particular, by taking $T(\mathbb{P}_q) = \mathbf{d}_{s,q}$ to be the distance function w.r.t. block S_q , the estimator $\mathbf{d}_{n,Q}$ satisfies the conditions of Lemma C.1. We also point out that the exponential concentration bound in Theorem 5.1 is strictly better than similar bounds appearing in other pointwise MoM estimators (e.g., Humbert et al., 2020, Theorem 2). This is owing to the Chernoff bound (instead of a Hoeffding bound) used for bounding the Binomial tail probability appearing in Lemma C.1. This provides a significant gain for Binomial random variables with shrinking probability (Hagerup and Rüb, 1990).

The next two results, Lemma C.2 and Lemma C.3 will be of assistance, and serve as generalizations of (Anai et al., 2019, Lemma 4.8 & Proposition 4.9).

We state the first result for a general metric space (\mathcal{M}, ρ) and an arbitrary weight function f . Here the ball of radius r centered at $\mathbf{x} \in \mathcal{M}$ is denoted $B_\rho(\mathbf{x}, r)$, and for a compact set $\mathbb{X} \subset \mathcal{M}$, the r -offset of \mathbb{X} w.r.t the metric ρ is given by $\mathbb{X}_\rho(r) = \bigcup_{\mathbf{x} \in \mathbb{X}} B_\rho(\mathbf{x}, r)$. The following result provides a handle for the interleavings between f -weighted filtrations computed on two nested sets using the same function f .

Lemma C.2. *Given a metric space (\mathcal{M}, ρ) , two subsets \mathbb{X}, \mathbb{Y} of \mathcal{M} such that $\mathbb{X} \subseteq \mathbb{Y}$, and a weight function $f : \mathcal{M} \rightarrow \mathbb{R}_{\geq 0}$, let $V_\rho[\mathbb{X}, f]$ and $V_\rho[\mathbb{Y}, f]$ be their respective f -weighted filtrations. If f satisfies the property that*

$$\inf_{\mathbf{x} \in \mathbb{X}} \rho(\mathbf{x}, \mathbf{y}) \leq f(\mathbf{y}) + a,$$

for $a \geq 0$ and for all $\mathbf{y} \in \mathbb{Y}$, then the filtrations are (id, α) -interleaved, i.e.,

$$V_\rho^t[\mathbb{X}, f] \subseteq V_\rho^t[\mathbb{Y}, f] \subseteq V_\rho^{\alpha(t)}[\mathbb{X}, f],$$

for $\alpha : t \mapsto 2^{1-\frac{1}{p}}t + a + \sup_{\mathbf{x} \in \mathbb{X}} f(\mathbf{x})$ and for all $t \geq 0$.

The proof of Lemma C.2 is provided in Appendix C.2. Since map α appearing in Lemma C.2 is not purely a translation map, it does not lead to a bound in the interleaving metric as per Eq. (18), and, therefore, a bound in the W_∞ metric cannot be characterized using Lemma C.2 alone. The next result, which is stated only for the Euclidean space $(\mathbb{R}^d, \|\cdot\|)$, establishes that for sufficiently large values of t , the map α may be replaced by a translation map. The proof is provided in Appendix C.3.

Lemma C.3. *Let $(\mathcal{M}, \rho) = (\mathbb{R}^d, \|\cdot\|)$. Suppose $\mathbb{X}, \mathbb{Y} \subset \mathbb{R}^d$ and $\mathbb{X} \subseteq \mathbb{Y}$, and f satisfies the same conditions as in Lemma C.2 for $a \geq 0$. Let $t(\mathbb{X})$ be the filtration value for the simplex corresponding to \mathbb{X} in $\text{nerve}\{\mathcal{V}_\rho[\mathbb{X}, f]\}$, i.e.,*

$$t(\mathbb{X}) \doteq \inf \left\{ t > 0 : \bigcap_{\mathbf{x} \in \mathbb{X}} B_{f, \rho}(\mathbf{x}, t) \neq \emptyset \right\},$$

and $\beta : t \mapsto t + c(\mathbb{X})$ be a non-decreasing map with

$$c(\mathbb{X}) \doteq a + \sup_{\mathbf{x} \in \mathbb{X}} f(\mathbf{x}) + \left(1 - \frac{1}{p}\right)t(\mathbb{X}).$$

Then for all $t \geq t(\mathbb{X})$, the homomorphisms $\phi_t^{\beta(t)} : \mathbb{V}_\rho^t[\mathbb{X}, f] \rightarrow \mathbb{V}_\rho^{\beta(t)}[\mathbb{X}, f]$ are trivial, i.e.,

$$\text{Im}(\phi_t^{\beta(t)}) \cong \begin{cases} \mathbf{F} & \text{if } \mathbb{V}_\rho^t[\mathbb{X}, f] = \text{Hom}_0(\mathbb{V}_\rho^t[\mathbb{X}, f]) \\ \{0\} & \text{if } \mathbb{V}_\rho^t[\mathbb{X}, f] = \text{Hom}_k(\mathbb{V}_\rho^t[\mathbb{X}, f]), k > 0 \end{cases}.$$

Furthermore, the bottleneck distance between the resulting f -weighted persistence diagrams is bounded above as

$$W_\infty\left(\mathfrak{Dgm}(\mathbb{V}_\rho[\mathbb{X}, f]), \mathfrak{Dgm}(\mathbb{V}_\rho[\mathbb{Y}, f])\right) \leq c(\mathbb{X}).$$

Remark C.1. *Unlike Lemma C.2, which is stated for general metric spaces, restricting ourselves to the Euclidean space $(\mathbb{R}^d, \|\cdot\|)$ in Lemma C.3 is sufficient for the objective of this work. However, as outlined in the proof, the only issue arises when Anai et al. (2019, Lemma B.1) is invoked. While Anai et al. (2019, Lemma B.1) (which holds for affine spaces satisfying the parallelogram identity) extends naturally to Banach spaces, the extension to general metric spaces will require some care on a case-by-case basis.*

The following lemma provide a useful characterization of the persistence diagram obtained using the sublevel sets of $\mathbf{d}_{n,Q}$.

Lemma C.4. *Given samples \mathbb{X}_n and $Q < n$, $V[\mathbf{d}_{n,Q}]$ and $\alpha : t \mapsto 2^{\frac{p-1}{p}}t$, $V[\mathbb{R}^d, \mathbf{d}_{n,Q}]$ are (id, α) -interleaved for for all $p \geq 1$. In particular, $V[\mathbf{d}_{n,Q}] = V[\mathbb{R}^d, \mathbf{d}_{n,Q}]$ when $p = 1$.*

The proof of Lemma C.4 is provided in Appendix C.4. Note that, $V^t[\mathbf{d}_{n,Q}]$ is the sublevel sets of $\mathbf{d}_{n,Q}$, whereas $V[\mathbb{R}^d, \mathbf{d}_{n,Q}]$ is the $\mathbf{d}_{n,Q}$ -weighted offset of all points in \mathbb{R}^d ; when $p \neq 1$, they are not necessarily the same.

C.1. Proof of Lemma C.1

For $t > 0$, define two events

$$E_1 = \{\|T_Q(\mathbb{P}_n) - T(\mathbb{P})\|_\infty \leq t\}, \text{ and } E_2 = \left\{ \#\{q \in [Q] : \|T(\mathbb{P}_q) - T(\mathbb{P})\|_\infty > t\} \leq \frac{Q}{2} \right\}.$$

First, we show that $E_2 \subseteq E_1$. To this end,

$$\begin{aligned} E_2 &\subseteq \left\{ \#\{q \in [Q] : \|T(\mathbb{P}_q) - T(\mathbb{P})\|_\infty > t\} \leq \frac{Q}{2} \right\} \\ &\subseteq \left\{ \#\{q \in [Q] : \|T(\mathbb{P}_q) - T(\mathbb{P})\|_\infty \leq t\} > Q - \frac{Q}{2} \right\} \\ &\subseteq \left\{ \#\{q \in [Q] : \forall \mathbf{x} \in \mathbb{R}^d, T(\mathbb{P})(\mathbf{x}) - t \leq T(\mathbb{P}_q)(\mathbf{x}) \leq T(\mathbb{P})(\mathbf{x}) + t\} > \frac{Q}{2} \right\} \\ &\subseteq \left\{ \forall \mathbf{x} \in \mathbb{R}^d, T(\mathbb{P})(\mathbf{x}) - t \leq \text{median}\{T(\mathbb{P}_q)(\mathbf{x}) : q \in [Q]\} \leq T(\mathbb{P})(\mathbf{x}) + t \right\} \\ &\subseteq \left\{ \forall \mathbf{x} \in \mathbb{R}^d, T(\mathbb{P})(\mathbf{x}) - t \leq T_Q(\mathbb{P}_n)(\mathbf{x}) \leq T(\mathbb{P})(\mathbf{x}) + t \right\} \\ &\subseteq \{\|T_Q(\mathbb{P}_n) - T(\mathbb{P})\|_\infty \leq t\} = E_1. \end{aligned}$$

Therefore, we have $E_2 \subseteq E_1$. Next, note that E_2 can be written as

$$E_2 = \left\{ \sum_{q=1}^Q \xi_q(2t; n, Q) \leq \frac{Q}{2} \right\},$$

where, for each $q \in [Q]$,

$$\xi_q(2t; n, Q) \doteq \mathbf{1}\left(\|T(\mathbb{P}_q) - T(\mathbb{P})\|_\infty > t\right).$$

Since $0 \leq \xi_q(2t; n, Q) \leq 1$ a.s., we have that

$$\begin{aligned} \sum_{q=1}^Q \xi_q(2t; n, Q) &= \sum_{q \in A} \xi_q(2t; n, Q) + \sum_{q \in A^c} \xi_q(2t; n, Q) \\ &\leq \sum_{q \in A} \xi_q(2t; n, Q) + |A^c| \leq \sum_{q \in A} \xi_q(2t; n, Q) + m. \end{aligned} \tag{49}$$

As a result, we can further bound the probability of E_2 from below as

$$\mathbb{P}(E_2) \geq \mathbb{P}\left(\sum_{q \in A} \xi_q(2t; n, Q) \leq \frac{Q}{2} - m\right). \tag{50}$$

Combining Eq. (50) with the fact that $E_2 \subseteq E_1$, we obtain

$$\mathbb{P}\left(\|T_Q(\mathbb{P}_n) - T(\mathbb{P})\|_\infty > t\right) = \mathbb{P}(E_1^c) \leq \mathbb{P}(E_2^c) \leq \mathbb{P}\left(\sum_{q \in A} \xi_q(2t; n, Q) > \frac{Q}{2} - m\right),$$

which gives us the desired result. ■

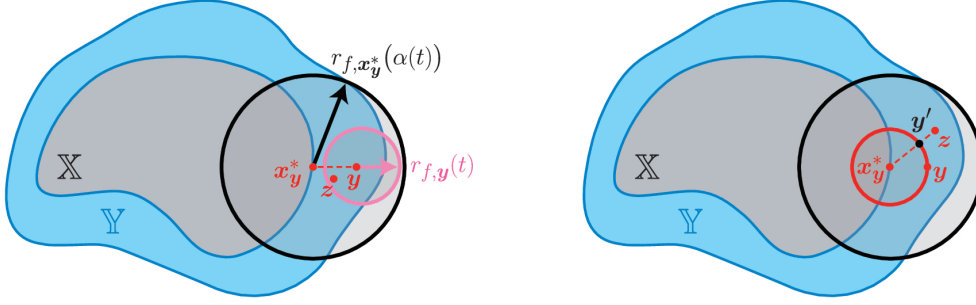


Figure 10: Illustration of Case I (Left) and Case II (Right).

C.2. Proof of Lemma C.2

Since $X \subseteq Y$, the inclusion $V_\rho^t[X, f] \subseteq V_\rho^t[Y, f]$ holds trivially. For the next part, let $V^t = V_\rho^t[X, f]$ and $U^t = V_\rho^t[Y, f]$ denote the respective f -weighted filtrations, so as to avoid the notational overload. In order to show the second inclusion, i.e., $U^t \subseteq V^{\alpha(t)}$, consider $z \in U^t$. Then, there exists $y \in Y$ such that $z \in B_{f, \rho}(y, t)$. If $y \in X \subset Y$, then it immediately follows that $z \in V^t \subseteq V^{\alpha(t)}$. In what remains, for $y \in Y \setminus X$, it is sufficient to show that there exists $x \in X$ such that $z \in B_{f, \rho}(x, \alpha(t))$.

To this end, let $x_y^* = \arg \inf_{x \in X} \rho(x, y)$ be the projection of y onto X via ρ . Then two following cases arise: (I) $\rho(x_y^*, z) \leq \rho(x_y^*, y)$, and (II) $\rho(x_y^*, z) \geq \rho(x_y^*, y)$ (see Figure 10).

Case I. The distance between x_y^* and z will satisfy

$$\begin{aligned} \rho(x_y^*, z) &\leq \rho(x_y^*, y) \stackrel{(i)}{\leq} f(y) + a \\ &\stackrel{(ii)}{\leq} (t^p - \rho(y, z)^p)^{\frac{1}{p}} + a \\ &\leq t + a \end{aligned}$$

where (i) follows from the assumption on f , and (ii) follows from the fact that if $z \in B_{f, \rho}(y, t)$, then $\rho(y, z) \leq r_{f, y}(t) = (t^p - f(y)^p)^{1/p}$. Furthermore, from Lemma D.1 (vi) we obtain

$$\begin{aligned} \rho(x_y^*, z) &\leq \left((t + a + f(x_y^*))^p - f(x_y^*)^p \right)^{\frac{1}{p}} \\ &\leq \left((t + a + \sup_{x \in X} f(x))^p - f(x_y^*)^p \right)^{\frac{1}{p}} \\ &\leq \left((2^{1-\frac{1}{p}}t + a + \sup_{x \in X} f(x))^p - f(x_y^*)^p \right)^{\frac{1}{p}} \\ &= (\alpha(t)^p - f(x_y^*)^p)^{\frac{1}{p}} = r_{f, x_y^*}(\alpha(t)), \end{aligned}$$

where the last inequality holds because $2^{1-\frac{1}{p}} \geq 1$. The last line implies that

$$z \in B_{f, \rho}(x_y^*, \alpha(t)) \subseteq V^{\alpha(t)}.$$

Case II. For $r = \rho(x_y^*, y)$ let y' be the projection of z onto $\partial B(x_y^*, r)$, i.e.,

$$y' = \arg \inf_{x' \in \partial B(x_y^*, r)} \rho(x', z).$$

The point \mathbf{y}' satisfies the following three properties: (PI) $\rho(\mathbf{x}_y^*, \mathbf{y}') = \rho(\mathbf{x}_y^*, \mathbf{y})$, since $\mathbf{y}' \in \partial B_{f,\rho}(\mathbf{x}_y^*, r)$; (P-II) $\rho(\mathbf{z}, \mathbf{y}') \leq \rho(\mathbf{z}, \mathbf{y})$ by definition of \mathbf{y}' ; and (PIII) $\rho(\mathbf{x}_y^*, \mathbf{y}') + \rho(\mathbf{y}', \mathbf{z}) \geq \rho(\mathbf{x}_y^*, \mathbf{z})$ from the triangle inequality.

Since $\mathbf{z} \in B_{f,\rho}(\mathbf{y}, t)$, when $\rho(\mathbf{x}_y^*, \mathbf{y}) \leq a$ we may use the triangle inequality to obtain

$$\rho(\mathbf{x}_y^*, \mathbf{z}) \leq \rho(\mathbf{x}_y^*, \mathbf{y}) + \rho(\mathbf{z}, \mathbf{y}) \leq a + (t^p - f(\mathbf{y})^p)^{\frac{1}{p}} \leq a + t \leq a + 2^{1-\frac{1}{p}}t. \quad (51)$$

Alternatively, when $\rho(\mathbf{x}_y^*, \mathbf{y}) > a$ we obtain the following inequality,

$$\begin{aligned} t^p &\geq \rho(\mathbf{y}, \mathbf{z})^p + f(\mathbf{y})^p \\ &\stackrel{\text{(iii)}}{\geq} \rho(\mathbf{z}, \mathbf{y})^p + (\rho(\mathbf{x}_y^*, \mathbf{y}) - a)^p \\ &\stackrel{\text{(iv)}}{=} \rho(\mathbf{z}, \mathbf{y})^p + (\rho(\mathbf{x}_y^*, \mathbf{y}') - a)^p \\ &\stackrel{\text{(v)}}{\geq} \rho(\mathbf{z}, \mathbf{y}')^p + (\rho(\mathbf{x}_y^*, \mathbf{y}') - a)^p \\ &\stackrel{\text{(vi)}}{\geq} \left(\rho(\mathbf{x}_y^*, \mathbf{z}) - \rho(\mathbf{x}_y^*, \mathbf{y}') \right)^p + \left(\rho(\mathbf{x}_y^*, \mathbf{y}') - a \right)^p \\ &\stackrel{\text{(vii)}}{\geq} 2^{1-p} \left(\rho(\mathbf{x}_y^*, \mathbf{z}) - a \right)^p, \end{aligned} \quad (52)$$

where (iii) holds from the assumption on f , (iv–vi) follow from (PI–PIII) respectively, and (vii) uses Lemma D.1 (i). Rearranging the terms of Eq. (52) we get $\rho(\mathbf{x}_y^*, \mathbf{z}) \leq a + 2^{1-\frac{1}{p}}t$. Therefore, from Eq. (51) and Eq. (52), in case (II) we have that

$$\begin{aligned} \rho(\mathbf{x}_y^*, \mathbf{z}) &\leq 2^{1-\frac{1}{p}}t + a \\ &\stackrel{\text{(viii)}}{\leq} \left((2^{1-\frac{1}{p}}t + a + \sup_{\mathbf{x} \in \mathbb{X}} f(\mathbf{x}))^p - f(\mathbf{x}_y^*)^p \right)^{\frac{1}{p}} \\ &= r_{f, \mathbf{x}_y^*}(\alpha(t)), \end{aligned}$$

where (viii) uses Lemma D.1 (vi). Similar to case (I), we obtain $\mathbf{z} \in B_{f,\rho}(\mathbf{x}_y^*, \alpha(t)) \subseteq V^{\alpha(t)}$. ■

C.3. Proof of Lemma C.3

Let $t \geq t(\mathbb{X})$ where

$$t(\mathbb{X}) \doteq \inf \left\{ t > 0 : \bigcap_{\mathbf{x} \in \mathbb{X}} B_{f,\rho}(\mathbf{x}, t) \neq \emptyset \right\},$$

and let $\mathbf{x}_0 \in \bigcap_{\mathbf{x} \in \mathbb{X}} B_{f,\rho}(\mathbf{x}, t)$. To ease the notation, let $U^t = V_\rho^t[\mathbb{Y}, f]$ denote the usual f -weighted filtration, and let W^t be defined as

$$W^t = \left\{ \bigcup_{\mathbf{x} \in \mathbb{X}} B_{f,\rho}(\mathbf{x}, \beta(t)) \right\} \cup \left\{ \bigcup_{\mathbf{y} \in \mathbb{Y} \setminus \mathbb{X}} B_{f,\rho}(\mathbf{y}, t) \right\},$$

such that $U^t \subset W^t \subset U^{\beta(t)}$. With this background, the proof closely follows that of Anai et al. (2019, Proposition 4.8). Specifically, the proof is based on the following outline:

- ① We first establish that for any $\mathbf{y} \in \mathbb{Y} \setminus \mathbb{X}$, there exists $\mathbf{x} = \mathbf{x}_y^* \in \mathbb{X}$ such that for all $t \geq t(\mathbb{X})$, $B_{f,\rho}(\mathbf{y}, t) \cup B_{f,\rho}(\mathbf{x}, \beta(t))$ is star-shaped around \mathbf{x}_0 . Since this holds for all $\mathbf{y} \in \mathbb{Y} \setminus \mathbb{X}$, it also holds for $\bigcup_{\mathbf{y} \in \mathbb{Y} \setminus \mathbb{X}} B_{f,\rho}(\mathbf{y}, t)$, and, therefore, W^t is star-shaped and contractible to \mathbf{x}_0 .

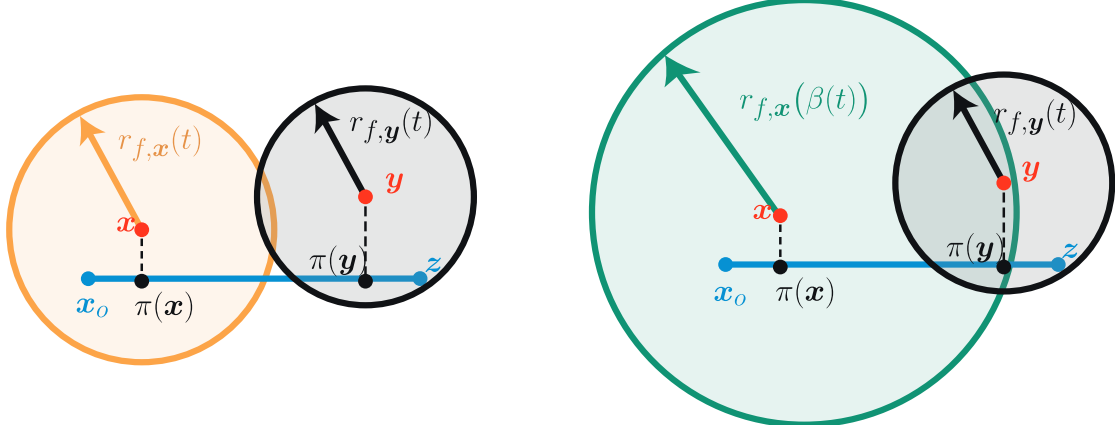


Figure 11: Illustration of Claim ①.

- ② The inclusion map $\iota_t : U^t \hookrightarrow U^{\beta(t)}$ can be decomposed as $\iota_t = j_t \circ \kappa_t$ where $j_t : U^t \hookrightarrow W^t$ and $\kappa_t : W^t \hookrightarrow U^{\beta(t)}$. Since W^t is star-shaped and contractible, i.e., $W^t \sim \{\mathbf{x}_0\}$, the linear map between the homology groups induced by κ_t , i.e., $v_t : \mathbb{W}^t \rightarrow \mathbb{U}^{\beta(t)}$ will be trivial.
- ③ The interleavings $\alpha(t)$ (Lemma C.2) and $\beta(t)$ are combined to provide the bound in W_∞ .

Claim ①. Let $\mathbf{y} \in \mathbb{Y} \setminus \mathbb{X}$. We need to show that there exists $\mathbf{x} \in \mathbb{X}$ such that $B_{f,\rho}(\mathbf{x}, \beta(t)) \cup B_{f,\rho}(\mathbf{y}, t)$ is star-shaped around \mathbf{x}_0 , i.e., for any $\mathbf{z} \in B_{f,\rho}(\mathbf{y}, t)$ the segment $\Gamma[\mathbf{x}_0, \mathbf{z}]$ is contained inside the set $B_{f,\rho}(\mathbf{x}, \beta(t)) \cup B_{f,\rho}(\mathbf{y}, t)$. See Figure 11.

To this end, let $\mathbf{x} = \arg \inf_{\mathbf{z} \in \mathbb{X}} \rho(\mathbf{z}, \mathbf{y})$ be the projection of \mathbf{y} onto \mathbb{X} . Note that, from the definition of \mathbf{x}_0 , $\mathbf{x}_0 \in B_{f,\rho}(\mathbf{x}, t)$ for all $t \geq t(\mathbb{X})$. For simplicity, let $S^t = B_{f,\rho}(\mathbf{x}, \beta(t)) \cup B_{f,\rho}(\mathbf{y}, t)$. Additionally, let $\pi(\mathbf{x})$ and $\pi(\mathbf{y})$ be the projection of \mathbf{x} and \mathbf{y} onto $\Gamma[\mathbf{x}_0, \mathbf{z}]$, respectively, i.e.,

$$\pi(\mathbf{x}) = \arg \inf_{\mathbf{x}' \in \Gamma[\mathbf{x}_0, \mathbf{z}]} \rho(\mathbf{x}', \mathbf{x}),$$

mutatis mutandis, the same for $\pi(\mathbf{y})$.

By definition, $\rho(\mathbf{x}, \pi(\mathbf{x})) \leq \rho(\mathbf{x}, \mathbf{x}_0)$ and $\rho(\mathbf{y}, \pi(\mathbf{y})) \leq \rho(\mathbf{y}, \mathbf{z})$, and consequently, $\pi(\mathbf{y}) \in B_{f,\rho}(\mathbf{y}, t)$. This implies that $\Gamma[\pi(\mathbf{y}), \mathbf{z}] \subseteq S^t$. What remains to be established is that $\Gamma[\mathbf{x}_0, \pi(\mathbf{y})] \subseteq S^t$. In order to show this, note that it is sufficient to show that $\pi(\mathbf{y}) \in B_{f,\rho}(\mathbf{x}, \beta(t))$. Indeed, if this holds, then $\Gamma[\mathbf{x}_0, \pi(\mathbf{y})] \subseteq B_{f,\rho}(\mathbf{x}, \beta(t)) \subseteq S^t$, and it will follow that $\Gamma[\mathbf{x}_0, \pi(\mathbf{y})] \cup \Gamma[\pi(\mathbf{y}), \mathbf{z}] = \Gamma[\mathbf{x}_0, \mathbf{z}] \subseteq S^t$.

Let $\tau = \rho(\mathbf{y}, \pi(\mathbf{y}))$. Since $\pi(\mathbf{y}) \in B_{f,\rho}(\mathbf{y}, t)$, when $\rho(\mathbf{x}, \mathbf{y}) > a$ it follows that

$$\begin{aligned} \tau &\leq r_{f,\mathbf{y}}(t) \\ &\leq \left(t^p - f(\mathbf{y})^p \right)^{\frac{1}{p}} \\ &\leq \left(t^p - (\rho(\mathbf{x}, \mathbf{y}) - a)^p \right)^{\frac{1}{p}}, \end{aligned}$$

where the last inequality follows from the assumption on f . Thus, we have

$$\rho(\mathbf{x}, \mathbf{y}) \leq \left(t^p - \tau^p \right)^{\frac{1}{p}} + a. \quad (53)$$

Alternatively, when $\rho(\mathbf{x}, \mathbf{y}) \leq a$, Eq. (53) holds trivially. Since $\pi(\mathbf{x}) \in B_{f,\rho}(\mathbf{x}, t)$ and $\rho(\mathbf{x}, \pi(\mathbf{x})) \leq \rho(\mathbf{x}, \mathbf{x}_0)$, it follows that

$$\rho(\mathbf{x}, \pi(\mathbf{x})) \leq t(\mathbb{X}). \quad (54)$$

Since $\rho = \|\cdot\|$, Anai et al. (2019, Lemma B.2) holds, which, combined with Eqs.(53) and (54) yields

$$\begin{aligned}
\rho(\mathbf{x}, \pi(\mathbf{y}))^2 &\stackrel{(i)}{\leq} \left((t^p - \tau^p)^{\frac{1}{p}} + a \right)^2 + \tau(2t(\mathbb{X}) - \tau) \\
&\leq (t^p - \tau^p)^{\frac{2}{p}} + \tau(2t(\mathbb{X}) - \tau) + a^2 + 2a(t^p - \tau^p)^{\frac{1}{p}} \\
&\stackrel{(ii)}{\leq} (t + \kappa t(\mathbb{X}))^2 + a^2 + 2at \\
&\leq (t + \kappa t(\mathbb{X}))^2 + a^2 + 2a(t + \kappa t(\mathbb{X})) \\
&= (t + a + \kappa t(\mathbb{X}))^2,
\end{aligned}$$

where (i) is a consequence of Anai et al. (2019, Lemma B.2), (ii) follows from (Anai et al., 2019, Lemma B.3) and noting that $t^p - \tau^p \leq t^p$ since $\tau \leq t$, and $\kappa = (1 - \frac{1}{p})$. The proofs of Anai et al. (2019, Lemma B.2 & B.3) require that the metric $\rho(\cdot, \cdot)$ admits the parallelogram identity for the result to hold. Additionally, from Lemma D.1 (vi) we obtain

$$\rho(\mathbf{x}, \pi(\mathbf{y})) \leq t + a + \kappa t(\mathbb{X}) \leq \left((t + a + \kappa t(\mathbb{X}) + \sup_{\mathbf{x} \in \mathbb{X}} f(\mathbf{x}))^p - f(\mathbf{x})^p \right)^{\frac{1}{p}} = r_{f, \mathbf{x}}(\beta(t)).$$

This implies that $\pi(\mathbf{y}) \in B_{f, \rho}(\mathbf{x}, \beta(t))$, and establishes claim ①.

For claim ②, note that since $W^t \sim \{\mathbf{x}_0\}$, for the k th homology group \mathbb{W}^t , we have that $\mathbb{W}^t \simeq \mathbf{F}$ for $k = 0$, and $\mathbb{W}^t \simeq \{0\}$ for $k > 0$. Therefore, the map $w_t : \mathbb{W}^t \rightarrow \mathbb{U}^{\beta(t)}$ is trivial, and consequently, so is the linear map $\mathbb{U}^t \rightarrow \mathbb{U}^{\beta(t)}$.

In order to show claim ③, observe that the persistence modules \mathbb{U} and \mathbb{V} are

$$\begin{cases} \text{(id, } \alpha\text{)-interleaved} & \text{for all } t \text{ and for } \alpha : t \mapsto 2^{1-\frac{1}{p}}t + a + \sup_{\mathbf{x} \in \mathbb{X}} f(\mathbf{x}) \\ \text{(id, } \beta\text{)-interleaved} & \text{for } t \geq t(\mathbb{X}) \text{ and for } \beta : t \mapsto t + a + \kappa t(\mathbb{X}) + \sup_{\mathbf{x} \in \mathbb{X}} f(\mathbf{x}) \end{cases}.$$

When $t \leq t(\mathbb{X})$, from (Anai et al., 2019, Lemma B.1),

$$\alpha(t) = t + \left(2^{1-\frac{1}{p}} - 1 \right) t + a + \sup_{\mathbf{x} \in \mathbb{X}} f(\mathbf{x}) \leq t + \kappa t(\mathbb{X}) + a + \sup_{\mathbf{x} \in \mathbb{X}} f(\mathbf{x}) = \beta(t).$$

Thus, $\alpha(t) \leq \beta(t)$ for $t \leq t(\mathbb{X})$. Since $\beta : t \mapsto t + c(\mathbb{X})$ is an additive interleaving for $c(\mathbb{X}) = \kappa t(\mathbb{X}) + a + \sup_{\mathbf{x} \in \mathbb{X}} f(\mathbf{x})$, this implies that

$$W_\infty(\mathfrak{Dgm}(\mathbb{U}), \mathfrak{Dgm}(\mathbb{V})) \leq c(\mathbb{X}),$$

which establishes claim ③. ■

C.4. Proof of Lemma C.4

For simplicity, let $f = d_{n, Q}$ denote the MoM Dist function. By definition, $V[f]$ and $V[\mathbb{R}^d, f]$ are (id, α)-interleaved if the following relationship holds

$$V^t[f] \subseteq V^t[\mathbb{R}^d, f] \subseteq V^{\alpha(t)}[f] \quad \text{for all } t \geq 0.$$

The first inclusion is straightforward since

$$V^t[f] \subseteq \bigcup_{\mathbf{x} \in V^t[f]} B_f(\mathbf{x}, t) = \bigcup_{\mathbf{x} \in \mathbb{R}^d} B_f(\mathbf{x}, t) = V^t[\mathbb{R}^d, f].$$

For the second inclusion, suppose $\mathbf{x} \in V^t[\mathbb{R}^d, f]$, i.e., there exists $\mathbf{y} \in \mathbb{R}^d$ such that $\|\mathbf{x} - \mathbf{y}\| \leq r_{f, \mathbf{y}}(t)$. It suffices to show that $\mathbf{x} \in V^{\alpha(t)}[f]$. To this end, note that since $d_{n, Q}$ is 1-Lipschitz by Lemma 4.1 it follows that

$$\begin{aligned} f(\mathbf{x}) &\leq f(\mathbf{y}) + \|\mathbf{x} - \mathbf{y}\| \\ &\leq f(\mathbf{y}) + r_{f, \mathbf{y}}(t) \\ &= f(\mathbf{y}) + (t^p - f(\mathbf{y})^p)^{\frac{1}{p}} \\ &\stackrel{(i)}{\leq} 2^{\frac{p-1}{p}} (f(\mathbf{y})^p + (t^p - f(\mathbf{y})^p))^{\frac{1}{p}} = 2^{\frac{p-1}{p}} t, \end{aligned}$$

where (i) follows from an application of Lemma D.1 (iii). Since $f(\mathbf{x}) \leq 2^{\frac{p-1}{p}} t = \alpha(t)$, it implies that $\mathbf{x} \in V^{\alpha(t)}[f]$ and the result follows. When $p = 1$, note that $\alpha(t) = t$, and therefore $V[f] = V[\mathbb{R}^d, f]$. \blacksquare

D. Auxiliary Results

Consider the Huber contamination model with parameter $\eta \in (0, 1/2)$, i.e.,

$$\mathbb{P}_{\eta, \mathbb{Q}} = (1 - \eta)\mathbb{P} + \eta\mathbb{Q}, \quad (55)$$

where \mathbb{P} is the nominal distribution and \mathbb{Q} is the contaminating distribution. The key tool for establishing minimax rates under contamination models is the *modulus of continuity* associated with a loss function.

Definition D.1. Let $\{\mathbb{P}_\theta : \theta \in \Theta\}$ be a class of distributions, and let $L : \Theta \times \Theta \rightarrow \mathbb{R}$ be a loss function. The modulus of continuity of L with respect to the contamination model is given by

$$\omega(\eta, \Theta) = \sup \left\{ L(\theta, \theta') : \text{TV}(\mathbb{P}_\theta, \mathbb{P}_{\theta'}) \leq \frac{\eta}{1 - \eta}, \theta_1, \theta_2 \in \Theta \right\}.$$

In other words, the modulus of continuity ‘‘measures the difficulty of the hardest one-dimensional subproblem’’ (Donoho, 1994). The modulus of continuity is used in the following theorem by Chen et al. (2018) to establish lower bounds on the minimax risk under η -Huber contamination.

Theorem D.1 (Theorem 5.1, Chen et al. 2018). *Suppose there is $\mathfrak{R}_n(0)$ such that for $\eta = 0$,*

$$\inf_{\hat{\theta}} \sup_{\theta \in \Theta} \sup_{\mathbb{Q}} \mathbb{P}_{\eta, \mathbb{Q}} \left\{ L(\hat{\theta}, \theta) > \mathfrak{R}_n(\eta) \right\} \gtrsim c \quad (56)$$

holds for some $c > 0$. Then for any $\eta \in (0, 1/2)$, the minimax bound Eq. (56) holds for $\mathfrak{R}_n(\eta) = \mathfrak{R}_n(0) \wedge \omega_L(\eta, \Theta)$.

The following lemma is a collection of well-known inequalities (and their slight variants). We state them here for reference, as they are used frequently in the proofs.

Lemma D.1. *For $0 < y \leq x$ and $p \geq 1$, the following inequalities hold:*

- (i) $x^p + y^p \leq (x + y)^p \leq 2^{p-1}(x^p + y^p)$;
- (ii) $2^{1-p}x^p - y^p \leq (x - y)^p \leq x^p - y^p$;
- (iii) $(x + y)^{\frac{1}{p}} \leq x^{\frac{1}{p}} + y^{\frac{1}{p}} \leq 2^{\frac{p-1}{p}}(x + y)^{\frac{1}{p}}$;

$$(iv) \quad x^{\frac{1}{p}} - y^{\frac{1}{p}} \leq (x - y)^{\frac{1}{p}} \leq 2^{\frac{p-1}{p}} x^{\frac{1}{p}} - y^{\frac{1}{p}};$$

$$(v) \quad y^{1-\frac{1}{p}} x^{\frac{1}{p}} \leq x \leq y^{1-p} x^p;$$

$$(vi) \quad x \leq \left((x + y)^p - y^p \right)^{\frac{1}{p}}.$$

Proof. *Part (i).* Let $f(y) = (x + y)^p - x^p - y^p$ on the interval $0 < y \leq x$. The derivative,

$$f'(y) = p(x + y)^{p-1} - py^{p-1} \geq 0$$

for all $0 < y \leq x$ and $p \geq 1$. Therefore f is non-decreasing, and $f(y) \geq f(0) = 0$. This gives us the first inequality. For the second inequality, note that $g(z) = z^p$ is convex for $z \geq 0$. This follows from the fact that $g''(z) = p(p-1)z^{p-2} \geq 0$ for all $z \geq 0$ and $p \geq 1$. By convexity, we obtain

$$2^{-p}(x + y)^p = \left(\frac{1}{2}x + \frac{1}{2}y \right)^p \leq \frac{x^p + y^p}{2},$$

which leads to the second inequality.

Part (ii). Let $z = (x - y)$. Applying the first inequality from the preceding part to z and y we get $z^p \leq (y + z)^p - y^p$, i.e., $(x - y)^p \leq x^p - y^p$. Similarly, from the second inequality, $(z + y)^p \leq 2^{p-1}(z^p + y^p)$, which is the same as $2^{1-p}x^p - y^p \leq (x - y)^p$.

Part (iii). Taking $a = x^{1/p}$ and $b = y^{1/p}$, from (i) it follows that

$$(x + y) \leq (x^{1/p} + y^{1/p})^p \leq 2^{p-1}(x + y),$$

and by noting that the map $t \mapsto t^{1/p}$ is increasing on \mathbb{R}_+ , the result in (iii) follows.

Part (iv). The proof is identical to the proof in Part (ii). The inequalities are obtained by taking $z = (x - y)$, and applying the results of Part (iii).

Part (v). Since $y \leq x$, it follows that $1 \leq (x/y)^{\frac{1}{p}} \leq x/y \leq (x/y)^p$ for $p \geq 1$. By rearranging the terms, we get $x \leq y^{1-p}x^p$ and $x \geq y^{1-\frac{1}{p}}x^{\frac{1}{p}}$.

Part (vi). We have $x = (x + y - y) = ((x + y - y)^p)^{\frac{1}{p}}$. From Part (ii) we have

$$(x + y - y)^p \leq (x + y)^p - y^p,$$

which, on rearranging, yields $x \leq ((x + y)^p - y^p)^{\frac{1}{p}}$. ■

Lemma D.2 (Chernoff-Hoeffding bound simplified). *Suppose Z_1, Z_2, \dots, Z_N are i.i.d. Bernoulli(p) random variables. Then, for $0 < \epsilon < 1$,*

$$\mathbb{P} \left(\frac{1}{N} \sum_{1 \leq i \leq N} Z_i > \epsilon \right) \leq \min \left\{ 1, \exp \left(N \left(\frac{2}{e} + \epsilon \log(p) \right) \right) \right\}.$$

Proof. For $0 < \epsilon < 1$, using the Chernoff-Hoeffding bound for binomial random variables (Hoeffding, 1963, Theorem 1) we have

$$\mathbb{P} \left(\frac{1}{N} \sum_{1 \leq i \leq N} Z_i > \epsilon \right) \leq \exp \left(-N \cdot \text{KL}(\text{Ber}(\epsilon) || \text{Ber}(p)) \right), \quad (57)$$

where $\text{Ber}(\epsilon)$ and $\text{Ber}(p)$ are Bernoulli distributions with parameters ϵ and p respectively, and $\text{KL}(\mathbb{P}||\mathbb{Q})$ is the Kullback-Leibler divergence of \mathbb{Q} w.r.t \mathbb{P} . Simplifying the quantity in the exponent, we get

$$\begin{aligned} \text{KL}(\text{Ber}(\epsilon)||\text{Ber}(p)) &= \epsilon \log\left(\frac{\epsilon}{p}\right) + (1-\epsilon) \log\left(\frac{1-\epsilon}{1-p}\right) \\ &= \underbrace{\epsilon \log(\epsilon) + (1-\epsilon) \log(1-\epsilon)}_{\geq -2/e} - \epsilon \log(p) - (1-\epsilon) \log(1-p) \\ &\geq -\frac{2}{e} - \epsilon \log(p), \end{aligned}$$

where the last inequality uses the fact that $x \log(x) \geq -1/e$ for all $0 \leq x \leq 1$, and $-(1-\epsilon) \log(1-p) \geq 0$ for all $0 \leq \epsilon, p \leq 1$. By noting that $\text{KL}(\text{Ber}(\epsilon)||\text{Ber}(p)) \geq 0$, it follows that

$$\text{KL}(\text{Ber}(\epsilon)||\text{Ber}(p)) \geq \max\left\{-\frac{2}{e} - \epsilon \log(p), 0\right\}.$$

Substituting this in Eq. (35) yields the result. \blacksquare

E. Additional Experiments

The tools for data-adaptive construction of $\mathbf{d}_{n,Q}$ -weighted filtrations, in addition to the code for all experiments, are made publicly available in the `RobustTDA.jl` Julia package⁷. In all experiments, the persistence diagrams are computed using the `Ripsrerer.jl` backend Čufar (2020), and we set the parameter $p = 1$ for the weighted-filtrations.

E.1. Comparison of $V[\mathbf{d}_{n,Q}]$ and $V[\mathbb{X}_n, \mathbf{d}_{n,Q}]$

The objective of this experiment is to illustrate that the $\mathbf{d}_{n,Q}$ -weighted filtration $V[\mathbb{X}_n, \mathbf{d}_{n,Q}]$ reasonably approximates the sublevel filtration $V[\mathbf{d}_{n,Q}]$. For the same setup as 9.1, \mathbb{X}_n comprises of $n = 550$ points obtained by sampling 500 points on a circle with additive Gaussian noise ($\sigma = 0.01$) and $m = 50$ outliers added from a Matérn cluster process. For $Q = \hat{Q}$ selected using Lepski's method, Figure 12 (a) depicts the MoM Dist function $\mathbf{d}_{n,Q}$. Figure 12 (b) illustrates the scatter plot for \mathbb{X}_n with the points colored by the weights $\mathbf{d}_{n,Q}(\mathbf{x}_i)$ for each $\mathbf{x}_i \in \mathbb{X}_n$. The shaded regions show the $\mathbf{d}_{n,Q}$ -weighted offsets $V^t[\mathbb{X}_n, \mathbf{d}_{n,Q}]$ for $t \in \{1.5, 1.75, 2, 2.25\}$ colored from white to blue. Figure 12 (c) depicts the sublevel persistence diagram $\mathfrak{Dgm}(V[\mathbf{d}_{n,Q}])$ computed using cubical homology on a grid of resolution 0.5. As expected by the result of Proposition B.1, the $\mathbf{d}_{n,Q}$ -weighted persistence diagram $\mathfrak{Dgm}(V[\mathbb{X}_n, \mathbf{d}_{n,Q}])$ in Figure 12 (d) captures the essential topological information in $\mathfrak{Dgm}(V[\mathbf{d}_{n,Q}])$.

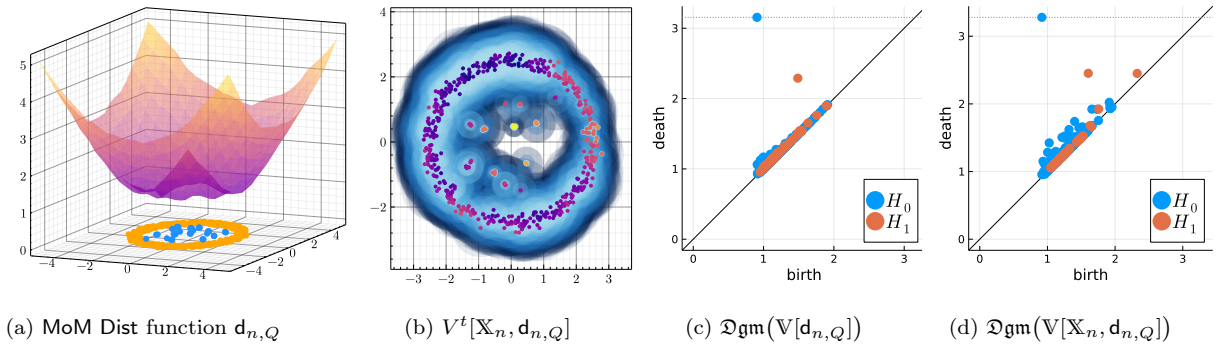


Figure 12: Comparison of sublevel filtrations with the $\mathbf{d}_{n,Q}$ -weighted filtration.

⁷<https://www.github.com/sidv23/RobustTDA.jl/>

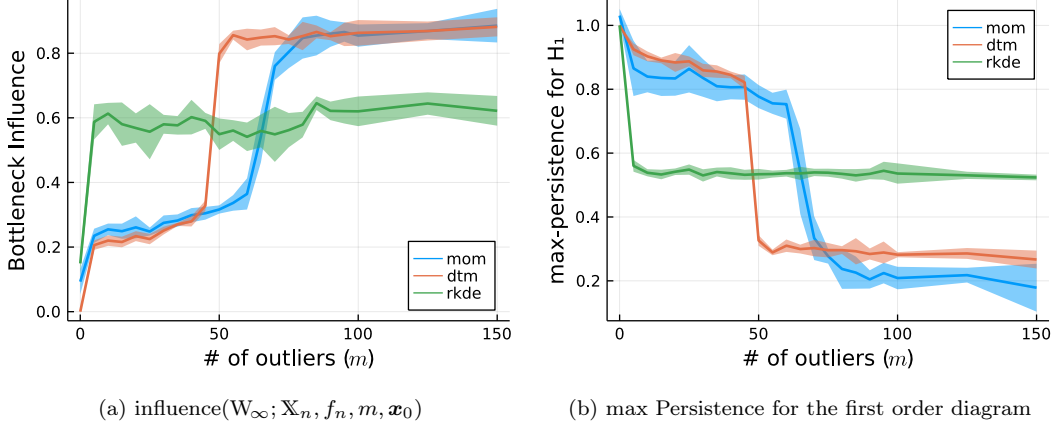


Figure 13: Influence analysis for $d_{n,Q}$ -weighted filtrations vis-à-vis DTM-based and unweighted filtrations.

E.2. Empirical influence analysis

In this experiment, we examine the influence of outliers on $d_{n,Q}$ -weighted filtrations. For $n = 500$, points \mathbf{X}_n are sampled uniformly from a circle. We compute the unweighted persistence diagram $D_n = \mathfrak{Dgm}(\mathbb{V}[\mathbf{X}_n])$. In a small neighborhood around the center of the circle, outliers \mathbf{Y}_m are sampled uniformly from $[-0.1, 0.1]^2$. For the composite sample $\mathbf{X}_n \cup \mathbf{Y}_m$ and a fixed value of $Q = 100$ & $k = 50$, we compute the MoM Dist weighted persistence diagram $D_{n+m,Q}^{MoM} = \mathfrak{Dgm}(\mathbb{V}[\mathbf{X}_n \cup \mathbf{Y}_m, \mathbf{d}_{n+m,Q}])$, the DTM weighted persistence diagram $D_{n+m,k}^{DTM} = \mathfrak{Dgm}(\mathbb{V}[\mathbf{X}_n \cup \mathbf{Y}_m, \delta_{n+m,k}])$, and the RKDE weighted persistence diagram $D_{n+m,\rho,\sigma}^{RKDE}$ from the RKDE $f_{\rho,\sigma}^{n+m}$ using the Hampel loss ρ and a Gaussian kernel K_σ . Since the RKDE $f_{\rho,\sigma}^{n+m} \doteq \sum_{i=1}^{n+m} w_i K_\sigma(\cdot, \mathbf{X}_i)$ does not behave like a distance function, we convert $f_{\rho,\sigma}^{n+m}$ to a distance-like function $\mathbf{d}_{n+m,\rho,\sigma}$ using a similar approach as Phillips et al. (2015) to obtain

$$\begin{aligned} \mathbf{d}_{n+m,\rho,\sigma}(\mathbf{x}) &\doteq \|K_\sigma(\cdot, \mathbf{x}) - f_{\rho,\sigma}^{n+m}\|_{\mathcal{H}} \\ &= \sqrt{\sum_{1 \leq i, j \leq n+m} w_i w_j K_\sigma(\mathbf{X}_i, \mathbf{X}_j) + K_\sigma(\mathbf{x}, \mathbf{x}) - 2f_{\rho,\sigma}^{n+m}(\mathbf{x})}. \end{aligned} \quad (58)$$

The RKDE-weighted persistence diagram $D_{n+m,\rho,\sigma}^{RKDE} = \mathfrak{Dgm}(\mathbb{V}[\mathbf{X}_n \cup \mathbf{Y}_m, \mathbf{d}_{n+m,\rho,\sigma}])$ is then computed using the $\mathbf{d}_{n+m,\rho,\sigma}$ -weighted filtration on the composite sample. The bandwidth of the kernel and the parameters for the Hampel loss function are selected using the same approach as in Vishwanath et al. (2020). For each diagram, we compute the birth time $b(\{\mathbf{x}_0\})$ for the first outlier $\mathbf{x}_0 \in \mathbf{Y}_m$, and the bottleneck influence $W_\infty(D_{n+m}, D_n)$, as described in Section 7. We generate 10 such samples for each value of m , and report the average in Figure 13.

From Figure 13 (a), we note that $D_{n+m,Q}^{MoM}$ and $D_{n+m,k}^{DTM}$ show similar behavior, although the outliers consistently appear earlier in the DTM persistence diagram $D_{n+m,k}^{DTM}$. Furthermore, for $D_{n+m,Q}^{MoM}$, we observe the sharp transition that occurs between $m = 50$ and $m = 80$, which is due to the fact that the theoretical guarantees for $\mathbf{d}_{n,Q}$ from Theorem 7.1 are valid only when $2m < Q = 100$. Similarly, from Theorem 6.2, the outliers are guaranteed to have little influence on $D_{n+m,Q}^{MoM}$ whenever $m \leq 50$, as seen in Figure 13 (a). In addition to the influence of the outliers in the bottleneck metric, we also compute the maximum persistence for the order-1 persistence diagram in Figure 13 (b). While the RKDE remains resilient to uniform outliers, we note that $D_{n+m,\rho,\sigma}^{RKDE}$ is significantly impacted by the outliers placed at a single point in the center of the circle. This is evidenced by the sharp transitions for $D_{n+m,\rho,\sigma}^{RKDE}$ in Figures 13 (a, b). However, unlike $\mathbf{d}_{n+m,Q}$ and $\delta_{n+m,k}$, by construction $\|\mathbf{d}_{n+m,\rho,\sigma}\|_\infty \leq \sup_{\mathbf{x}} \sqrt{2K_\sigma(\mathbf{x}, \mathbf{x})} < \infty$. Therefore, the impact the outliers have on $D_{n+m,\rho,\sigma}^{RKDE}$ is bounded; and despite being more sensitive to the high-density outliers, the resulting influence on $D_{n+m,\rho,\sigma}^{RKDE}$ in Figures 13 (a, b, c) is bounded.